Optical measurements of aurora

Kari Kaila
University of Oulu, Department of Physics
14.11.2011

What we can measure?

- We can
  - Take white light images of aurora
    - Earlier films were used, later intensifies tv-cameras
    - At present CCD or CMOS chips
    - Integration time about 1 sec, downloading time short or seconds
  - Take monochromatic images of aurora
    - Needs telecentric optical system including narrow band filters in between optics and camera
  - Measure the intensity of an aurora in selected color
    - Needs photosensitive device
      - Photomultiplier tube (PMT)
      - Light sensitive diode

What we can measure?

- Measure the intensity of several auroral emissions
  - Multichannel auroral photometer
    - Several auroral emissions can be measured simultaneously
    - Directed to one point at a time
    - Integration and repetition times very small (down to ms)
    - Fields of view about 1° (0.5 ° - 40 °).
  - Auroral spectrometer
    - Will measure a spectral band at a time
    - Directed to one direction in the sky
    - Field of view 0.5° x 15°
    - Long integration time, about 10 sec

Auroral CCD camera

Kilpisjärvi auroral station

Multichannel auroral photometer

Zenith photometer and auroral video camera

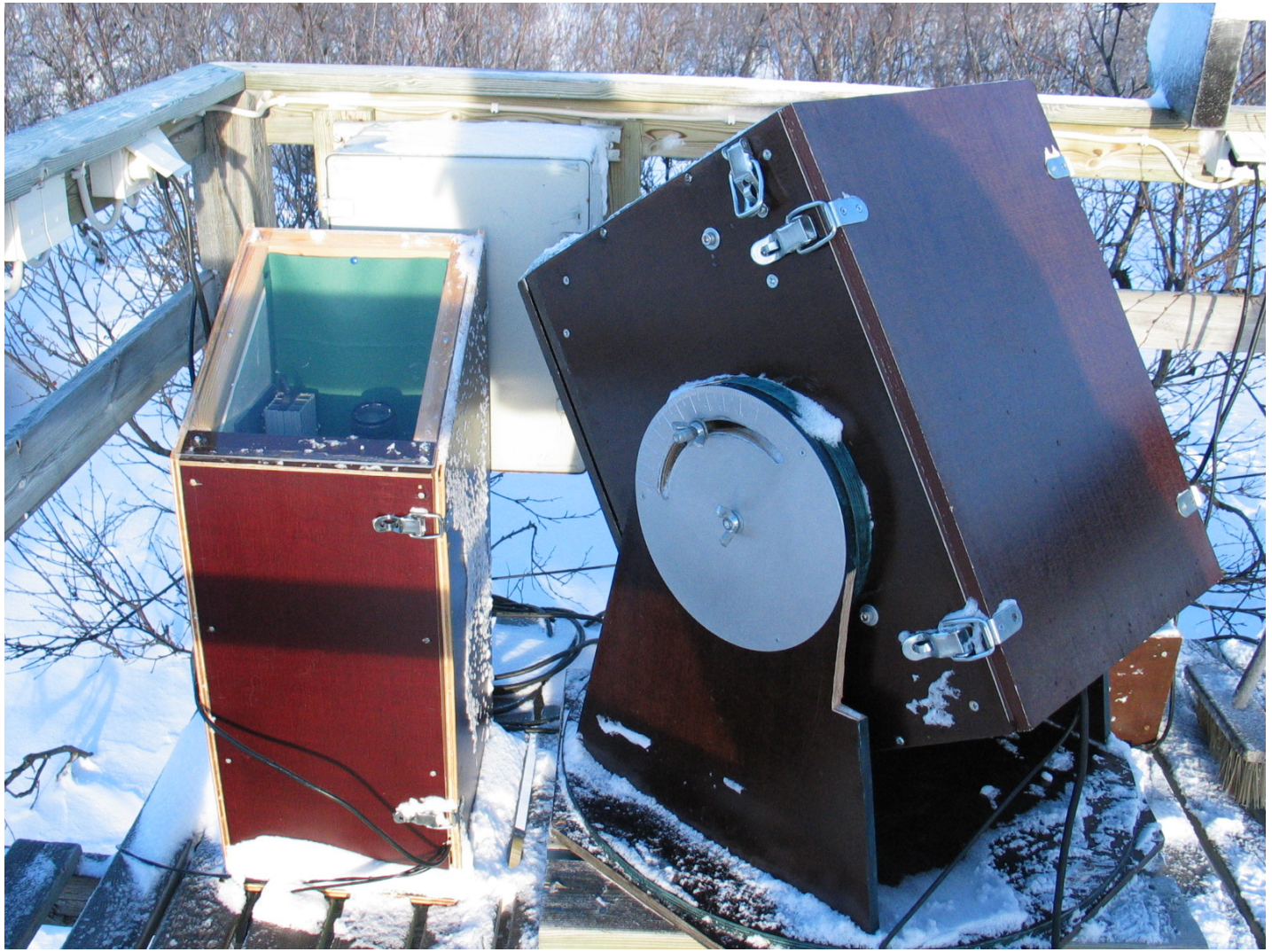

Control room inside a house

Karesuvanto station

Kilpisjärvi since 2009

Photometer

- The idea of a photometer is to measure the intensity of the target
- We use photomultiplier (pmt) tubes, which typically have 10-12 dynods
- A high voltage of about 1000 V is needed to drive the pmt. The voltage has been coupled to cathode and anode. A voltage divider divides the voltage to different dynods.

Photomultiplier tube

- The pmt photocathodes are sensitive to light
- The dynode chain multiplies the electrons from cathode by 10^6 times
- The small pulse has to be amplified
- The amplified pulse can be counted
- The quantum efficiency of pmt is less than 30%

Photomultiplier tubes (PMT)

Figure 1: Schematic Representation of PMT

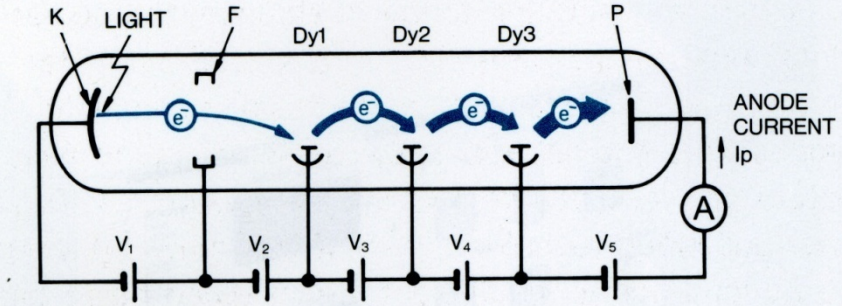

FIGURE 1
Cross-Section of Head-On Type Photomultiplier Tube

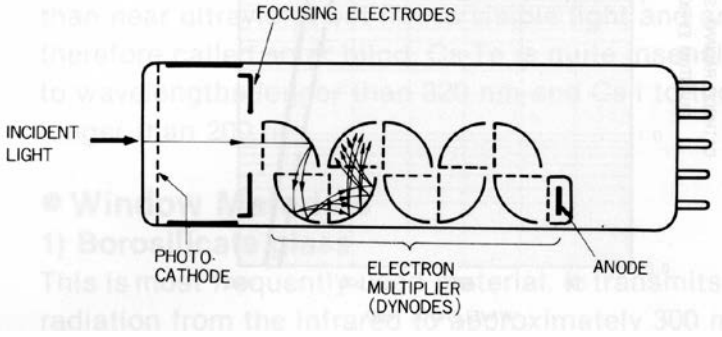

FIGURE 2
External Appearance

a) Side-On Type

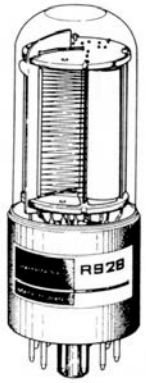

b) Head-On Type

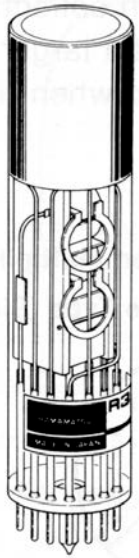

Figure 3: Voltage Divider Circuit with Cathode Grounded

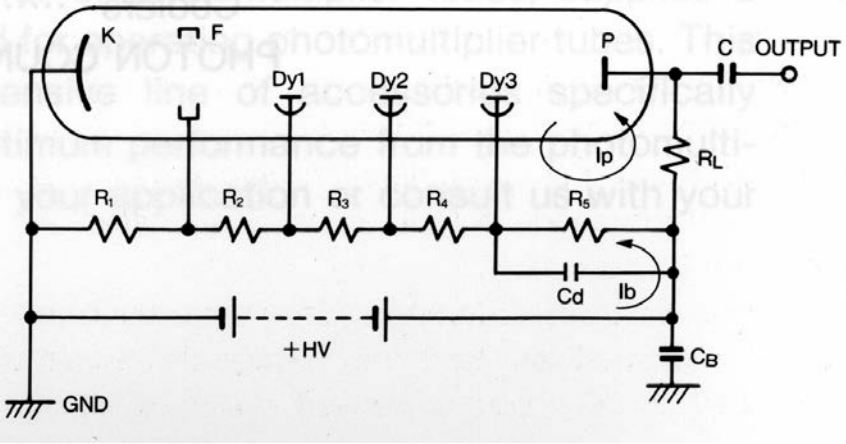

Characteristics of PMT

FIGURE 18
Anode Pulse Rise Time and Electron Transit Time

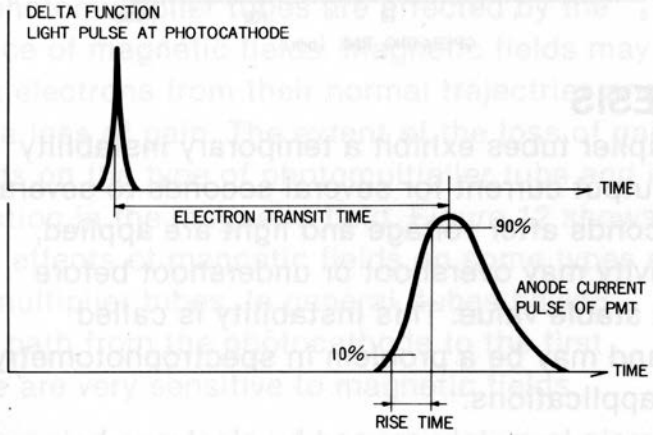

FIGURE 10
Typical Dark Current vs. Supply Voltage

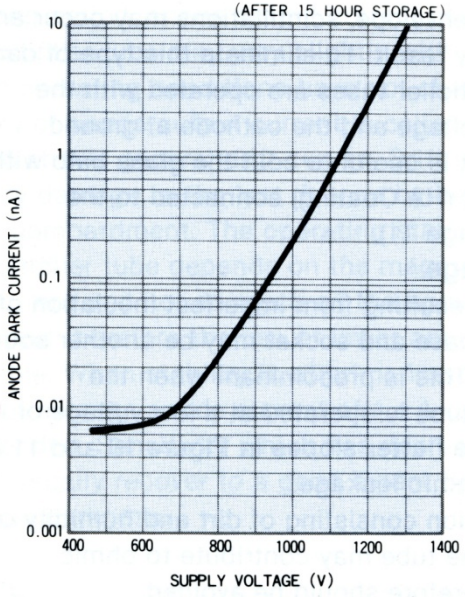

FIGURE 11
Temperature Characteristics of Dark Current

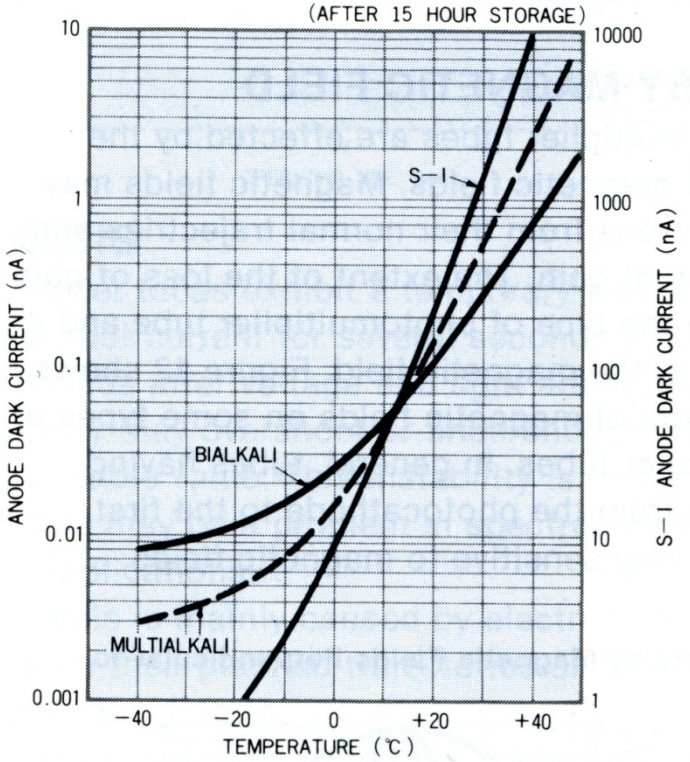

Bialkali photocathode sensitivity

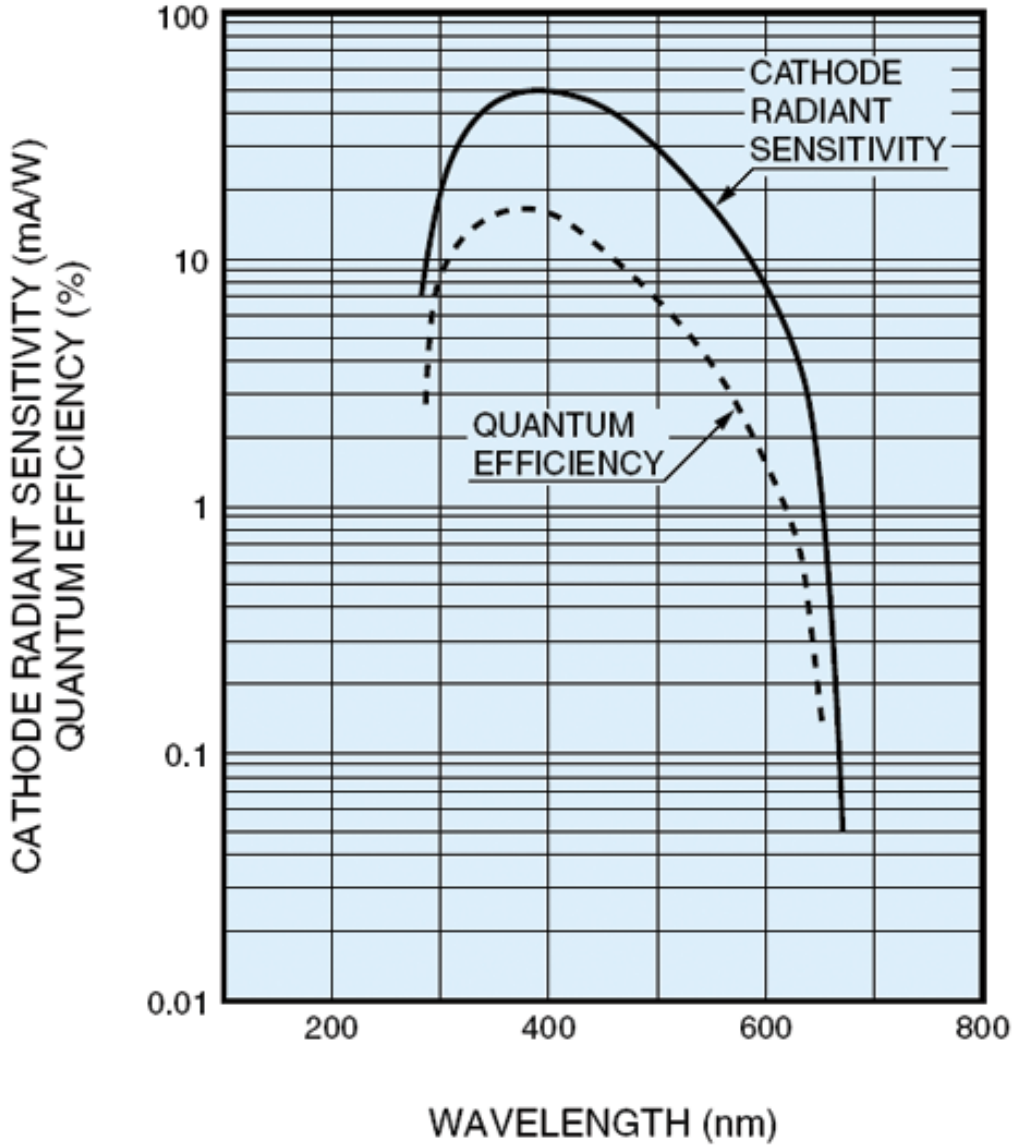

Photocathode sensitivities

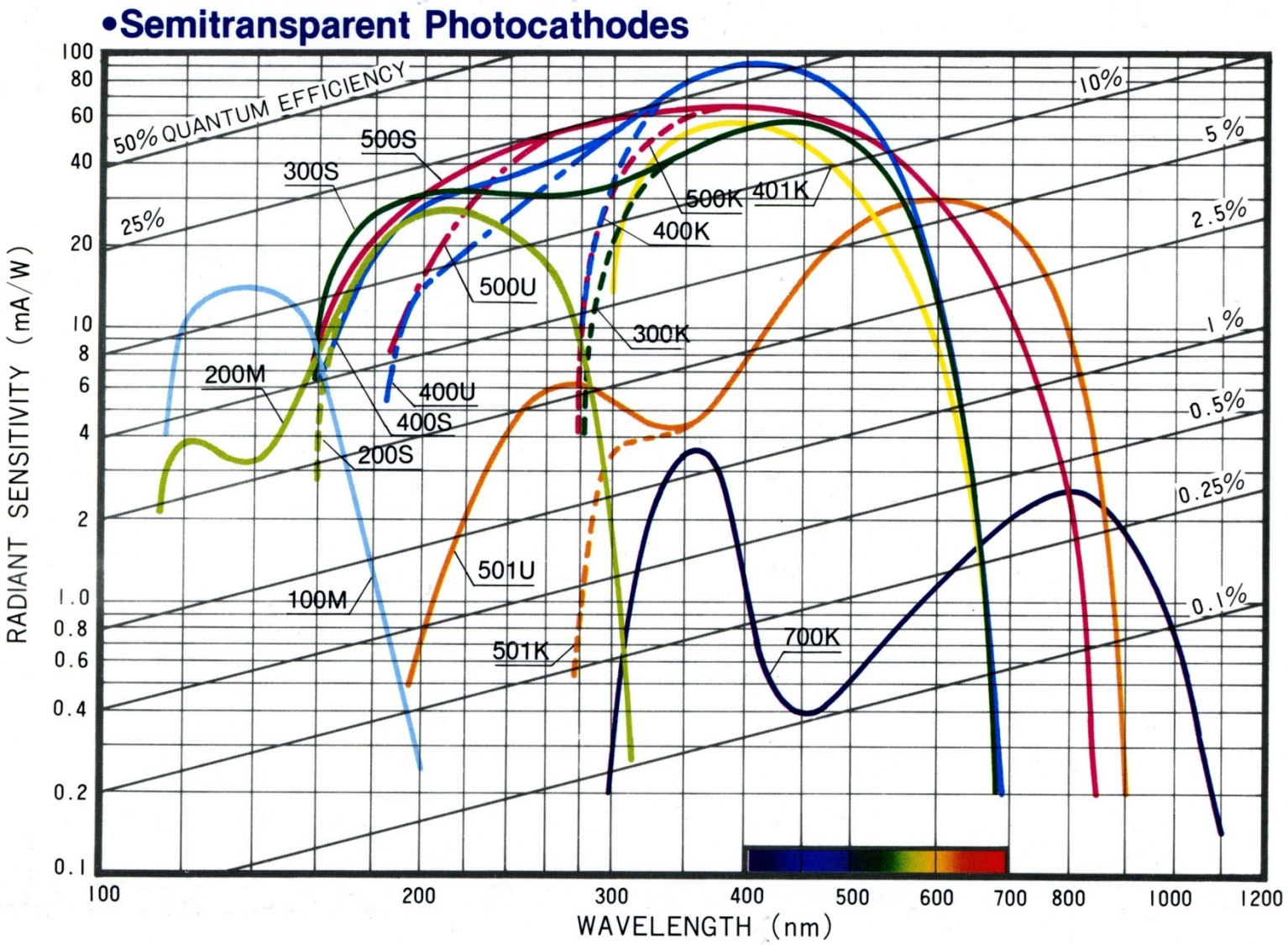

Photodiode characteristics

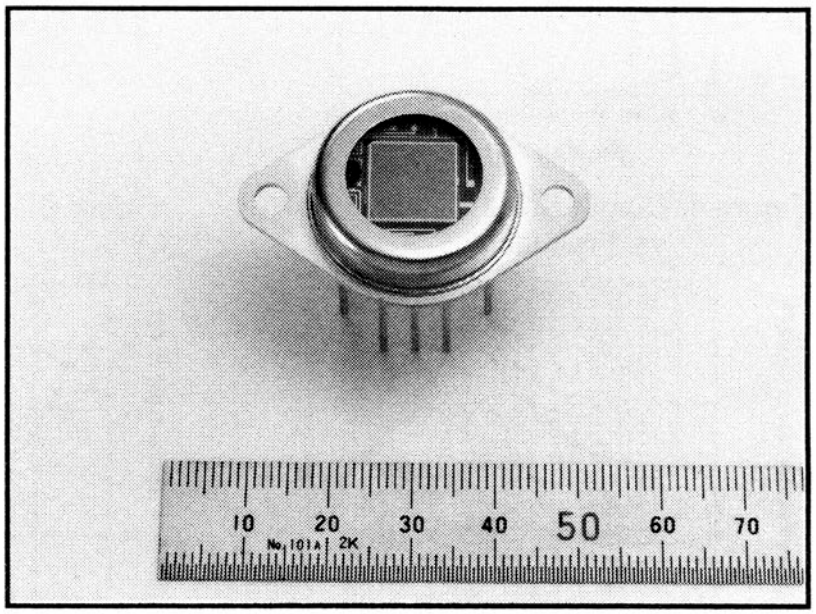

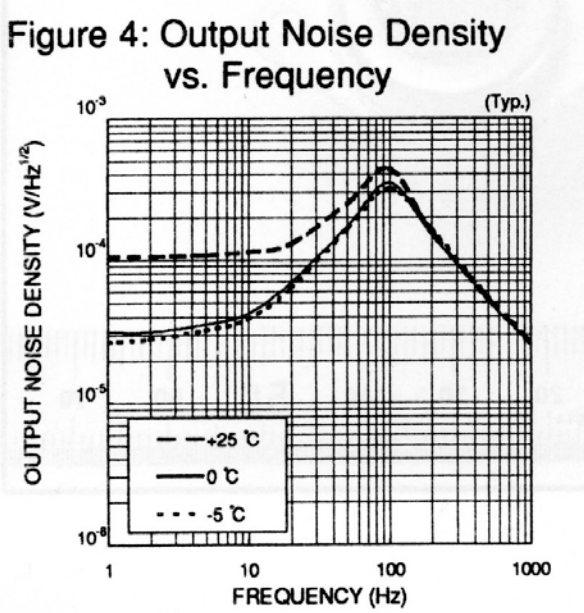

Si PHOTODIODE WITH PRE-AMP S6204-02

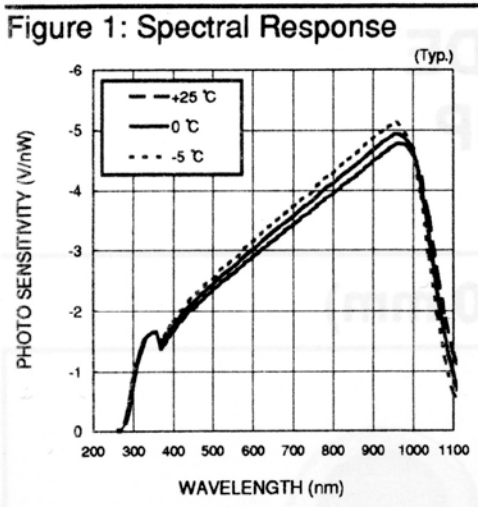

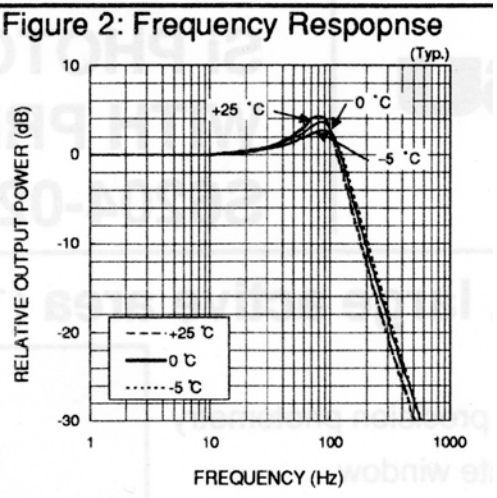

CCD chip and camera

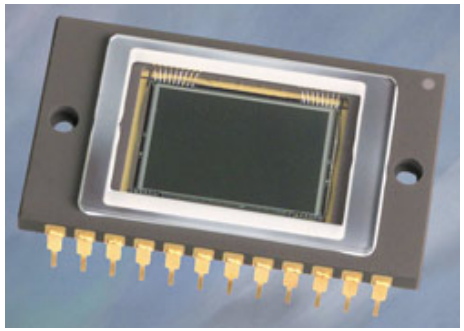

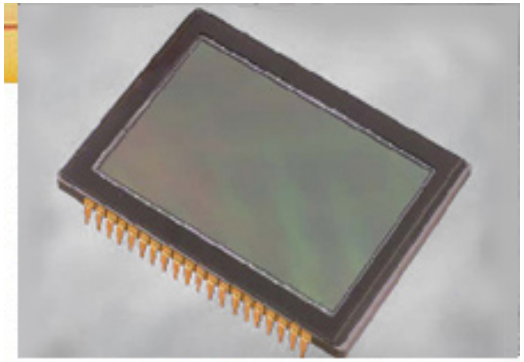

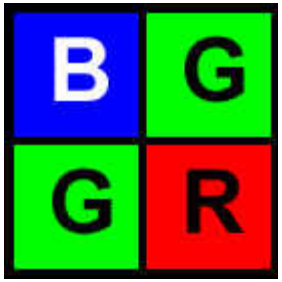

DEVICE DESCRIPTION

Architecture

Overall

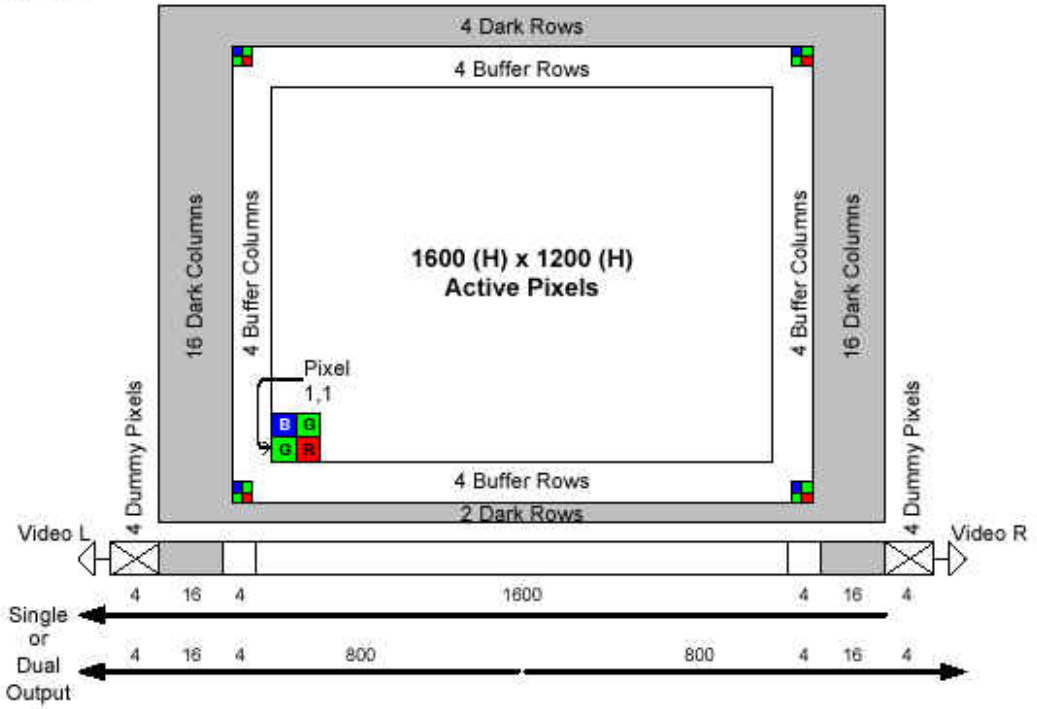

CCD camera sensitivity

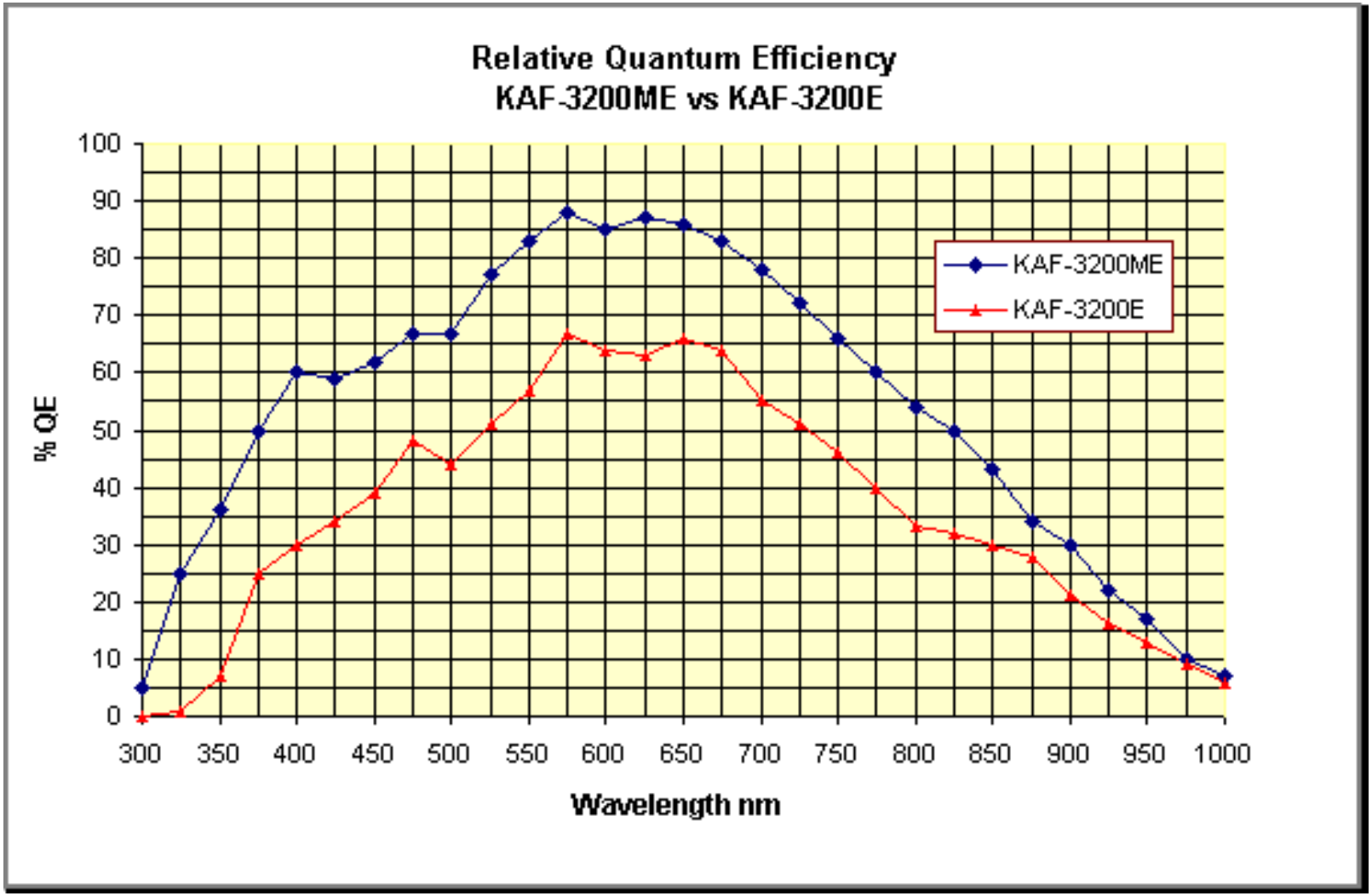

CCD color vrs bw chip sensitivity

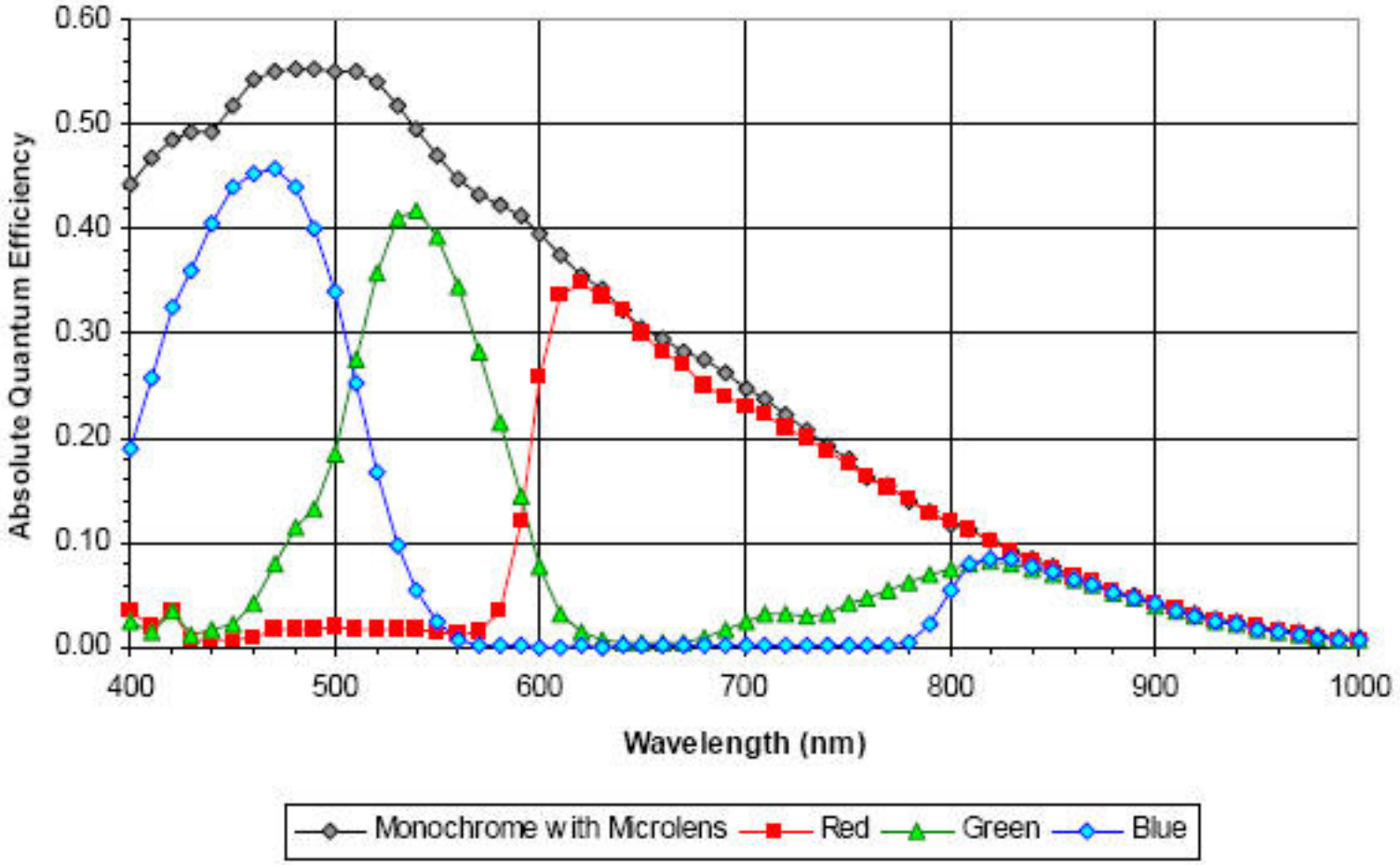

Different spectral curves

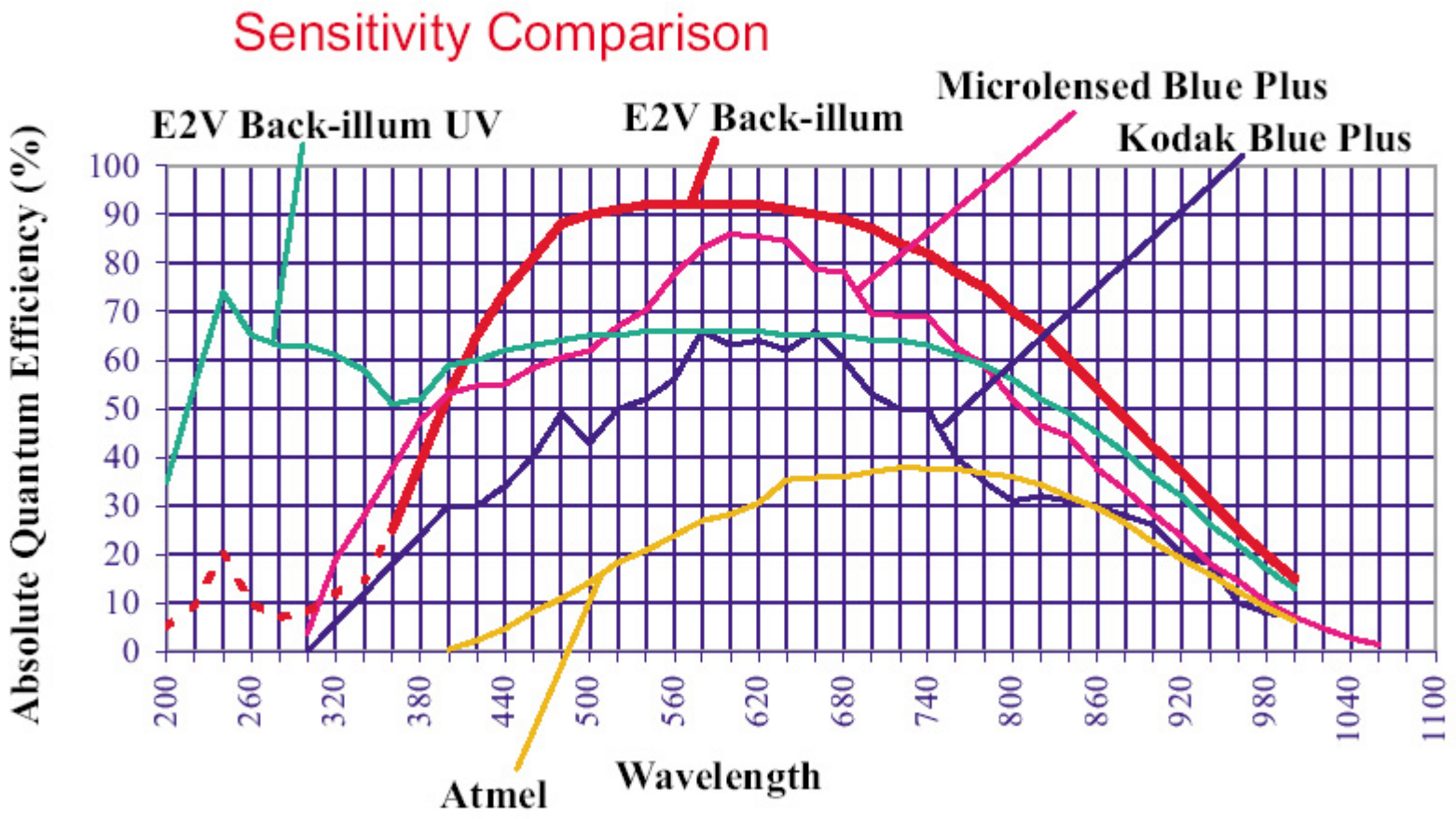

Filters

- Measurements need filters
- They are typically narrow band interference filters
- Their FWHM is typically 1 nm (0.6-3.0 nm)
- They have own characteristics
- By tilting their central wavelength can be shifted
- Problems: temperature dependent, aging

Narrow band interference filters

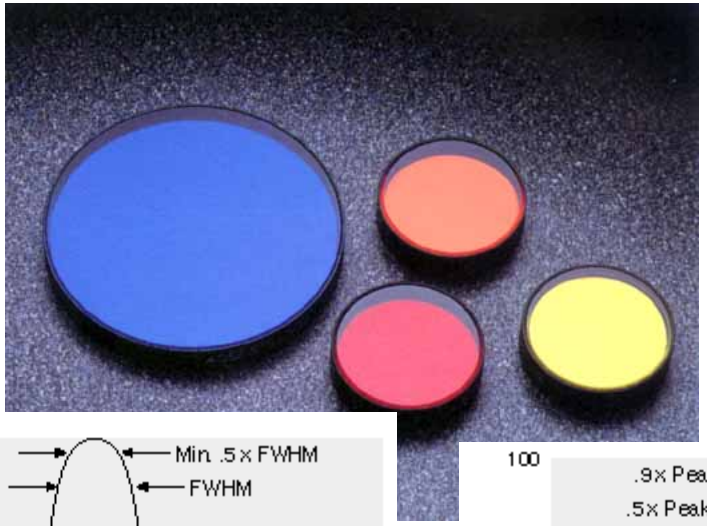

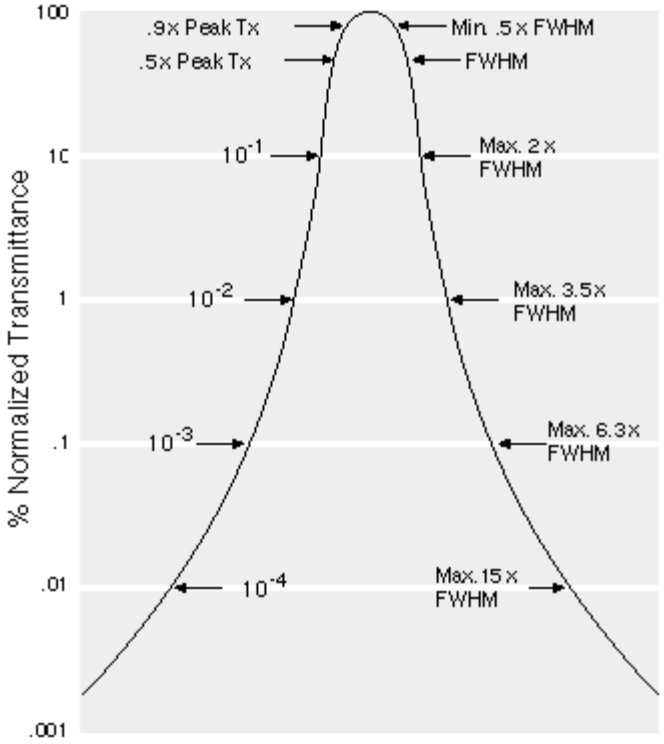

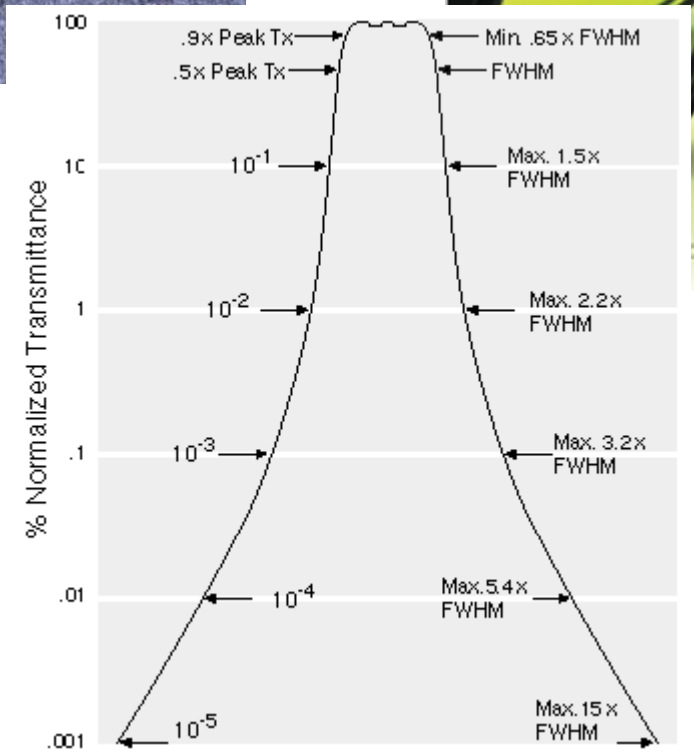

Measured transmission curve

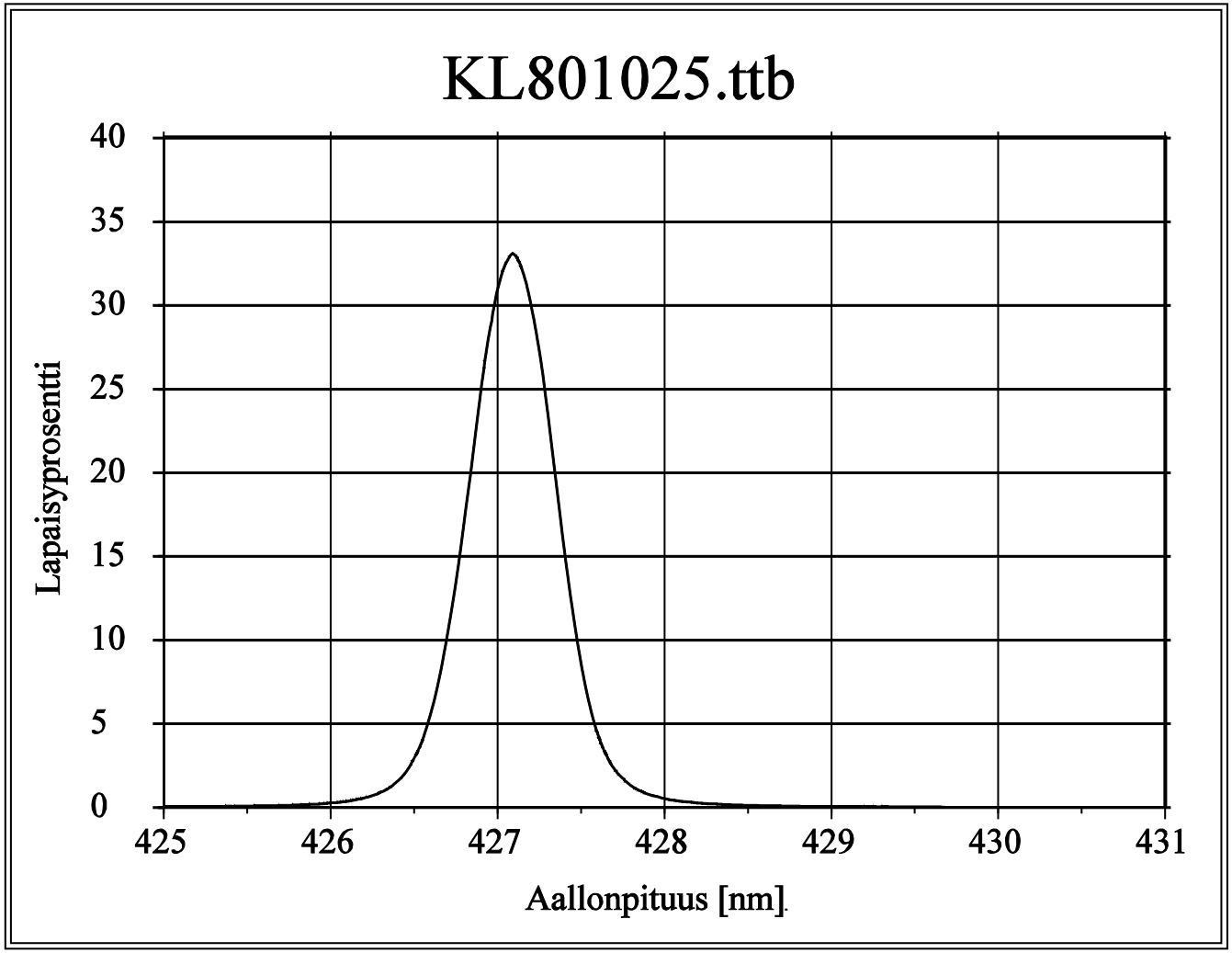

What is our target

- Our target is aurora, usually faint extend luminosity in the night sky.
- The light consists of atomic emission lines and molecular bands.
- When measuring the wanted emission, the filter has to be tuned correctly by tilting it.

Atomic transitions

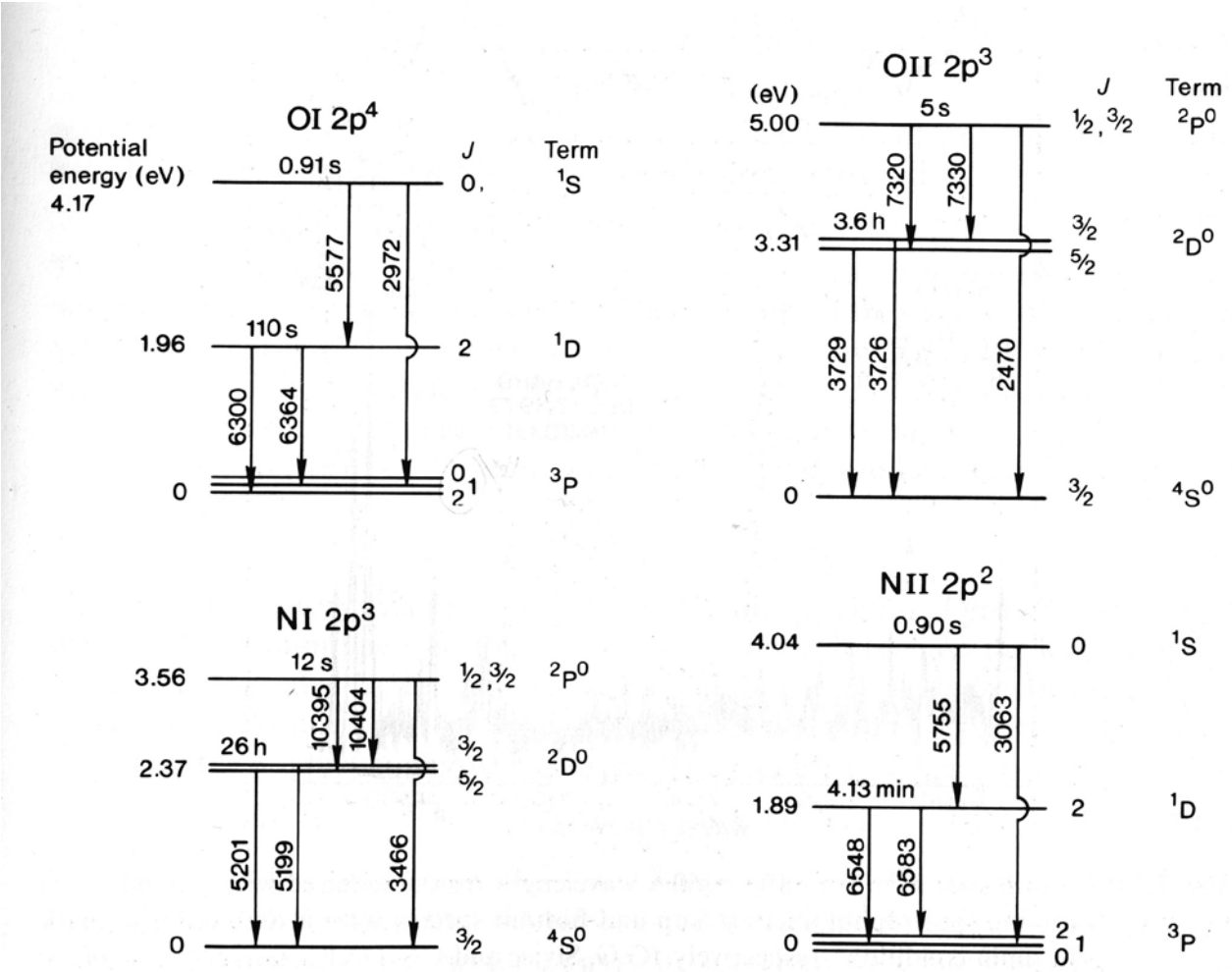

Fig. 7.4.4 Partial energy level diagrams for O, O^+, N and N^+ showing states in the ground configuration of the atoms and ions.

Molecular transitions

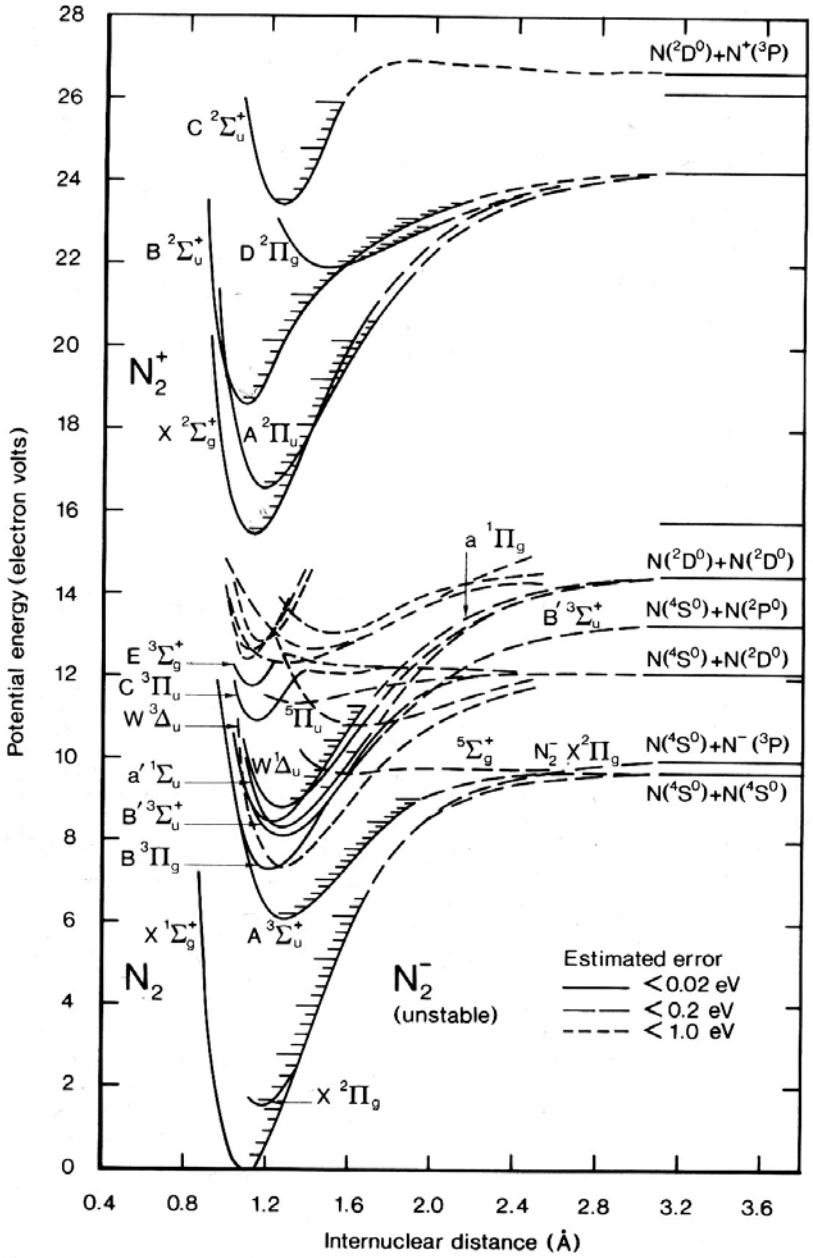

Fig. A3.5 Potential energy curves for N_2^- (unstable), N_2, and N_2^+.

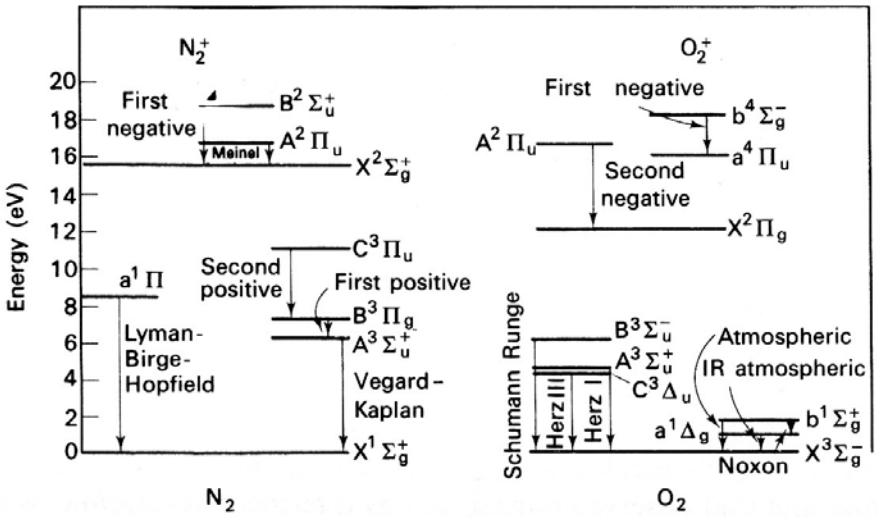

Fig. 5.2 Low lying energy states of O_2, O_2^+, N_2 and N_2^+.

Auroral spectrum

- Auroral spectrum consists of atomic lines and molecular bands
- Atomic lines are narrow
- Molecules produce vibrational bands, which consist of numerous rotational lines

Auroral spectrum 1

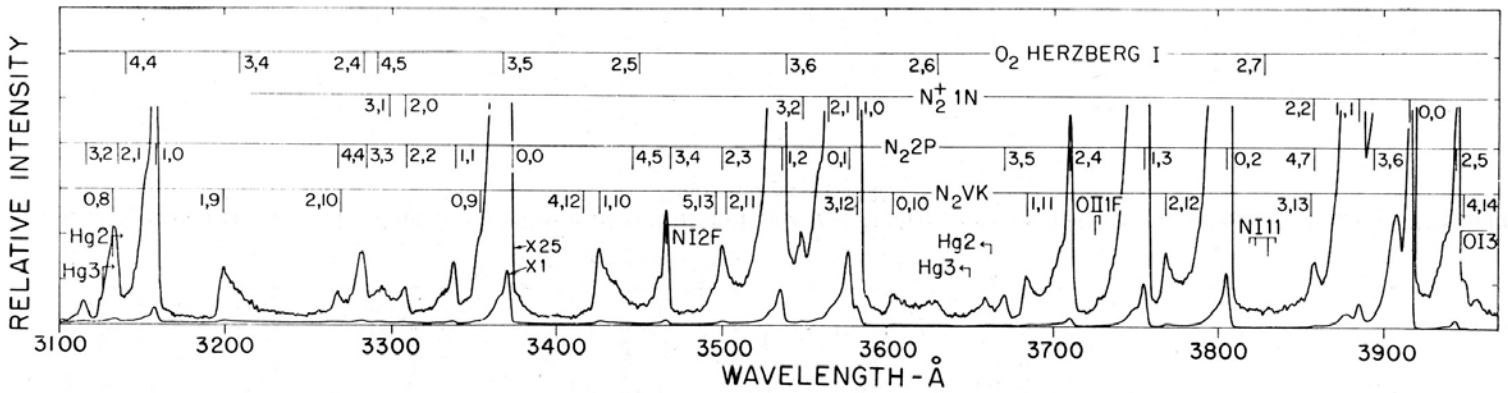

Fig. 4.2. Spectrum of aurora 3100–3950 Å and 3 Å resolution. The two curves are at the gains indicated. Bands and atomic features present or possibly present are indicated. The ordinates are relative intensity uncorrected for atmospheric transmission. I am very much indebted to Dr R. L. Gattinger for preparing this spectrum from data recently obtained at the NRC Auroral Observatory, Ft. Churchill.

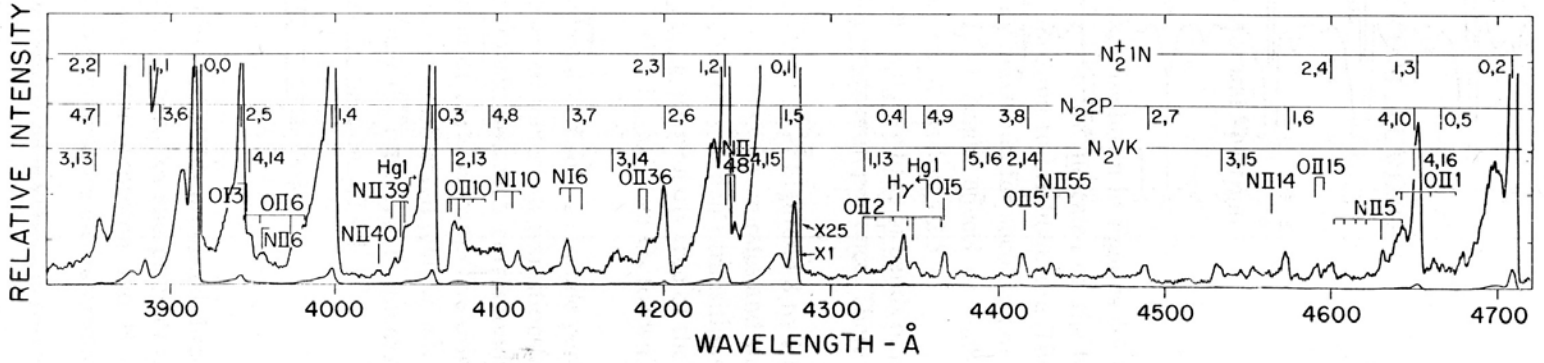

Fig. 4.3. Spectrum of aurora 3850–4700 Å as for Figure 4.2. I am very much indebted to Dr R. L. Gattinger for preparing this spectrum from data recently obtained at the NRC Auroral Observatory, Ft. Churchill.

Auroral spectrum 2

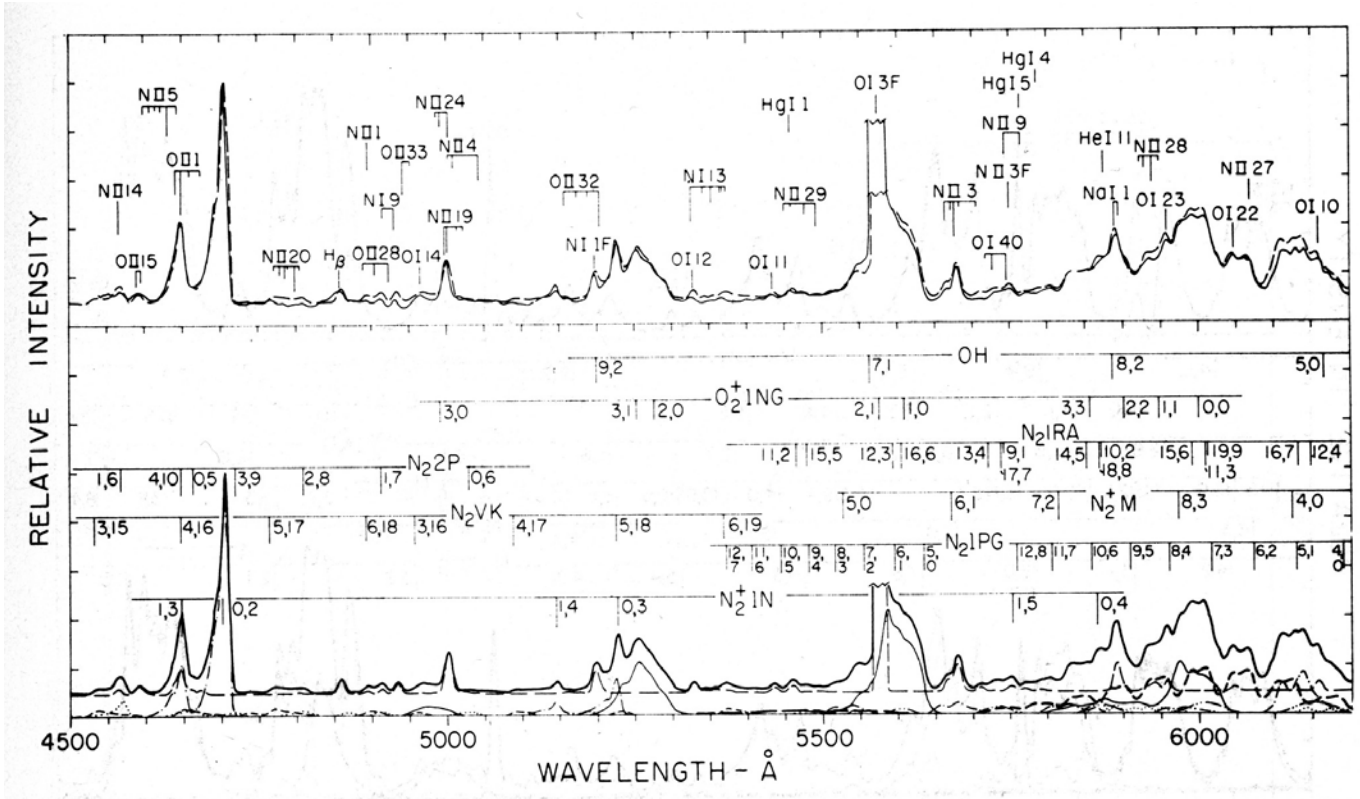

Fig. 4.4. Spectrum of aurora 4500 Å to 6200 Å at 10 Å resolution. Upper panel: solid line is the observed averaged spectrum of aurora with $I(5577)$ in the range 20–60 kR; dashed line is total synthetic spectrum. Lower panel: Heavy solid line is the total synthetic spectrum; N_2 1P – heavy long dashes; N_2^+ M and 1N – alternating dot and dash; OH-dots; O_2^+ 1N – light solid line; atomic lines plus continuum-light long dashes; O_2 At-short dashes; N_2 IRA – double dot and single dash; N_2 2P – dots; N_2 VK short dashes. From Gattinger and Vallance Jones (1974). (Courtesy *Canadian Journal of Physics*; reproduced by permission of the National Research Council of Canada.)

Auroral spectrum 3

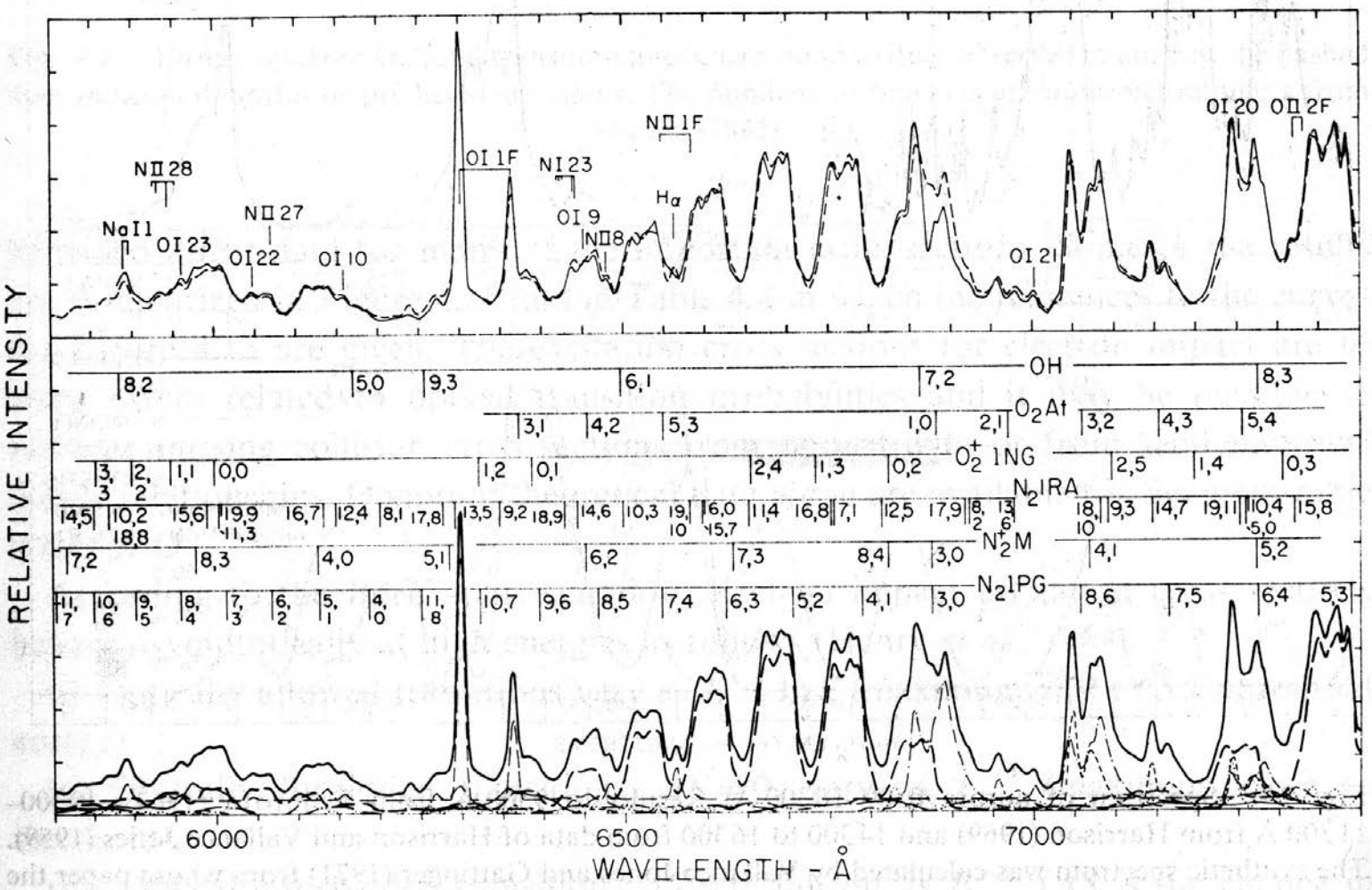

Fig. 4.5. Spectrum of aurora 5800–7400 Å; (continuation of Figure 4.4).

Auroral images with CCD

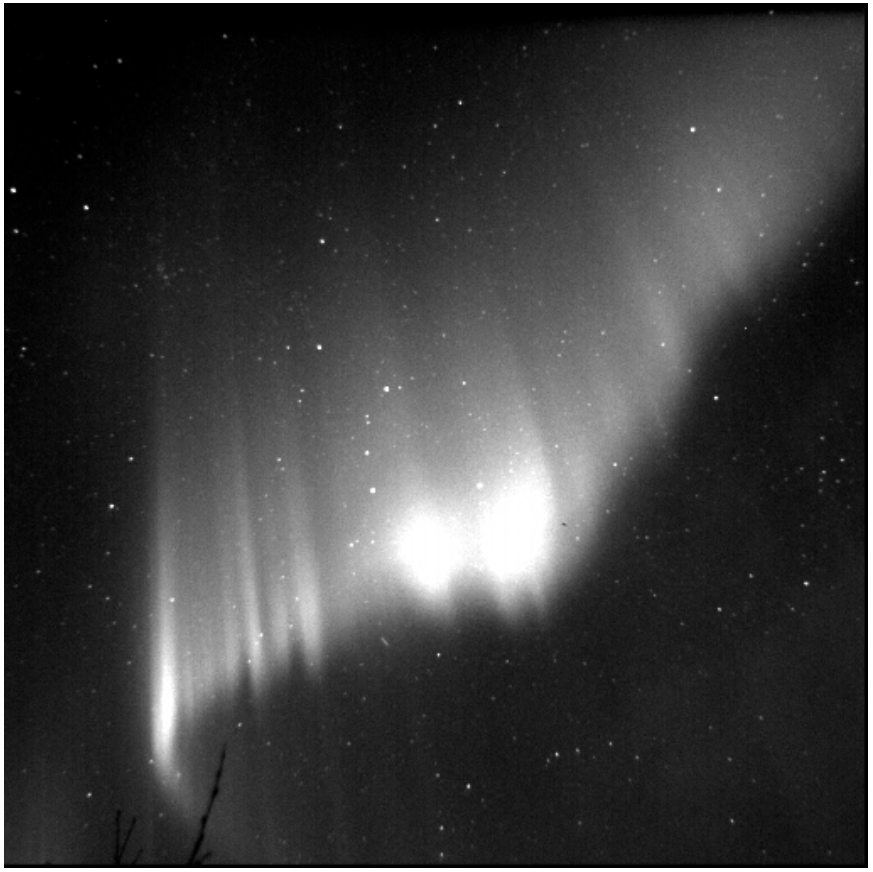

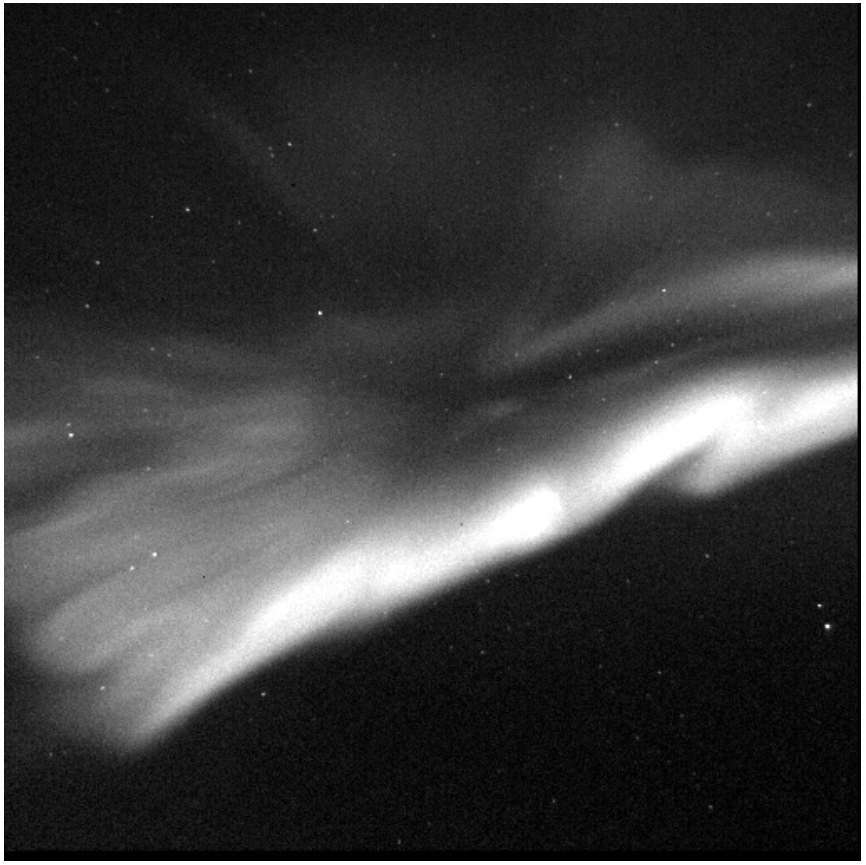

Auroral images with CCD

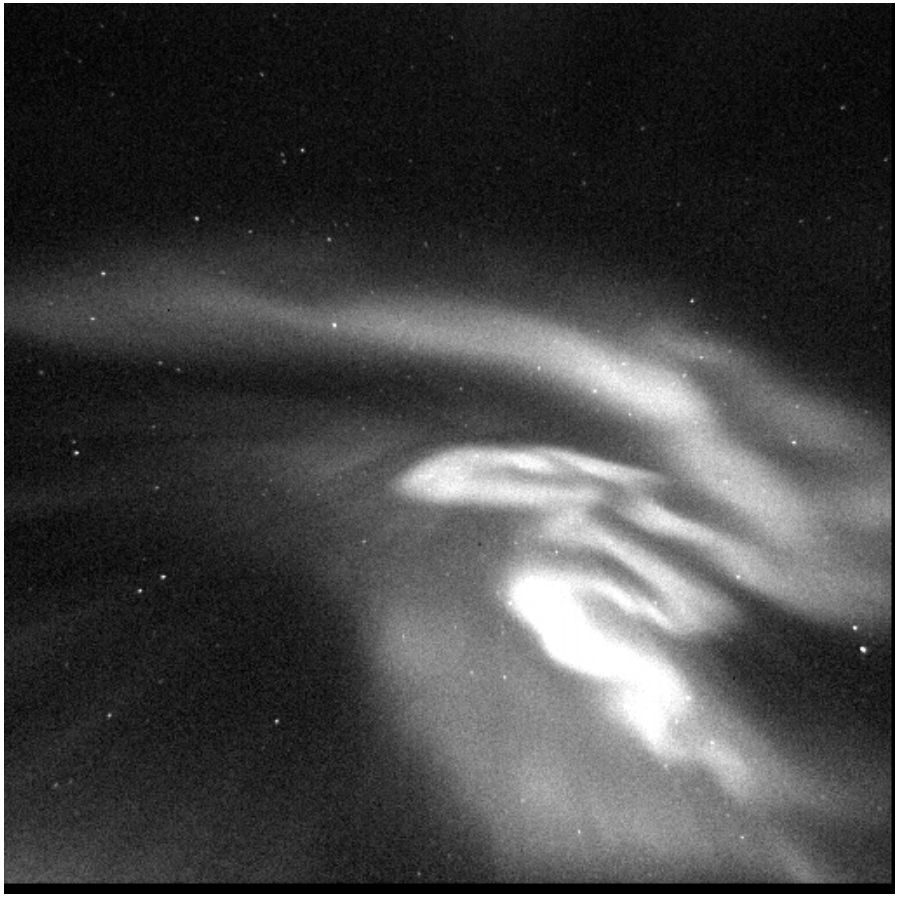

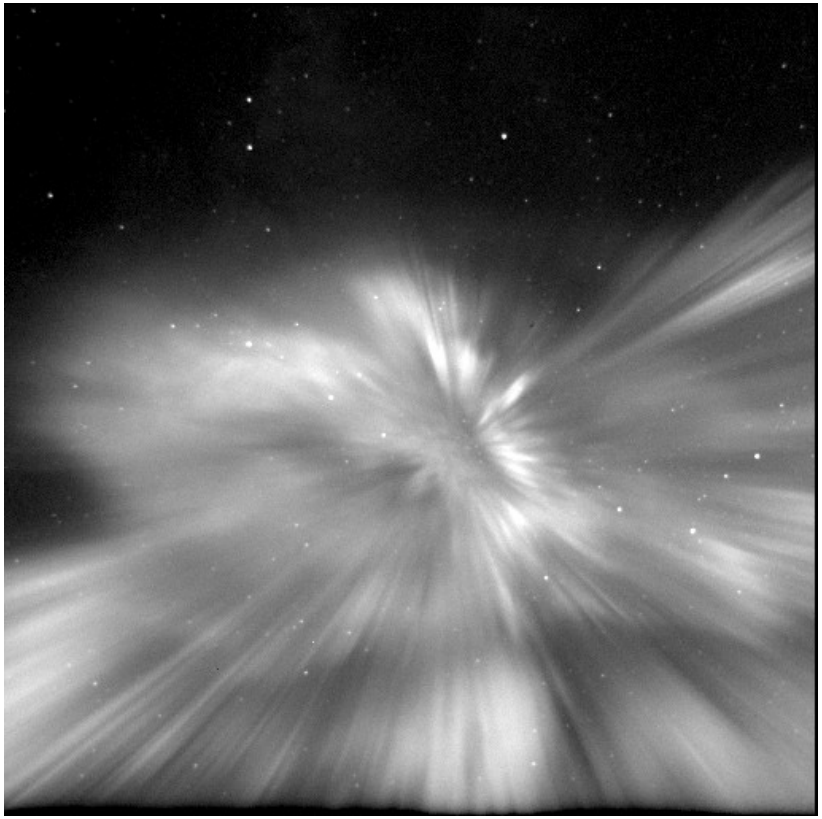

Auroral spectra

- Auroral spectra can be taken with spectrometers
- They have objective, which makes an image to the narrow slit. The with in the sky is typically 0.5° and length 20°
- A spectrum covers a range of about 200 nm
- As detector we use CCD type cameras

H alfa aurora

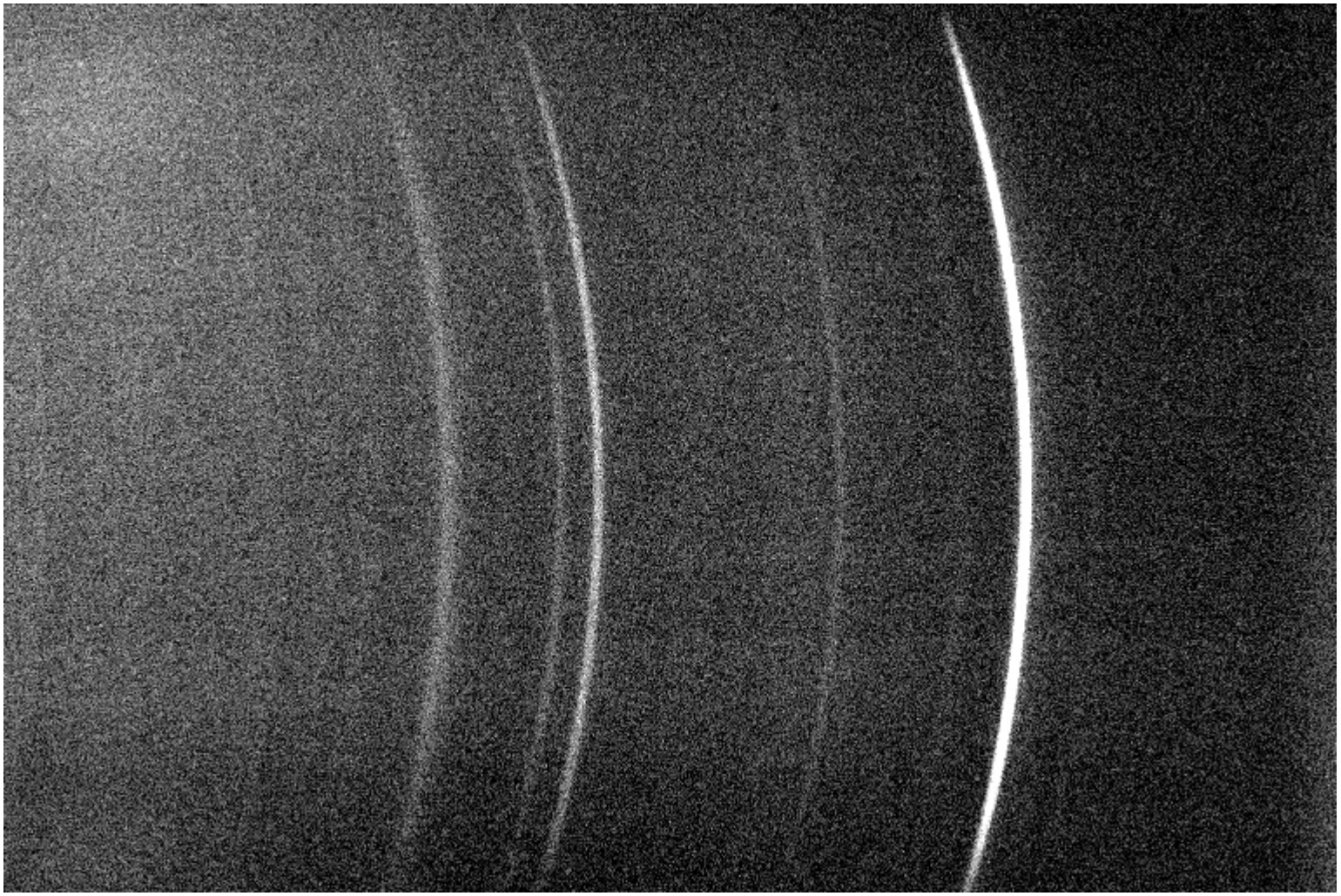

Electron aurora

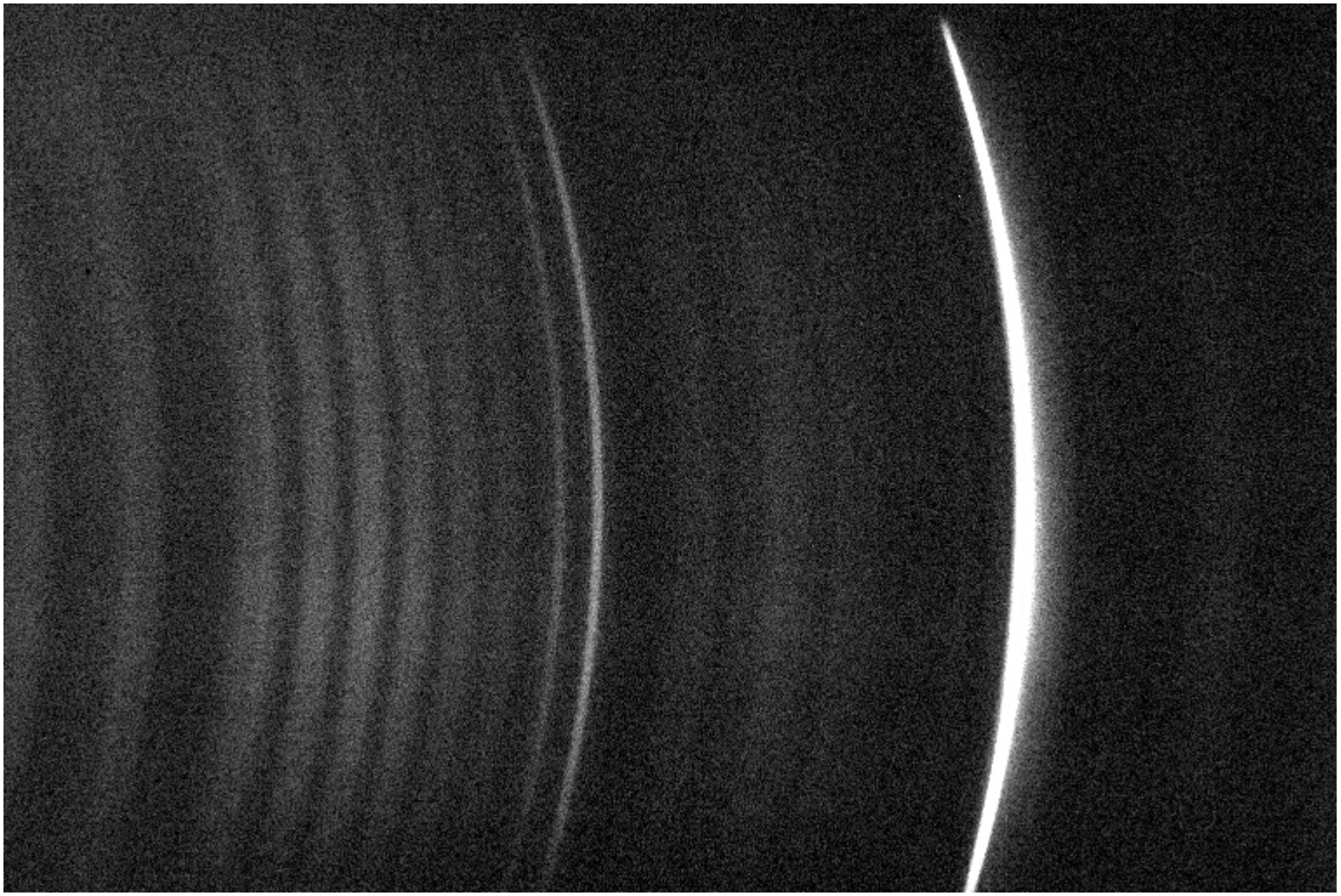

Electron aurora 2

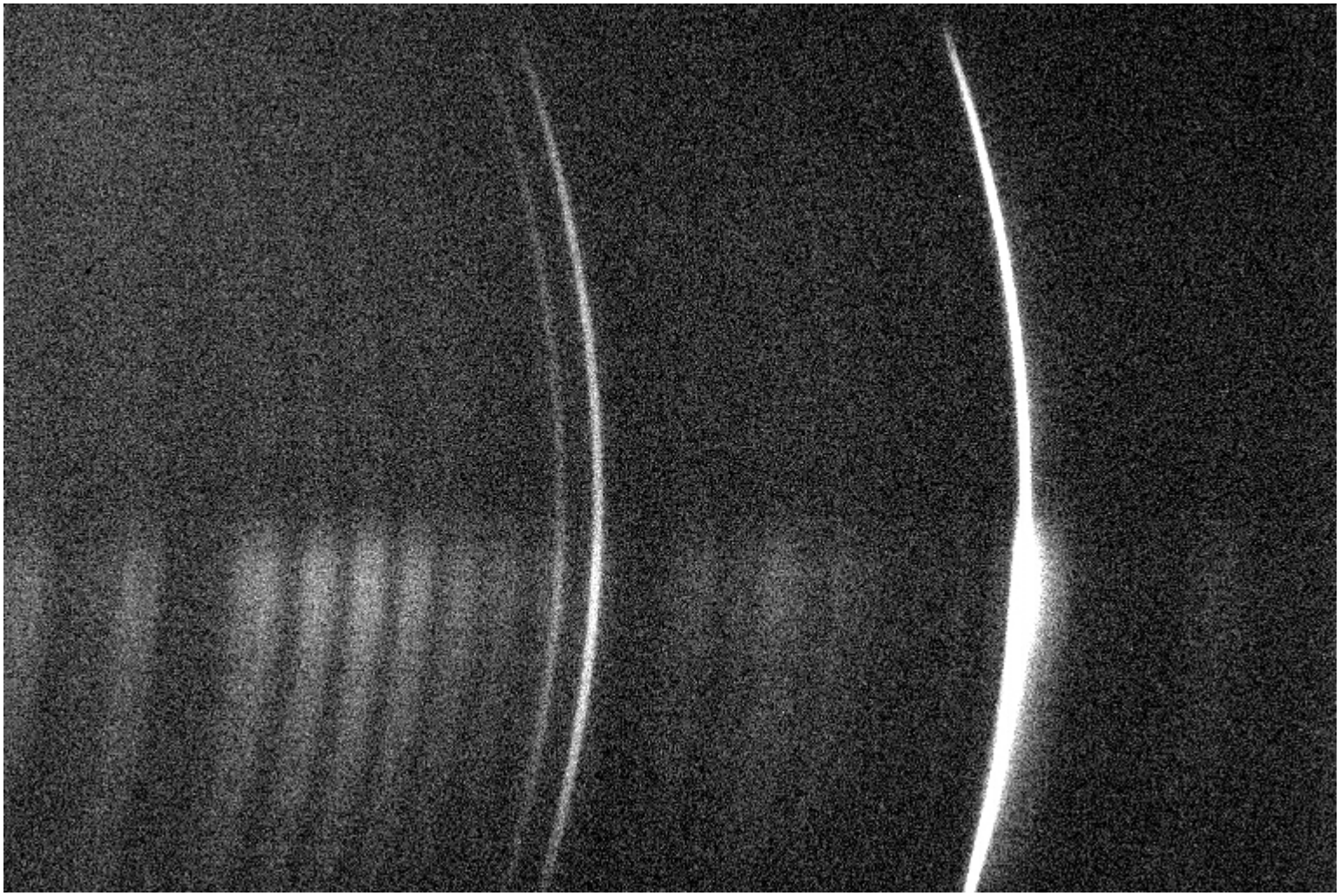

Aurora is complex

- Aurora consists of very many parameters
  - atmosphere, electron and proton fluxes, …
- Auroral instruments are possible to build
  - planning, design, components, calibration, …
- Measurements take its time
  - every instrument needs its own program, …
- Data handling is its own job
  - programming, checking, modelling, …

Optical measurements of aurora, interference filters

Kari Kaila
University of Oulu, Department of Physics
14.11.2011

Optical measurements

- Our target is aurora
- Our intrest is the light of aurora
  - Where they are located?
  - Their structure?
  - How high is their intensity?
  - How they moves?

Aurora

- *Excitation of atmospheric constituents due to collisions of energetic particles.*
- Aurora is the light, which is emitted from the exited atoms and molecules.
- It is three dimensional luminous phenomenon in the high latitude upper atmosphere.
- We see always the projection of this luminocity.

Optical measemenet devices

- Auroras can be measured optically by
  - Cameras or imaging devices
  - Photometers
  - Spectrometers
  - Interferometers

- All these intruments will be looked briefly

Cameras and photometers

- **Cameras** take images of the sky and auroras.
  - The images give information about the weather conditions and auroral forms.
  - They take images in white light or through filter.

- **Photometers** measure intensities of the aurora of one point at a time.
  - They have narrow bandwith filters, 0.5 – 2 nm.

Spectrometers and interferometers

- **Spectrometers** take spectral images of a narrow line of the sky.
  - The spectral range can be 10 – 300 nm.
  - The spectral resolution is 0.1 – 3 nm.

- **Interferometers** give very high spectral resolution of wide area.
  - The spectral resolution is below 0.01 nm.

Measurements

- Each instrument has its advantages and disadvantages.
- It will always be a compromice what you are measuring and how you are measuring.
- If you gain something you will lose something else.
- Think carefully what you want to measure and what you really need!

Features of different instruments

- **Cameras, white light:**
  + Weather conditions
  + Auroral forms
  + Wide field of view
  + Short integration times
  - Earlier long download time, no more
  - No spectral information
  - High or huge data flow

Features of different instruments

- **Cameras, filtered:**
  + Some kind spectral information from large area
  + Auroral forms
  - Filter bandwidth relative large, 2 - 10 nm
  - Not pure emissions
  - Only one filter at a time
  - Not very high temporal resolution
  - High or huge data flow

Features of different instruments

- **Photometers:**
  - – Only towards one direction at a time
  - + Several simultaneous channels possible
  - + Narrow bandwith filters used
  - + High temporal resolution -> ms
  - + High repetition rate -> kHz
  - + Sensitive equipment
  - + Possible to scan in one plane
  - + Low to moderate data flow

Features of different instruments

- **Spectrometers:**
  + Several spectral emissions simultaneously
  + Long but narrow line in the sky
  + Spectral shape of emissions
  + Background easy to subtract
  - Poor temporal resolution, integration times more than 5 sec
  + moderate data flow

Features of different instruments

- **Interferometers:**

  + Very high spectral resolution

  + Can give Doppler velocity and line width

  - Used only for atomic emission lines

Filters

- The spectral range in white light measurements depend only of the spectral sensitivity of the detector.
- Filters let a limited wavelength range pass through, other wavelengths are reflected or absorbed.
  - Color glas filters: very broad bans pass through
  - Interference filters: bandwidth 10 – 0.3 nm
  - Cut on and cut off filters, sharp edge

Interference filters

- Characteristic parameters are:
  - Central wavelength λc
  - Bandwidth FWHM (Full Width at Half Maximum)

- These parameters are valid if
  - The light passes perpendicular to the filter
  - The temperature is close to the room temperature

The structure of interference filter

- Interference filter is one type of Fabry-Perot interferometer.
- There the air gap is replaced by a thin layers of dielectric material with half-wave or quarter-wave optical thickness.
- A unity of an interference filter is cavity.
- The more cavities the more narrow filter bandwidth.

Two cavity filter layout

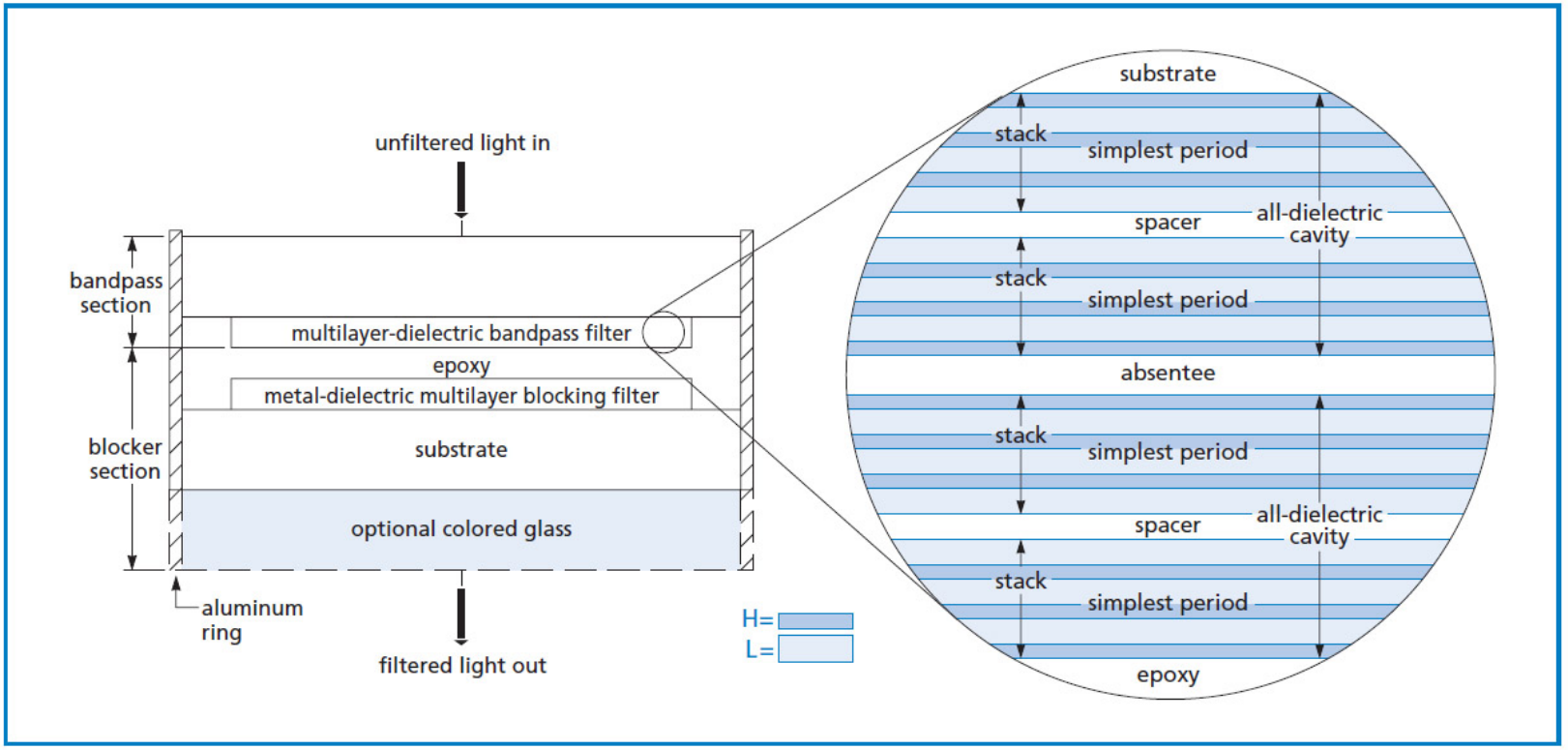

Cross section of a typical two-cavity interference filter

Bandwidth of

1

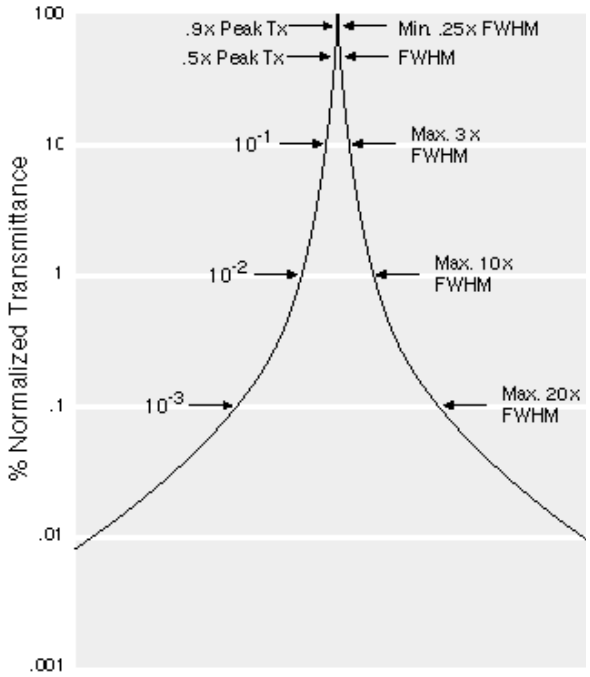

2

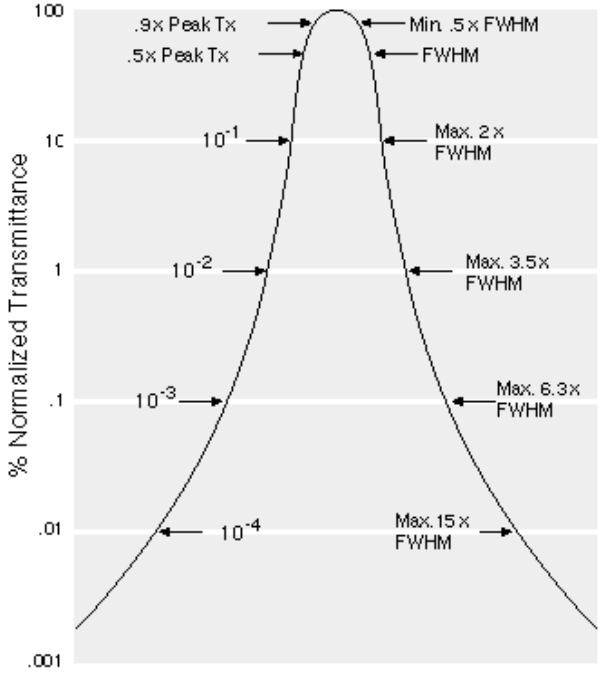

3 cavity filter

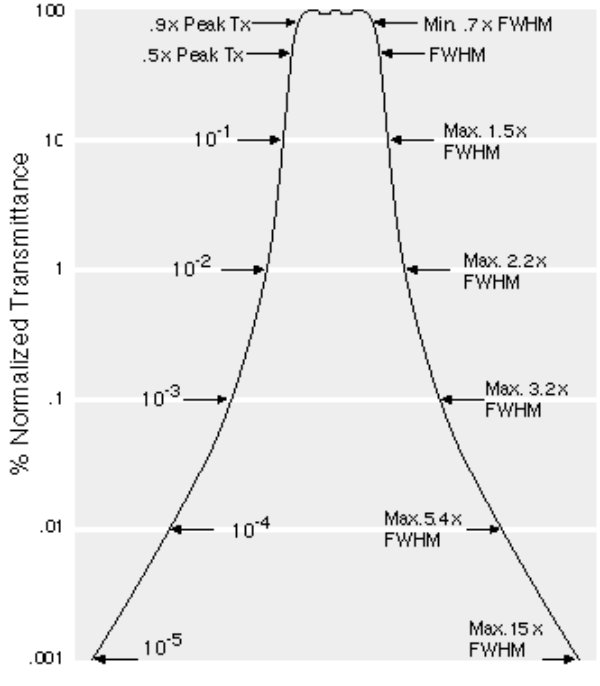

Wavelength adjustment

- Central wavelength changes towards shorter wavelengths when tilting the filter.

$$\lambda_\theta = \lambda_0 \left[1 - \left(\frac{n_0}{n_e}\right) sin^2\theta\right]^{1/2}$$

where
λ_θ = central wavelength at tilting angle θ,
λ_0 = the central wavelength at tilting angle $0°$,
n_0 = refractive index of the surrounding medium,
n_e = effective refranctive index of the filter material.

Temperature dependency

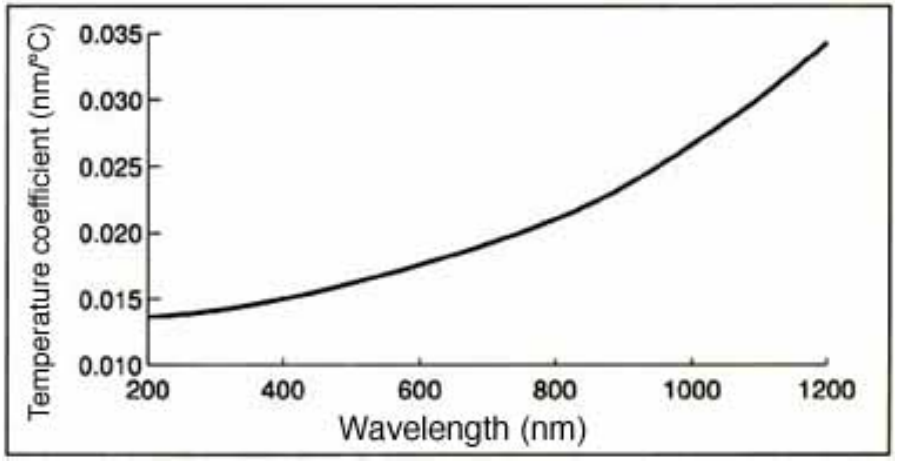

Temperature Dependence of Peak Transmittance

Wavelength (nm)	Temperature Coefficient of Shift (nm per °C)
400	0.016
476	0.019
508	0.020
530	0.021
557	0.021
608	0.023
630	0.023
643	0.024
710	0.026
820	0.027

Transmission and refractive index

- Typical maximum transmissions for different wavelengths are:

λ_c	T_{max}
< 400 nm	<30 %
400-500 nm	45 %
500-700 nm	60 %
700-800 nm	55 %

- Typical effective refractive indexes are:

λ_c	n_e
340-480 nm	1.45
480-1100 nm	2.05

Aging of interference filter

- Central wavelength shifts slowly towards shorter wavelengths!
- Filter transmissions decrease with the time!
- Humidity will destroy the filter with the time!

Wavelenngth adjustment

- Tilting the filter the central wavelength shifts towards lower wavelength
- At the same time the FWHM increases
- Also the peak transmission decreases
- The total area under the transmission profile stays constant

Example: 486.1 nm filter

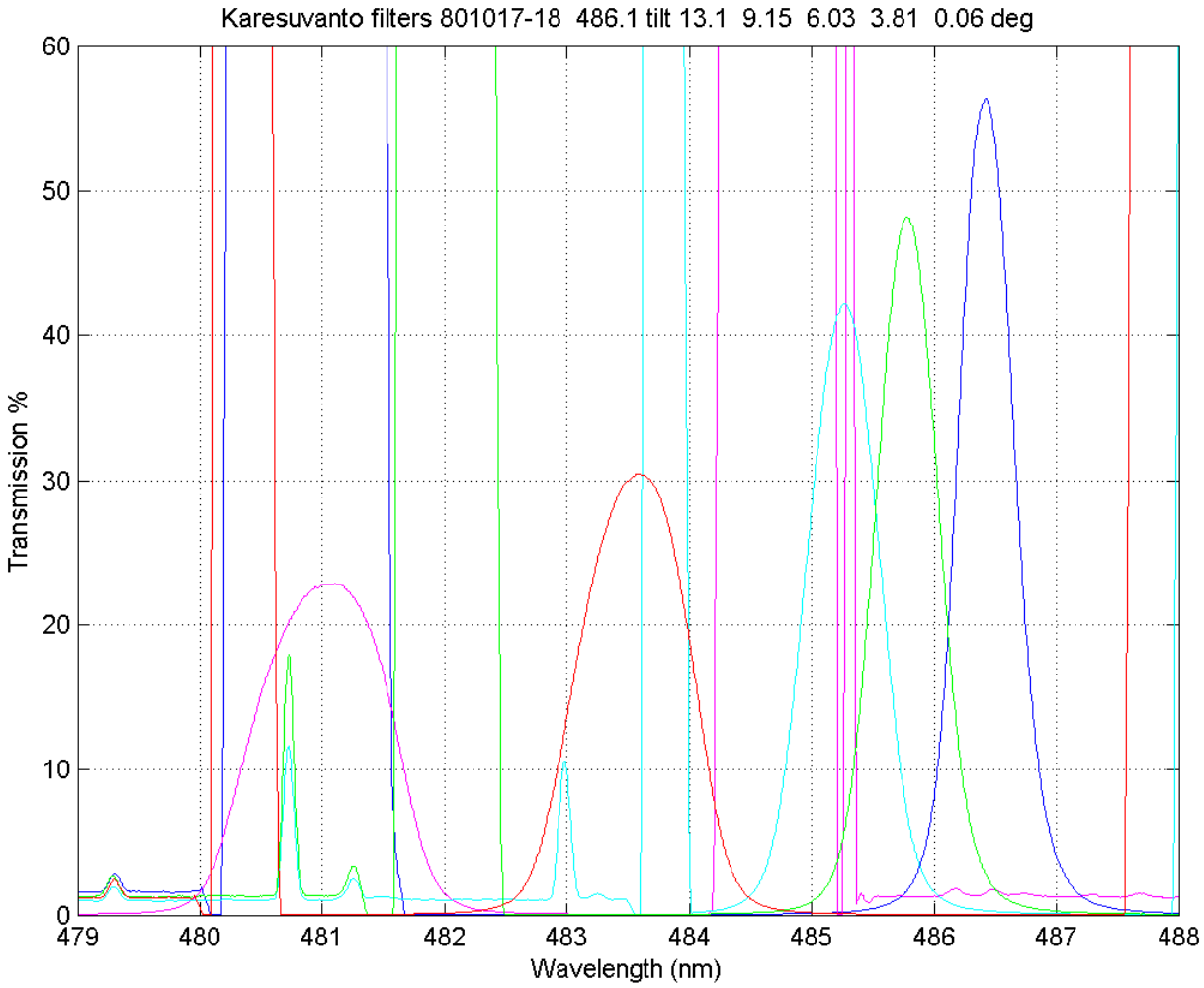

Gaussian transmission curve?

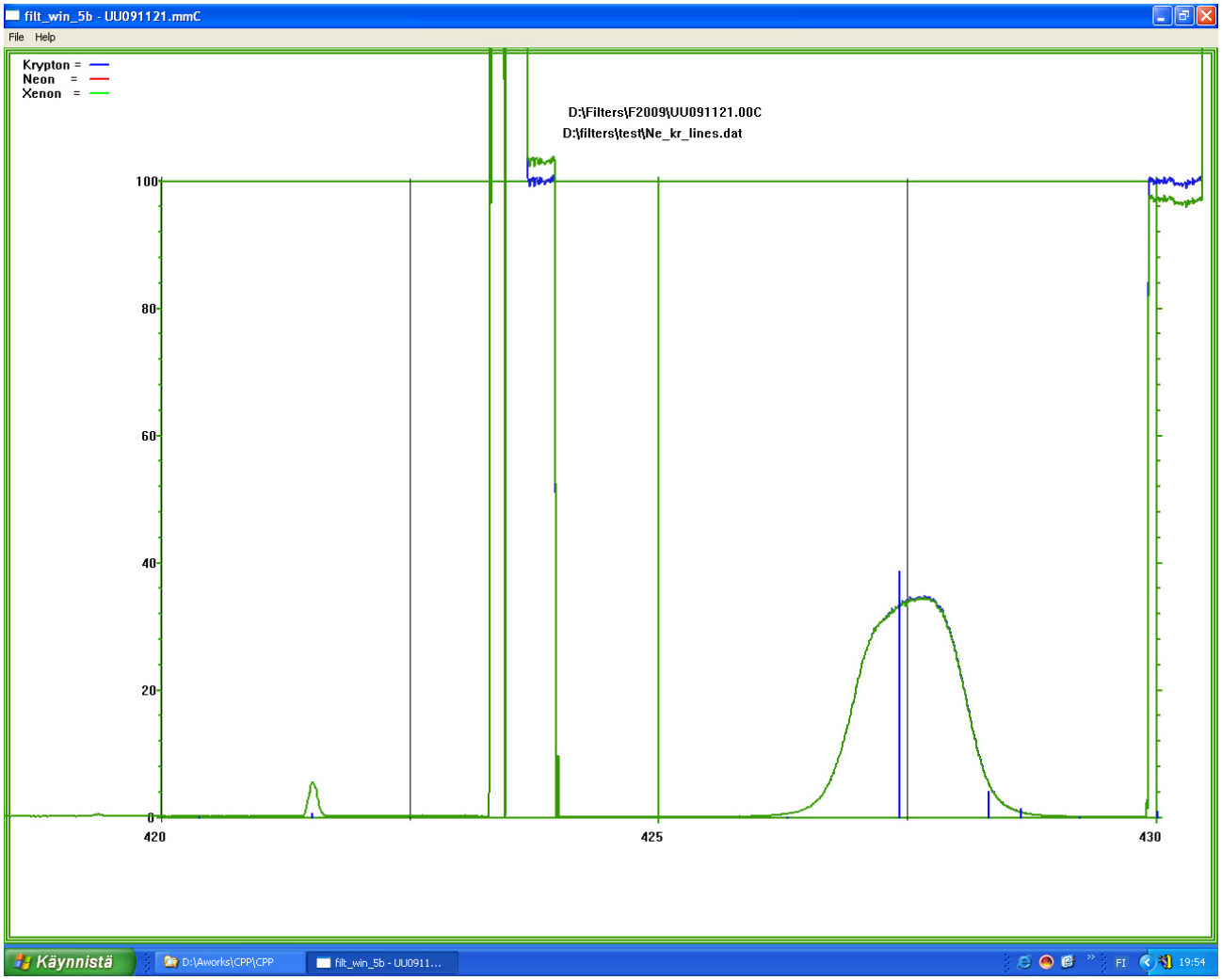

Filter aging effects

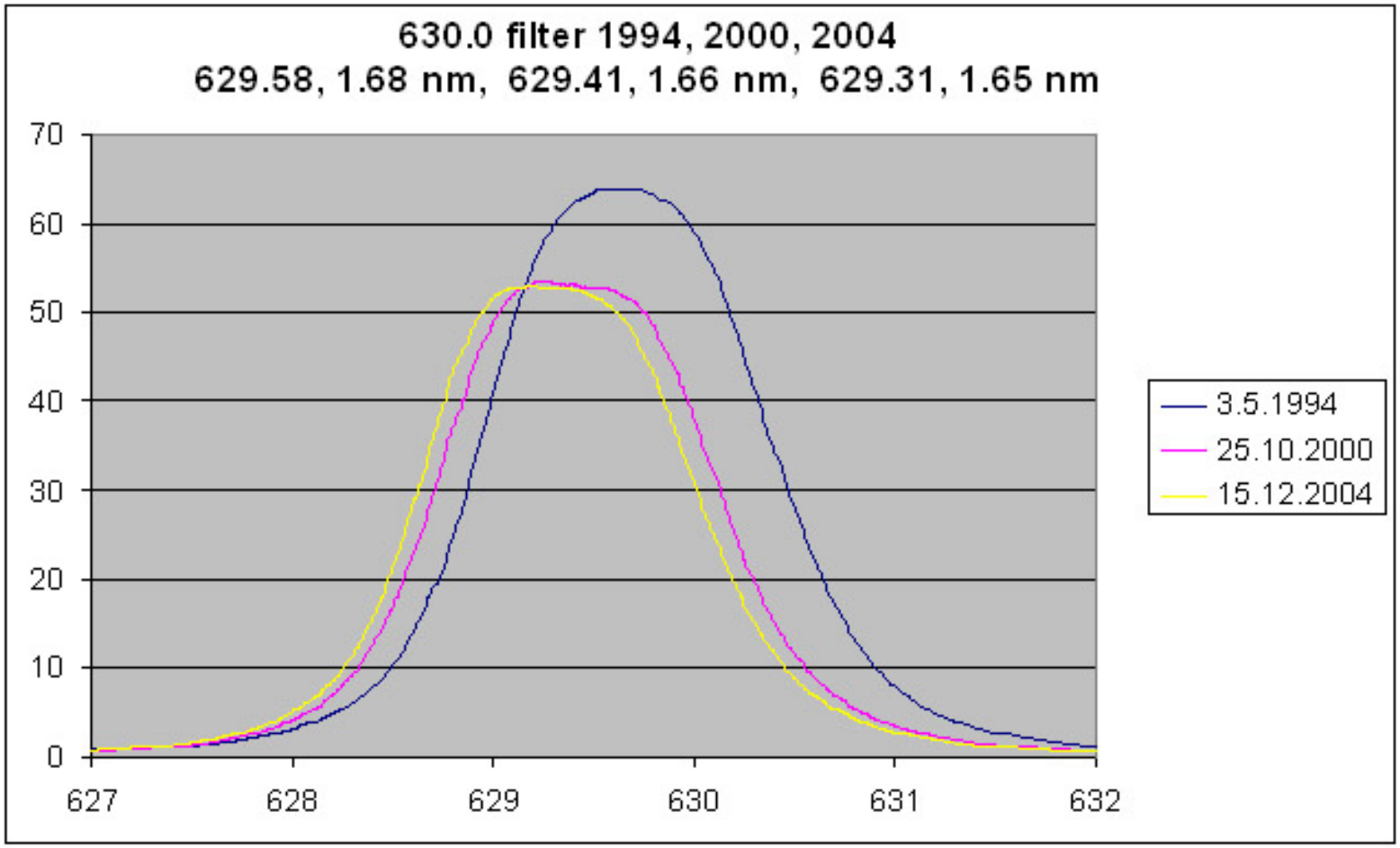

Temperature effect

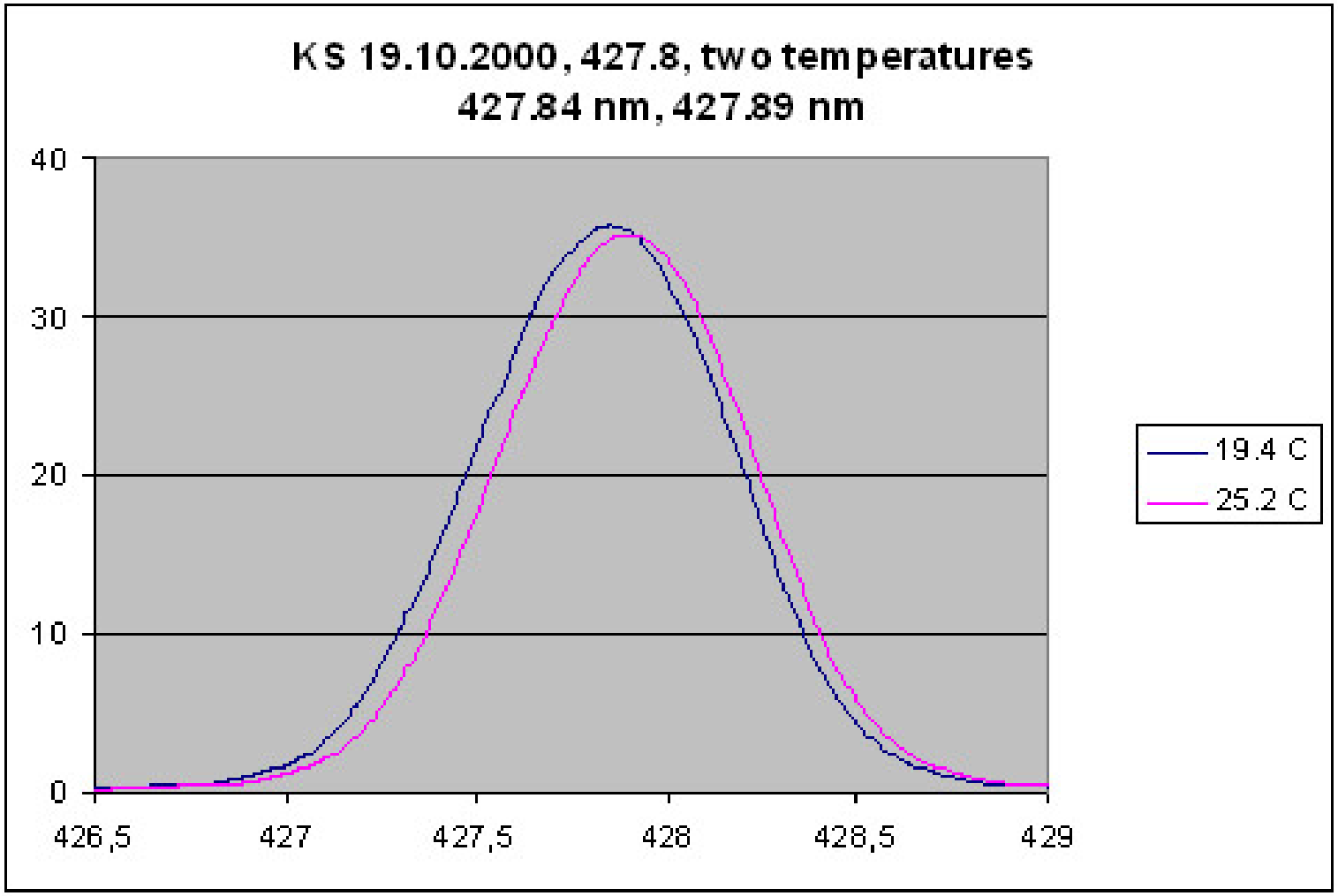

End

OPTICAL EMISSIONS

Optical transition probabilities

The atoms and molecules which enter the various excited states are eventually de-excited by emission of radiation or by loosing their energy of excitation in collisions. The probability of radiation is determined by the Einstein transition probability A_{nm}. In general this probability is given by the expression by Eyring et al. (1944)[1].

$$\begin{aligned} A_{nm} &= \frac{32\ \pi^3\ \overline{\nu}_{nm}^3}{3\hbar}\{| < m|\mathbf{M}_e|n > |^2 \\ &+ | < m| \sum_i^N \frac{e}{2mc}\mathbf{r}_i \times \mathbf{p}_i|n > |^2 \\ &+ \frac{3}{10}\ \pi^3\ \overline{\nu}_{nm}^2| < m| \sum_i^N e\ \mathbf{r}_i\mathbf{r}_i|n > |^2\} \end{aligned} \tag{1}$$

Where the summations are over all N electrons of the atom or molecule. The $\mathbf{M}_e = \sum_i^N e\mathbf{r}_i$ is the dipole moment of the electrons, $\mathbf{p}_i$ is the momentum operator of the ith electron.

The term $< m|\mathbf{M}_e|n >$ is called the electronic transition moment and is often denoted by $\mathbf{R}_e(n, m)$. Sometimes $|\mathbf{R}_e(n, m)|^2$ is denoted by S_{nm}, the line strength.

The first term in equation 1 represents the electronic dipole contribution to the transition probability and is normally dominant with a value of the order of 10^8 s^{-1}.

The second term represents magnetic dipole radiation and the third electric quadrupole radiation. These terms are of the order of 10^{-5} s^{-1} and 10^{-8} s^{-1} the value of the electric dipole term.

The two latter terms can become important if the electric dipole term is zero as a consequence of the symmetric properties of the wave functions.

[1]Eyring, H., Walter, J. and Kimball, G.E.: *Quantum chemistry*, Wiley, New York, 1944

Such a low probability transitions are examples of 'forbidden' transitions, but they are particularly important in the aurora.

States connected to the lower energy levels only by forbidden transitions are *metastable* and may have radiative lifetime of many seconds or even hours.

One important class of metastable states are the terms of O, O^+, N and N^+ belonging to the ground-state electron configuration. These are strictly forbidden by symmetry for electronic dipole radiation but can occur weakly through electric quadrupole or magnetic dipole radiation.

Another important class of 'forbidden' transition is forbidden to the approximation that electron spin and orbital angular momentum do not interact. In this approximation transition involving a change in spin quantum number do not occur. Since some interaction does occur, the electric dipole transition moment for such transitions can depart from zero.

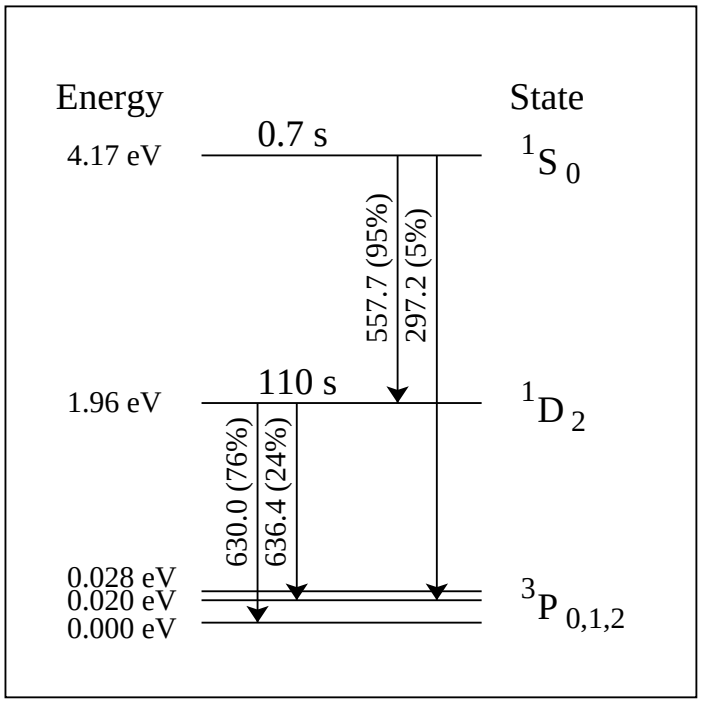

Figure 1: The lowest enery levels for O, O^+, N and N^+.

Emission intensities

The intensities of emission features in photon units is given by the relation

$$I_{nm} = N(n)\ A_{nm} \tag{2}$$

where $N(n)$ the population in the upper state depends on the balance between the various production and loss rates for the state.

When the upper and lower states are degenerate, i.e. consist of g_n and g_m states of equal or approximately equal energy, the individual transitions between these levels are taken together to give an effective A-value for electric dipole radiation of the form

$$A_{nm} = \frac{32\ \pi^3\ \overline{\nu}_{nm}^3}{3\hbar} S_{nm}/g_n \tag{3}$$

where

$$S_{nm} = \sum_{i,k} |R_e(n_i, m_k)|^2 \tag{4}$$

and the summation is over all the intercombinations between the sublevels. The g_n is the statistical weight of the upper level and S_{nm} is the line strength.

Electronic band system

The intensities of individual bands are determined by the equation

$$I(v', v'') = N(v')\ A(v', v'') \tag{5}$$

where $N(v')$ is the number of molecules in the v'th level of the upper state and $A(v', v'')$ is the Eistein transition probability for the transition from this level to the v''th level of the lower state.

The transition probabilities may be shown to be proportional to the $q(v', v'')$ according to the relation

$$A(v', v'') = constant\ \overline{\nu}^3(v', v'') R_e^2(v', v'') q(v', v'') \tag{6}$$

where

$$q(v', v'') = |\int \psi_v^*(v', S') \psi_v(v'', S'') dr|^2 \tag{7}$$

is the Franck-Condon factor for the transition from state S' to the state S'' and the ψ's are the corresponding wavefunctions. R_e is the electron transition moment

$$R_e(v', v'') = \frac{\int \psi_v(v')[\int \psi_e' M_e \psi_e'' d\tau_e]\psi_v(v'')dr}{\int \psi_v(v')\psi_v(v'')dr} \tag{8}$$

where ψ_e is the electronic wave function of all electrons within the molecule and ψ_v is the vibrational wave function.

The lifetime of a molecule in an excited state will be

$$\tau(v') = 1/\sum_{v''} A(v', v'') \tag{9}$$

Rotation and vibration spectra

The state of the molecule is described by a total wavefunction

$$\psi_{total} = \psi_e \ \psi_v \ \psi_r \tag{10}$$

where ψ_e is the electric wavefunction, ψ_v is the vibrational wavefunction and ψ_r is the rotational wavefunction. In principle the energy levels could be solved by Schrödinger wave equation.

Rotation spectrum

If we have a diatomic molecule where the masses of the atoms are m_1 and m_2 and the distances from the center of mass are r_1 and r_2, the inertial moment of the molecule is

$$I = m_1 r_1^2 + m_2 r_2^2 = \sum_i m_i r_i^2 \tag{11}$$

or simply

$$I = \mu r_o^2 \tag{12}$$

where μ is reduced mass and r_0 is the internuclear distance.

The obtained energy levels for molecular rotation are

$$E_j = \frac{h}{8\ \pi^2 I c} J(J+1) \qquad J = 0, 1, 2, ... \tag{13}$$

or in other way

$$E_j = BJ(J+1) \qquad J = 0, 1, 2, ... \tag{14}$$

where B is the rotational constant and J is the rotational quantum number.

For non-rigid rotator, where $r \neq$ constant the energy levels will be

$$E_J = BJ(J+1) + DJ^2(J+1)^2 + HJ^3(J+1)^3 + ... \quad cm^{-1} \tag{15}$$

where D is the centrifugal distortion constant.

The selection rules for rotational transition are $\Delta J = \pm 1$. The $-$sign produces P-branch and the + sign produces R-branch (the $\Delta J = 0$ produces Q-branch, but not in every molecule).

The spectral lines are transitions from one energy level to another energy level

$$E_{J+1} - E_J = 2B(J+1) - 4D(J+1)^3 \quad cm^{-1} \tag{16}$$

If $D = 0$ the distances of the spectral lines are equal (=$2B$). In reality that is not the case.

Vibrational spectrum

In a molecule the force between two atoms is of the type

$$F = -k(r_e - r) \tag{17}$$

where k is the force constant and r_e is the equilibrium distance of atoms.

In a diatomic molecule the atoms are vibrating with a frequency of

$$\overline{\omega} = \frac{1}{2\pi c}\sqrt{\frac{k}{\mu}} \quad cm^{-1} \tag{18}$$

Again the Schrödinger wave equation gives the energy levels, this time for the vibration

$$E_v = \left(v + \frac{1}{2}\right)\ \overline{\omega_e} - \left(v + \frac{1}{2}\right)^2\ \overline{\omega_e} x_e \tag{19}$$

where v= 0, 1, 2, ... is vibrational quantum number, $\overline{\omega}$ is the equilibrium frequency and x_e is anharmonic constant.

The selection rules for harmonic vibrational transitions are $\Delta v = \pm 1$ but generally $\Delta v = \pm 1, \pm 2, ...$

The transition between two vibrational energy levels is

$$\begin{aligned} 0 \longrightarrow 1: \quad & E_{\nu+1} - E_\nu = \overline{\omega_e}(1 - 2x_e) \quad cm^{-1} \\ 0 \longrightarrow 2: \quad & E_{\nu+2} - E_\nu = 2\overline{\omega_e}(1 - 3x_e) \quad cm^{-1} \end{aligned} \tag{20}$$

and generally

$$E_{\nu+\Delta v} - E_\nu = \Delta v \overline{\omega_e}\,[1 - (\Delta v + 2v + 1)x_e] \quad cm^{-1} \tag{21}$$

The difference of the wavenumbers in rotational lines is 1 - 10 cm^{-1} and the difference of the wavenumbers in vibrational lines is around 1000 cm^{-1}. In the first approximation the molecule is rotating and vibrating independently and

$$E_{tot} = E_{rot} + E_{vib} \tag{22}$$

end the energy levels will be obtained from the equation

$$\begin{aligned} E_J = \quad & BJ(J+1) + DJ^2(J+1)^2 + ... \\ & (v + \tfrac{1}{2})\ \overline{\omega_e} - (v + \tfrac{1}{2})^2\ \overline{\omega_e} x_e \quad cm^{-1} \end{aligned} \tag{23}$$

If the vibrational transition is $v = 0 \longrightarrow v = 1$ the rotational fine structure can be obtained from the differences of the energy levels according to the selection rules

$$\Delta E_{J,v} = E_{J',v=1} - E_{J",v=0} = \overline{\omega_0} + B(J' - J")(J' + J" + 1) \tag{24}$$

where $\overline{\omega_0} = \overline{\omega_e}(1 - 2x_e)$ is the band origin, ' is the upper state and " is the lower state. For P-branch $\Delta J = -1$ or $J' = J" + 1$ the spectral lines are in the positons of

$$\Delta E_{J,v} = \overline{\omega_0} - 2B(J" + 1) \quad cm^{-1} \tag{25}$$

and for R-branch $\Delta J = +1$ or $J" = J' + 1$ the spectral lines are in the positons of

$$\Delta E_{J,v} = \overline{\omega_0} + 2B(J" + 1) \quad cm^{-1} \tag{26}$$

The occupation number and the intensities

The energy of a rotational state J is $E_J = BJ(J+1)$ and the angular momentum is $\sqrt{J(J+1)}\frac{h}{2\pi}$. The angular momentum is a vector, which can have different degenerated states: $J, J-1, ..., 0, ..., -J+1, -J$. It means that the degeneration of the state is $2J+1$. The occupation number for the different states is according to the Boltzmann distribution

$$\frac{N_i}{N_j} = e^{-\frac{(E_i - E_j)}{kT}} \tag{27}$$

The occupation number N_J of rotational state J will be

$$N_J = (2J+1)N_0 e^{-\frac{(J(J+1)h^2)}{8\pi^2 IkT}} \tag{28}$$

The maximum occupation quantum number can be obtained from equation 28. by deriving the equation and putting

$$\frac{dN_J}{dJ} = 0 \tag{29}$$

Exercise: Show that the maximum occupation number is

$$J = \sqrt{\frac{kT}{2hcB}} - \frac{1}{2} \tag{30}$$

The intensity of the spectral line I is directly proportional to the occupation number of the upper level $I \propto N_J$. By using the previous equations the intensities and the positions of the rotational lines can be calculated.

The vibrational occupation numbers can also be calculated. Thus the ratio of the occupation numbers of the first and second vibrational levels is

$$\frac{N_{v=1}}{N_{v=0}} = e^{-\frac{(E_1 - E_0)}{kT}} \tag{31}$$

At room temperature the occupation number in vibrational state $v = 0$ is oler 99% and in the state $v = 1$ only about 0.5%. But this is not valid in the auroral spectrum.

Electronic transition for diatomic molecules

The energy differences in the electronic transitions are much bigger than the energy differences in the vibrational transitions. According to Born-Oppenheimer approximation

$$E_{tot} = E_{el} + E_{vib} + E_{rot} \tag{32}$$

and also

$$\Delta E_{tot} = \Delta E_{el} + \Delta E_{vib} + \Delta E_{rot} \tag{33}$$

In the electronic transition also the wave numbers are

$$\nu = \nu_{el} + \nu_{vib} + \nu_{rot} \tag{34}$$

where the first term is for electronic transition and is constant. The two other terms are the same than in the vibrational and rotational spectrum. The main difference is that the two electronic states have different $\overline{\omega_e}$ and $\overline{\omega_e} x_e$ values for vibration and different B_e and α_e values for rotation.

According to that it appears a band head to the spectrum. If $B_{\nu'} < B_{\nu"}$ the band head appears in the R-branch and if $B_{\nu'} > B_{\nu"}$ the band head appears in the P-branch.

In the electronic transitions the selection rules are similar than in atomic case:

$$\begin{aligned} \Delta\Lambda = &\quad 0, \pm 1 \\ \Delta S = &\quad 0 \\ symmetry: &\quad \Sigma^+ \leftrightarrow \Sigma^+ \; and \; \Sigma^- \leftrightarrow \Sigma^- \\ parity: &\quad g \leftrightarrow u \end{aligned} \tag{35}$$

The rotational structure of nitrogen N_2^+ ions

In electron precipitation the energetic electrons undergo collisions with ground state nitrogen molecule $N_2(X^2\Sigma_g^+)$. If the molecule ionize then

$$N_2(X^2\Sigma_g^+) + e \longrightarrow N_2^+(B^2\Sigma_u^+) + e + e_s \tag{36}$$

The original rotational occupation distribution of the ground state remains in the excited ion state. The B-state has very short life time, 70 ns, and it

Parameter	X $^2\sum_g^+$	B $^2\sum_g^+$	
T_e	0	25461.5	cm^{-1}
ω_e	2207.19	2419.87	cm^{-1}
$\omega_e x_e$	16.136	23.19	cm^{-1}
$\omega_e y_e$	-0.0400	-0.5375	cm^{-1}
B_e	1.932	2.083	cm^{-1}
α	0.020	0.0195	cm^{-1}
r_e	1.116	1.075	$\times 10^{-10}$ m

Table 1: The constants in the transition of $B^2\sum_u^+ - X^2\sum_g^+$. The $\nu_{00} = 25566.0$ cm^{-1}

will undergo a spontaneous emission before collisions with other atmospheric constituents.

$$N_2^+(B^2\Sigma_u^+) \longrightarrow N_2^+(X^2\Sigma_g^+) + h\nu \ (1 \ NG) \tag{37}$$

The emissions of the 1 NG are in the blue and violet region (Table 2). The different rotational and vibrational constants for the two different levels $X^2\sum_g^+$ and $B^2\sum_u^+$ are shown in the Table 1.

Because N_2 and N_2^+ are homonuclear molecules, which have $\Lambda = 0$, the odd and even rotational lines have different statistical weight. The ratio of the statistical weights is

$$\frac{\text{strong}}{\text{weak}} = \frac{I+1}{I} \tag{38}$$

where I is nuclear spin quantum number.

Transition	Band head [nm]	Relative intensity
0 - 0	391.44	98.51
0 - 1	427.81	30.00
0 - 2	470.92	6.04
0 - 3	522.83	0.99
0 - 4	586.47	0.14
1 - 0	358.21	6.80
1 - 1	388.43	3.93
1 - 2	423.65	3.87
1 - 3	465.18	1.34
2 - 0	330.80	0.02
2 - 1	356.39	0.15
2 - 2	385.79	0.01

Table 2: The band heads of the $N_2(X^2\Sigma_g^+)$ 1 NG bands.

The intensity of rotational lines on $N_2^+1\ NG$ bands

The intensity of the rotational lines can be obtained from the equation

$$I_{em} = \frac{C_{em}\nu^4}{Q_r}(J' + J" + 1)e^{-\frac{B'J'(J'+1)hc}{kT}} \tag{39}$$

where C_{em} is a constant for each band and Q_r is rotational state sum or partition function.

$$Q_r = \sum_{J'}^{\infty}(2J' + 1)e^{-\frac{B'J'(J'+1)hc}{kT}} \tag{40}$$

By taking the logaritm of the intensity equation 39 and by plotting the $ln(I_m/(J' + J" + 1))$ as a function of $J'(J' + 1)$ will be obtained a straight line. Its slope is $-B'hc/kT$.

We know the rotational constant B' and all the other constants and we can determine the temperature T. This temperature is called rotational temperature. It is close to the neutral temperature but not exactly the same. Rotational temperature can be measured by photometers with narrow bandwidth filters as well as with the spectrometers which have high enough spectral resolution.

Some spectroscopy

Kari Kaila
University of Oulu, Department of Physics
18.11.2011

Vibrating ideal diatomic molecyle

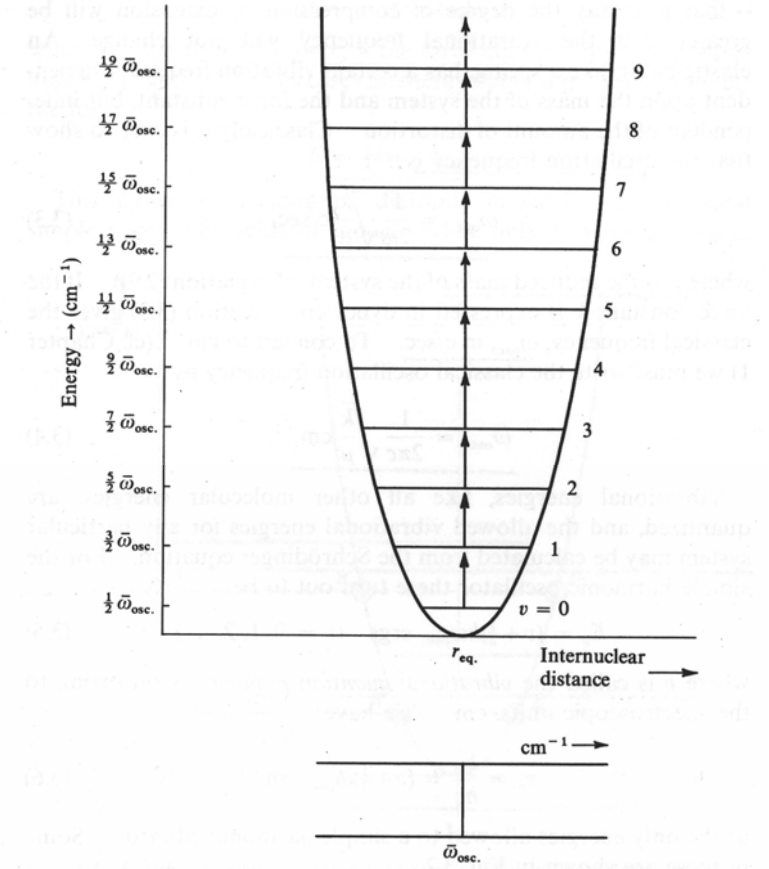

Fig. 3.2: The allowed vibrational energy levels and transitions between them for a diatomic molecule undergoing simple harmonic motion.

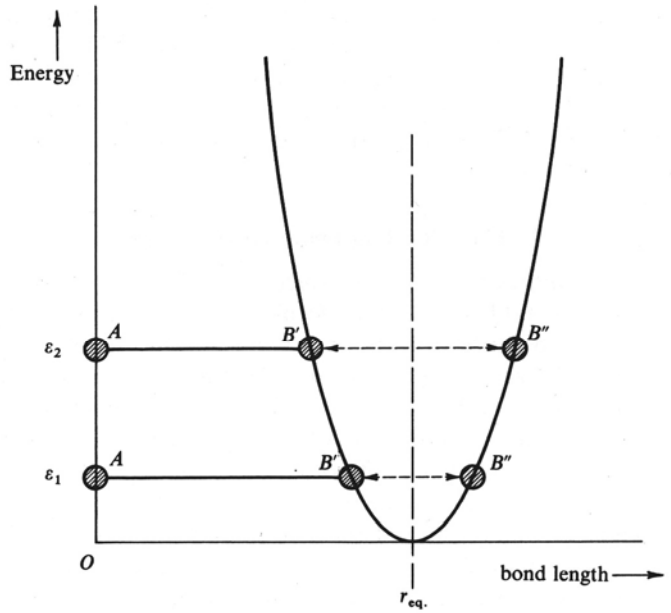

Fig. 3.1: Parabolic curve of energy plotted against the extension or compression of a spring obeying Hooke's law.

More real potential energy curve

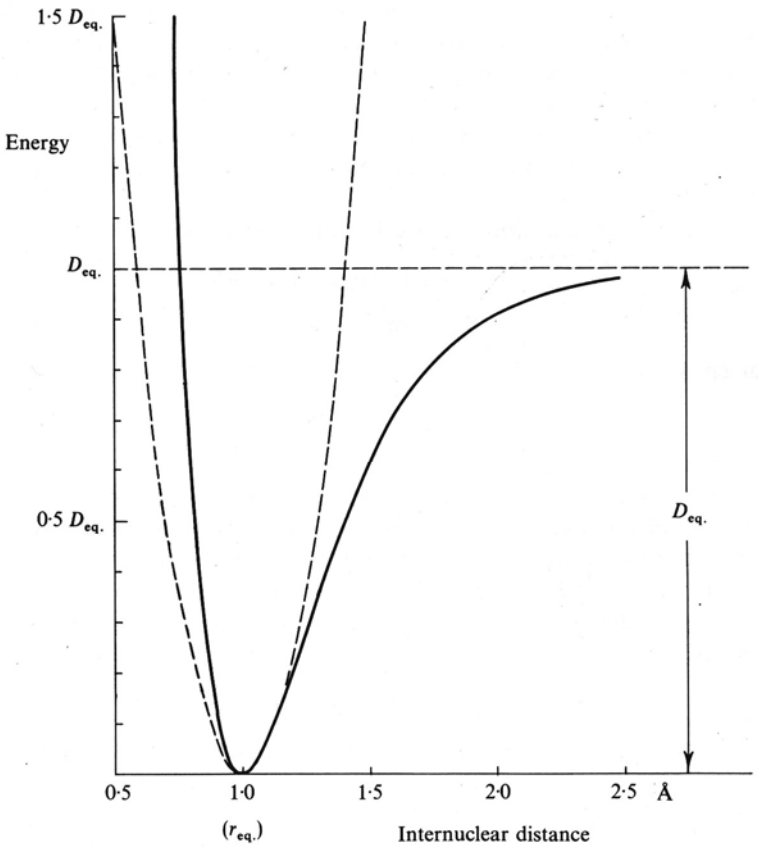

Fig. 3.3: The Morse curve: the energy of a diatomic molecule undergoing anharmonic extensions and compressions.

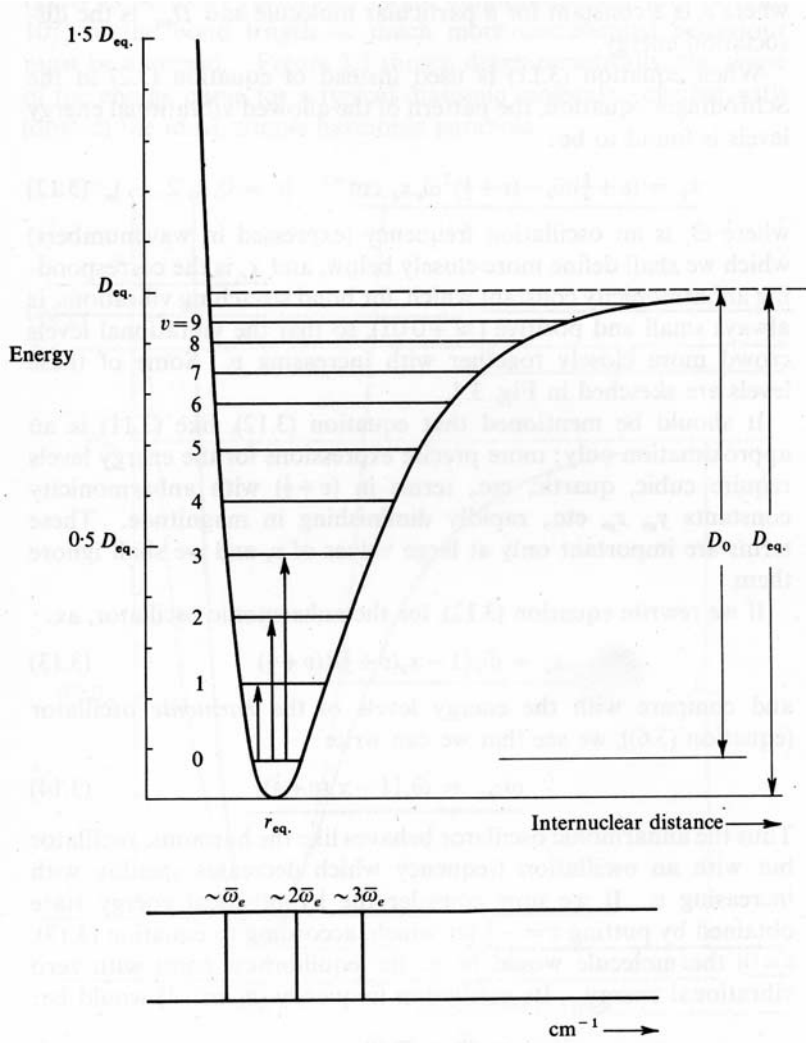

Fig. 3.4: The allowed vibrational energy levels and some transitions between them for a diatomic molecule undergoing anharmonic oscillations.

Rotational energy levels

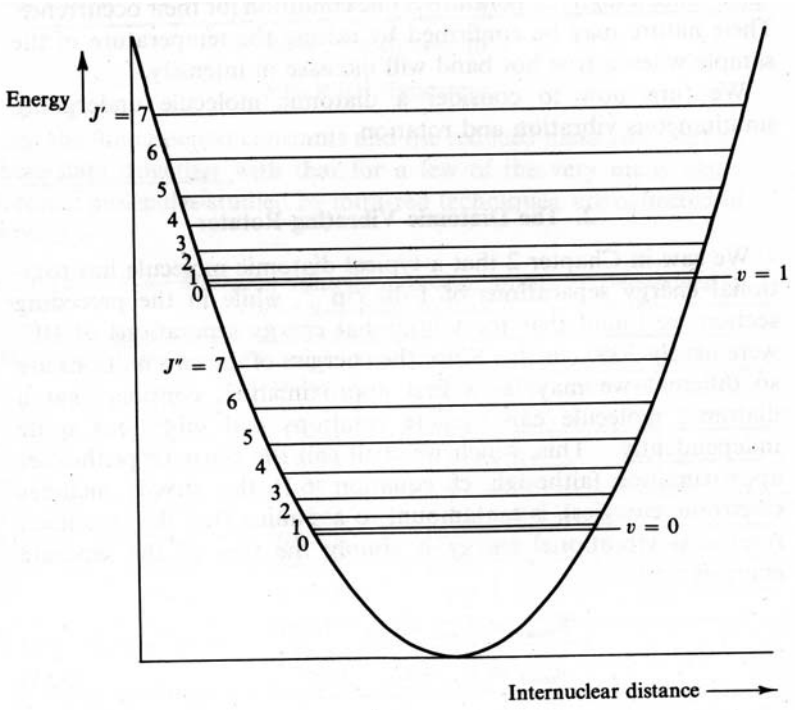

Fig. 3.5: The rotational energy levels for two different vibrational states of a diatomic molecule.

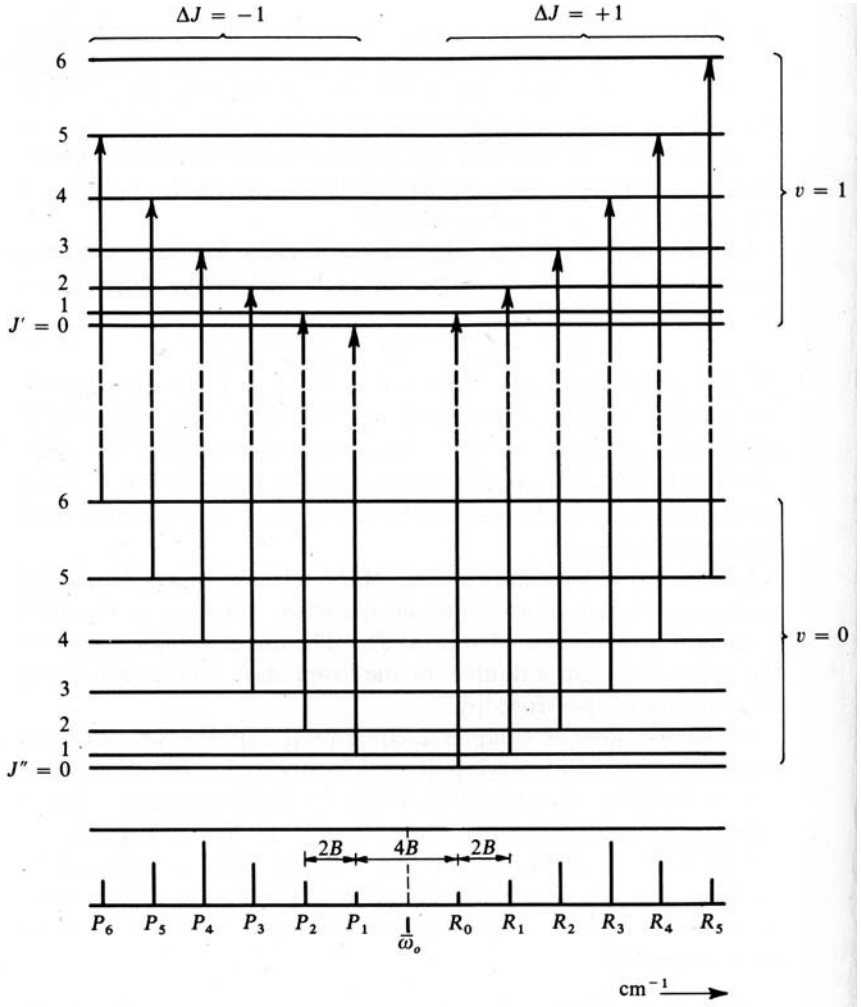

Fig. 3.6: Some transitions between the rotational–vibrational energy levels of a diatomic molecule together with the spectrum arising from them.

Rotation spectrum of CO

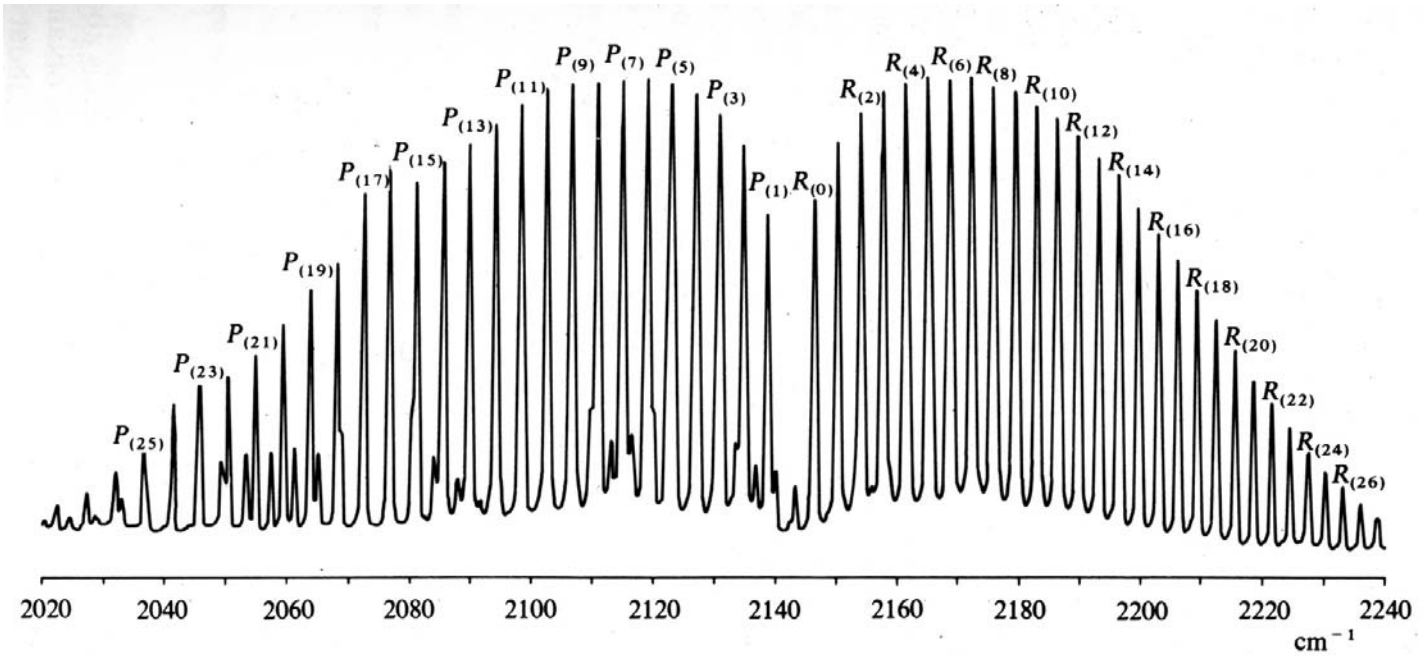

Fig. 3.7(b): *The centre of the fundamental band of carbon monoxide under higher resolution than in* (a). (*Gas pressure 100 mm* Hg *in a 10 cm cell.*) *The lines are labelled according to their J″ values. The P branch is complicated by the presence of a band centred at about 2100* cm^{-1} *due to the 1% of* ^{13}CO *in the sample; some of the rotational lines from this band appear between P branch lines, others are overlapped by a P branch line and give it an enhanced intensity* (*e.g. lines* $P_{(16)}$, $P_{(17)}$, $P_{(23)}$ *and* $P_{(24)}$).

Ψ^2 and transitions

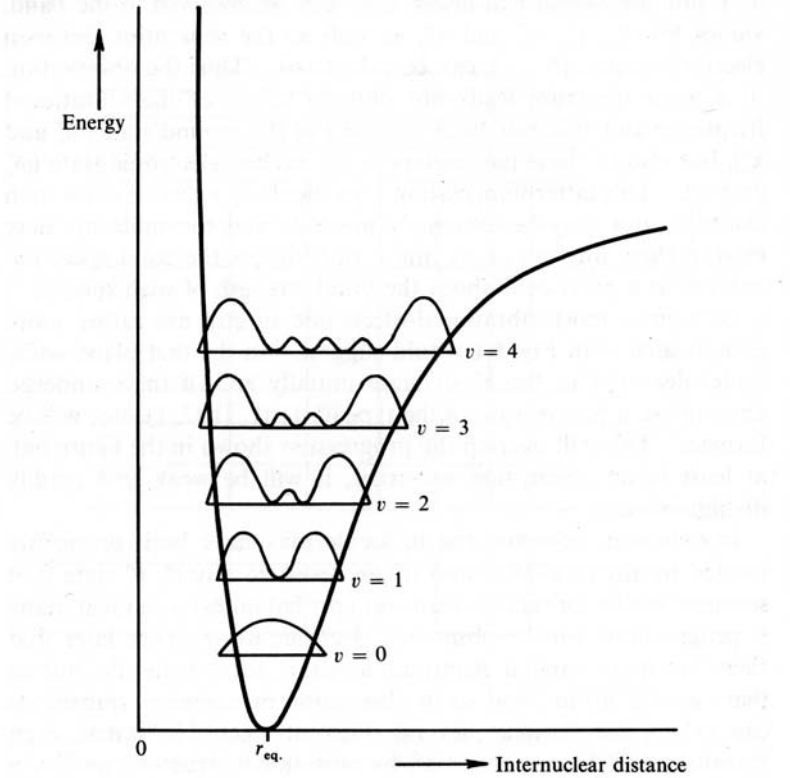

Fig. 6.2: The probability distribution for a diatomic molecule according to the quantum theory. The nuclei are most likely to be found at distances apart given by the maxima of the curve for each vibrational state.

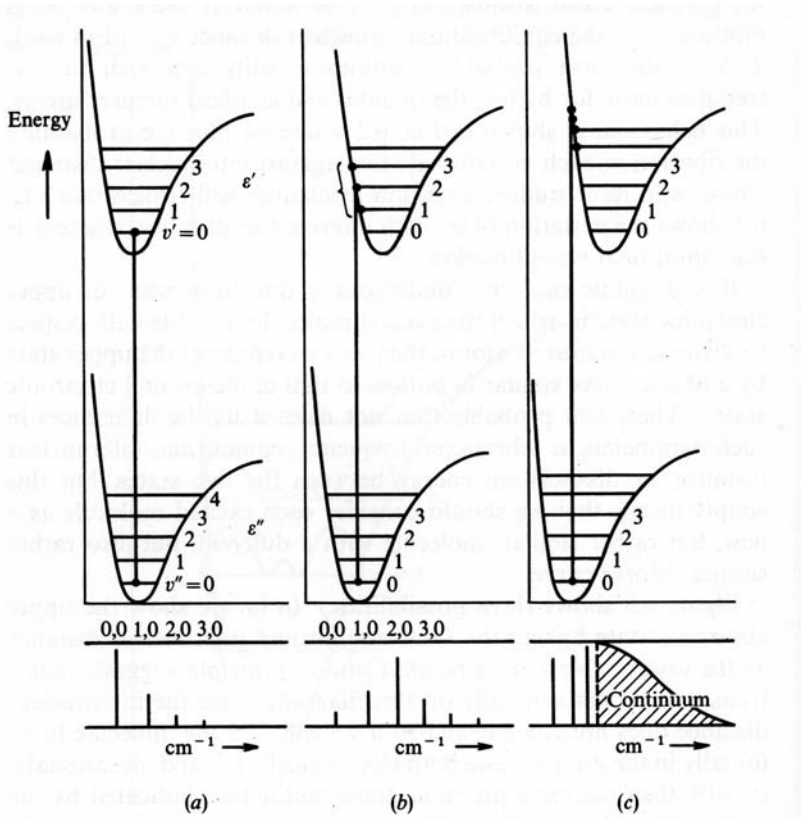

Fig. 6.3: The operation of the Franck–Condon principle for (a) *internuclear distances equal in upper and lower states,* (b) *upper state internuclear distance a little greater than that in the lower state, and* (c) *upper state distance considerably greater.*

Rotation lines in electric transition

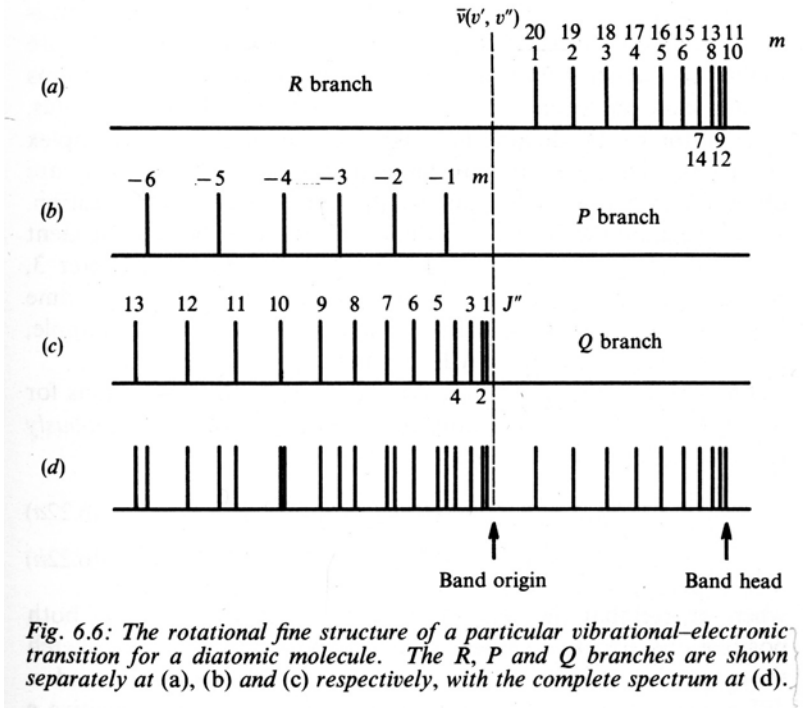

Fig. 6.6: The rotational fine structure of a particular vibrational–electronic transition for a diatomic molecule. The R, P and Q branches are shown separately at (a), (b) *and* (c) *respectively, with the complete spectrum at* (d).

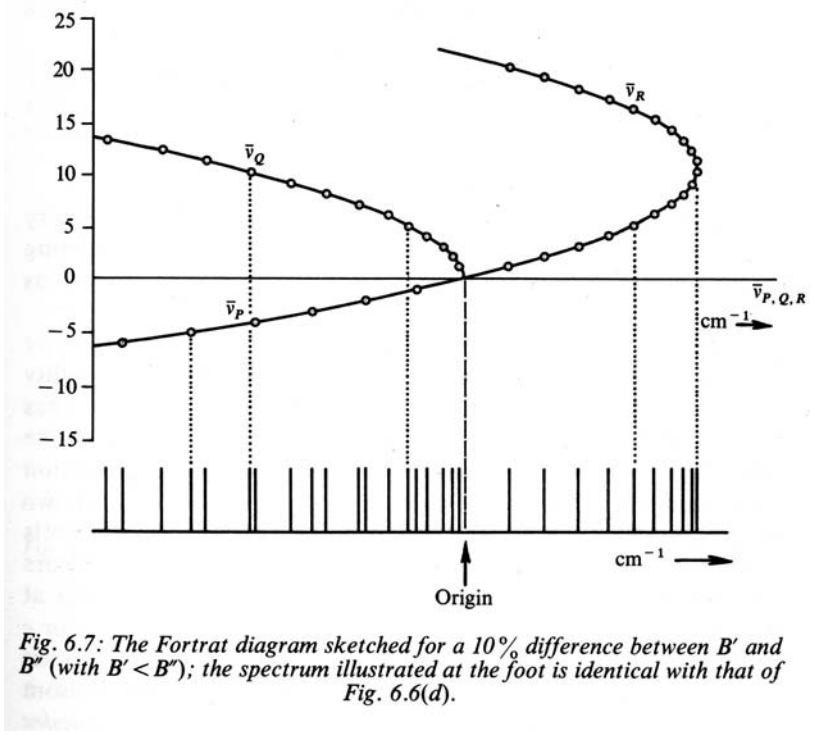

Fig. 6.7: The Fortrat diagram sketched for a 10% difference between B′ and B″ (with B′ < B″); the spectrum illustrated at the foot is identical with that of Fig. 6.6(d).

In the upper atmosphere

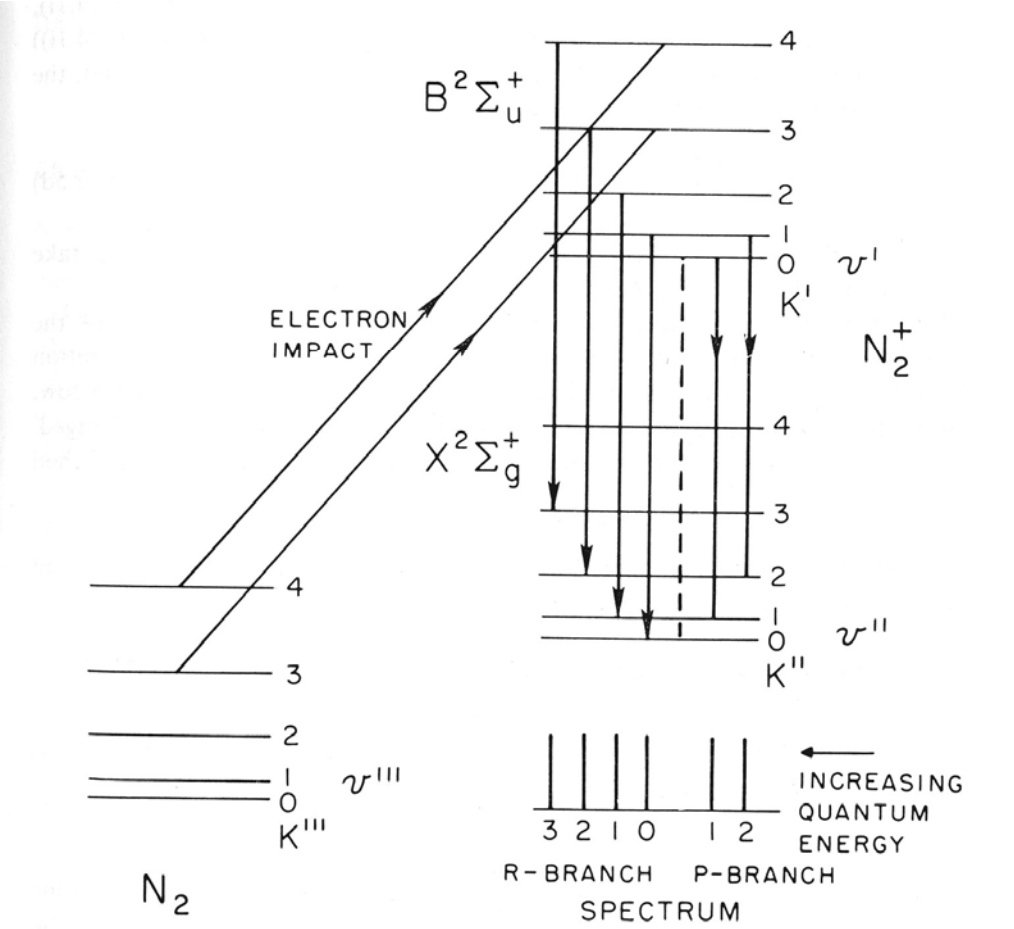

Fig. 4.35. Simplified energy level diagram illustrating typical excitation relations for an N_2^+ 1N rotation-vibration band v''', v' and v'' indicate respectively typical vibrational levels of the ground state of N_2 and the B and X states of N_2^+.

Simulated N_2^+ 0-1 transition

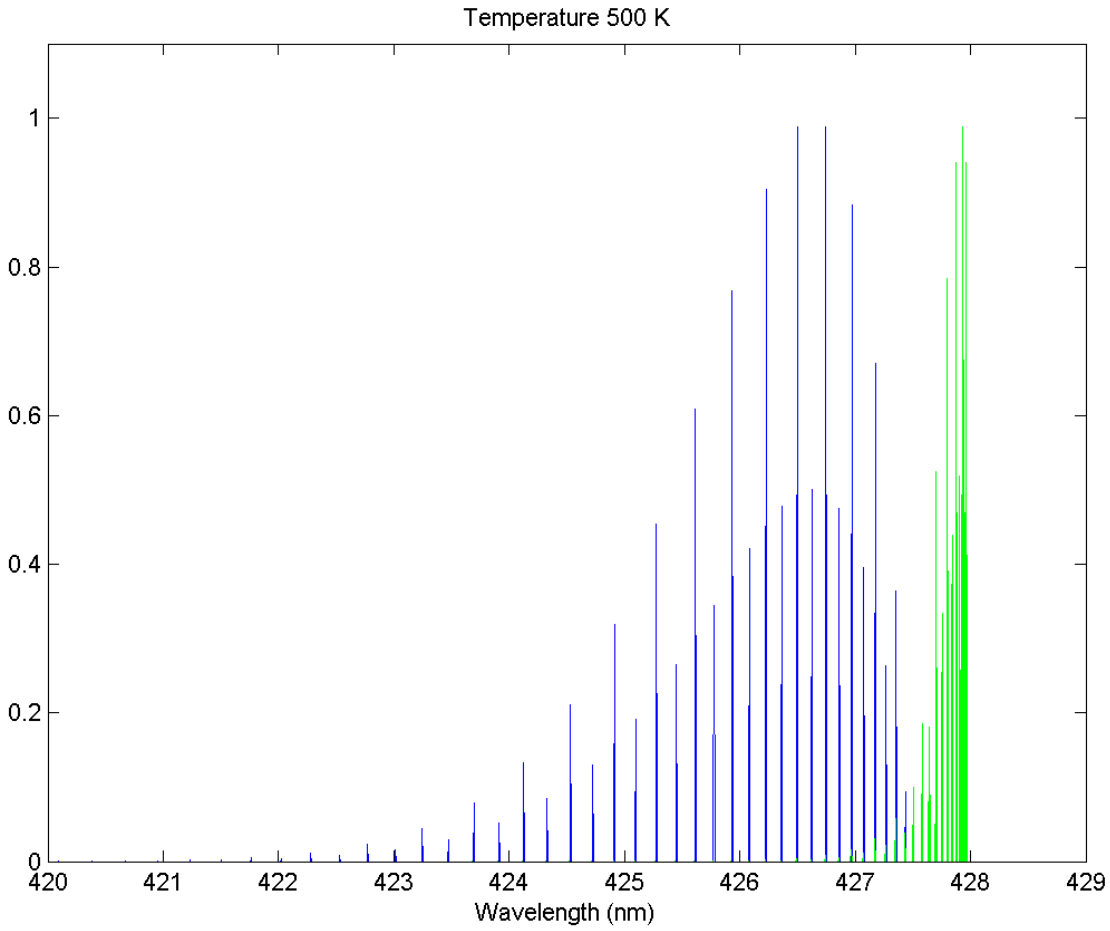

2 NEUTRAL ATMOSPHERE

2.1 ATMOSPHERIC MODELS

Earth atmosphere is densest at the Earth surface.

The density decreases when going upward. The pressure also decreases with a function of altitude. The temperature changes in different way.

The number density of the most important species, the neutral temperature T_n and pressure of the Earth atmosphere have been modelled since 1958. In the next table there are different models about in chronological order.

Model
U.S. Standard Atmosphere
Jacchia Reference Atmosphere
Atmospheric Handbook
CIRA-XX
MSIS-XX

We will look briefly each of these models.

U.S. Standard Atmosphere

The work of the U.S. Committee on Extension to the Standard Atmosphere (COESSA) led to the first U.S. Standard Atmosphere model in the year 1958. It was published with National Oceanic and Atmospheric Administration (NOAA), the National Aeronautics and Space Administration (NASA) ans U.S. Air Force.

Revised versions were published in 1962, 1966 and 1976.

The model was based on rocket and satellite data and perfect (ideal) gas law. It gave atmospheric densities and temperatures from sea level to 1000 km. Below 32 km it is identical with the Standard Atmosphere of the International Civil Aviation Organization (ICAO).

These standard atmospheres consist of single profiles representing the idealized, steady-state atmosphere for moderate Solar activity.

Output parameters: temperature, pressure, density, acceleration caused by gravity, ... for five northern latitudes (15, 30, 45, 60, 75) for summer and winter conditions.

Jacchia Reference Atmosphere

Jacchia Reference Atmospheres were publishes as reports in 1970, 1971 and 1977.

These includes explanatory text, formulas and tables, where density, temperature and composition are listed in the altitude range 90 km to 2500 km.

Variations with season, latitude and local time are considered.

Jacchia's models are based mostly on satellite drag data.

Assuming diffuse equilibrium, the atmospheric profiles are defined by the exospheric temperature.

Jacchia contributed the thermospheric part (110 - 200 km) to the CIRA-72 model.

Atmospheric Handbook The data set was compiled by V.E. Derr in 1984 and it presents atmospheric parameters for scattering, radiation and emission calculations.

This is available in hard copy or on magetic tape.

CIRA-XX

The COSPAR International Reference Atmosphere is shortly called CIRA-XX atmosphere. CIRA-XX is probably the most widely used and well established model of Commitee on Space Research (COSPAR).

Versions CIRA-61, CIRA-72, CIRA-86.

Below 50 km the atmosphere can be assumed to be homogenously mixed and can be treated as a perfest gas.

Above 80 km the hydrostatic equilibrium gradually braks down as diffusion and vertical transport become important.

The temperature varies from ground up to **exosphere** at 400 km, where the temperature is constant.

MSIS-XX

This Mass Spectrometer and Incoherent Scatter (MSIS) model is mainly developed by A.E. Hedin and co-workers. They have combined the data from the rocket borne mass spectrometer data and incoherent scatter radar data obtained by different research groups.

Versions MSIS-77, MSIS-83, MSIS-86.

The exension model MSISE-90 was developed around 1990.

Below 72.5 km the model is primarily on the MAP Handbook tabulation of zonal average temperature and pressure by Barnett and Corney, which was also used for CIRA-86. Above 72.5 km MSISE-90 is essentially a revised MSIS-86 model taking into account data derived from space shuttle flights and newer incoherent scatter results.

If the atmosphere above 120 km is interested, the model MSIS-86 is recommended.

All the major species are included: N_2, O, O_2, H, He, also T and T_{exo}.

This program can be run in the web page:
http://ccmc.gsfc.nasa.gov/modelweb/models/msis_vitmo.php

Reference: A.E.Hedin, Extension of the MSIS Thermospheric Model into Middle and Lower Atmosphere, J. Geophys. Res. **96**, 1159, 1991.

NRLMSISE-00

The revised MSIS model is called Naval Research Laboratory MSIS E model and is from 2000. This is the most recent atmospheric model, which gives the major and many minor species of atmosphere as a function of altitude, date, time, location, solar flux and magnetic index.

Basically all the atmospheric models are available in Fortran or C language.

Exercises:

Exercise 2.1: Go to this web page. Look and run some models and look the results it gives to you.

Exercise 2.2: Find the paper by Hedin and look it is one of the earlier MSIS versions. Look how the values have been determined and which parameters can be obtained from the model.

NSSDC
MSIS-E-90 Model
You submitted the following name/value pairs:
DATE: year=2000 month=01 day=15 TIME: hour=10.UT
Geographical latitude = 65. Geographical longitude = 335. height = 0 start height = 0 stop height = 190 step = 10

Results of MODEL calculations:
NUMBER DENSITIES, MASS DENSITY, TEMPERATURE

Taulukko 1: Table 1: Results from MSISE-90 atmospheric model

Height	O	N_2	O_2	mass density	T_n	T_{Exo}
km	$1/cm^3$	$1/cm^3$	$1/cm^3$	g/cm^3	K	K
0.0	0.000E+00	2.149E+19	5.764E+18	1.322E-03	263.6	1037
10.0	0.000E+00	6.248E+18	1.676E+18	3.844E-04	215.8	1037
20.0	0.000E+00	1.317E+18	3.533E+17	8.103E-05	203.1	1037
30.0	0.000E+00	2.408E+17	6.459E+16	1.481E-05	205.3	1037
40.0	0.000E+00	4.492E+16	1.205E+16	2.764E-06	238.2	1037
50.0	0.000E+00	1.076E+16	2.886E+15	6.619E-07	258.0	1037
60.0	0.000E+00	2.999E+15	8.044E+14	1.845E-07	248.8	1037
70.0	0.000E+00	7.994E+14	2.141E+14	4.916E-08	227.9	1037
80.0	3.287E+09	1.900E+14	5.066E+13	1.167E-08	210.4	1037
90.0	1.755E+11	3.920E+13	1.026E+13	2.401E-09	193.8	1037
100.0	3.578E+11	6.908E+12	1.685E+12	4.246E-10	202.9	1037
105.0	2.911E+11	2.927E+12	6.637E+11	1.807E-10	218.6	1037
110.0	2.048E+11	1.277E+12	2.620E+11	7.933E-11	246.7	1037
115.0	1.339E+11	5.816E+11	1.064E+11	3.647E-11	295.8	1037
120.0	8.688E+10	2.870E+11	4.703E+10	1.824E-11	366.5	1037
125.0	6.020E+10	1.613E+11	2.409E+10	1.042E-11	437.2	1000
130.0	4.444E+10	1.005E+11	1.395E+10	6.617E-12	498.1	1000
135.0	3.415E+10	6.688E+10	8.756E+09	4.495E-12	552.4	1000
140.0	2.707E+10	4.666E+10	5.827E+09	3.206E-12	600.8	1000
145.0	2.197E+10	3.374E+10	4.047E+09	2.373E-12	643.9	1000
150.0	1.818E+10	2.507E+10	2.902E+09	1.807E-12	682.2	1000
155.0	1.528E+10	1.905E+10	2.134E+09	1.408E-12	716.4	1000
160.0	1.301E+10	1.473E+10	1.600E+09	1.117E-12	746.9	1000
165.0	1.120E+10	1.153E+10	1.219E+09	9.002E-13	774.0	1000
170.0	9.724E+09	9.160E+09	9.405E+08	7.355E-13	798.3	1000
175.0	8.506E+09	7.348E+09	7.339E+08	6.077E-13	819.8	1000
180.0	7.487E+09	5.945E+09	5.780E+08	5.070E-13	839.1	1000
185.0	6.626E+09	4.845E+09	4.589E+08	4.265E-13	856.3	1000
190.0	5.890E+09	3.973E+09	3.667E+08	3.615E-13	871.6	1000

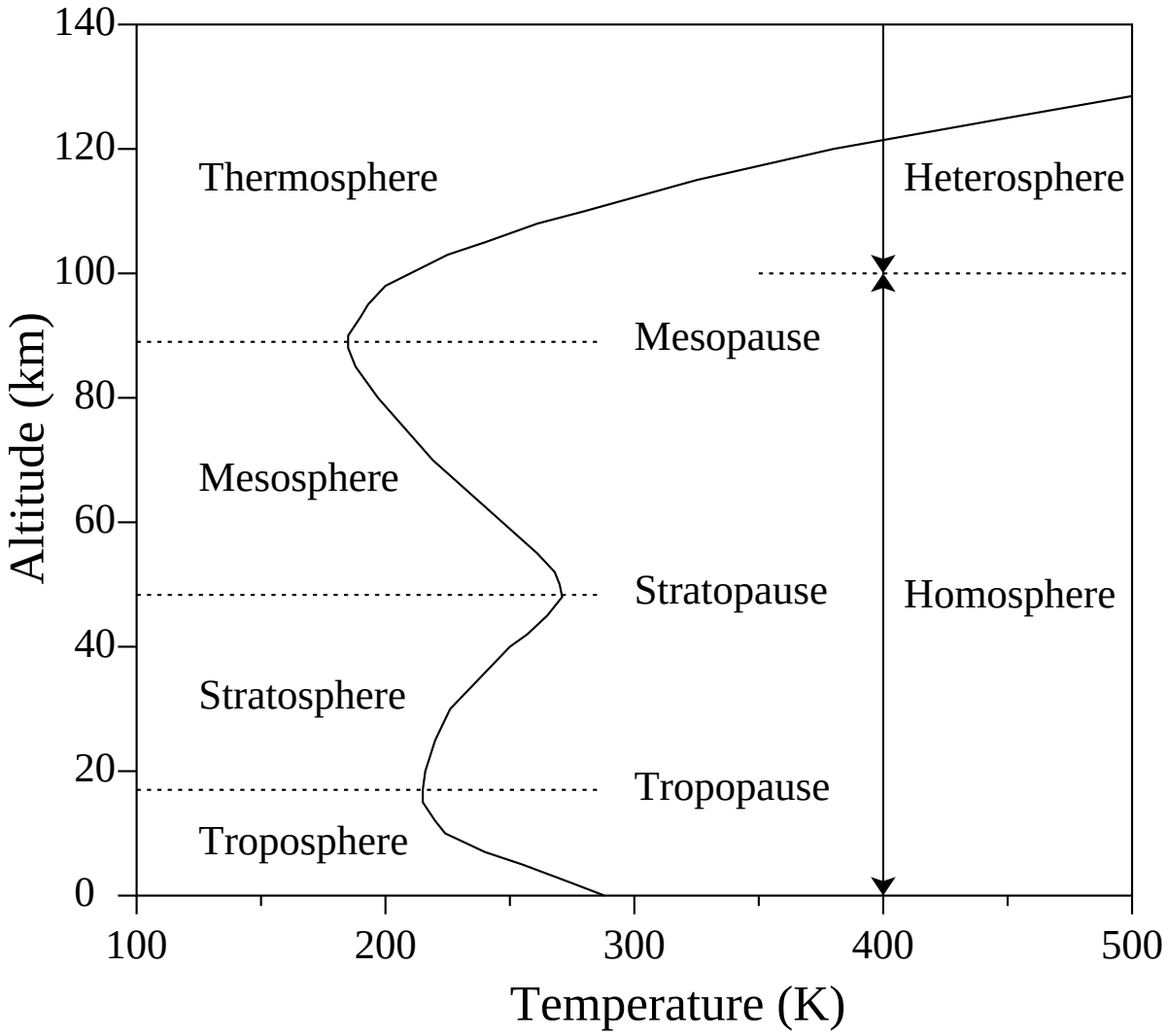

Kuva 1: The temperature of the atmosphere 0 - 140 km and the names of the layers.

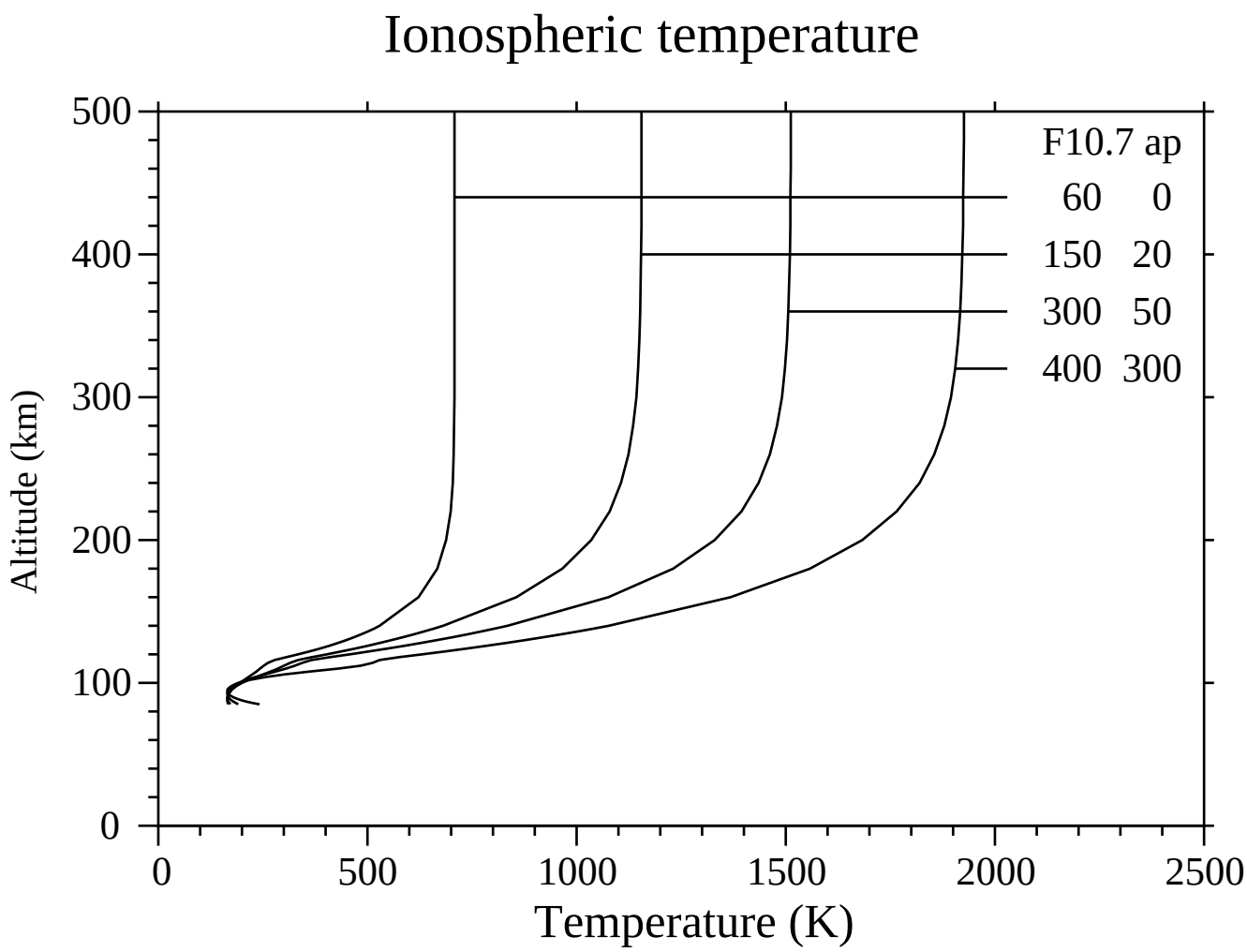

Kuva 2: The temperatures of upper atmosphere at different 10.7 cm Solar flux and magnetic ap-index pairs.

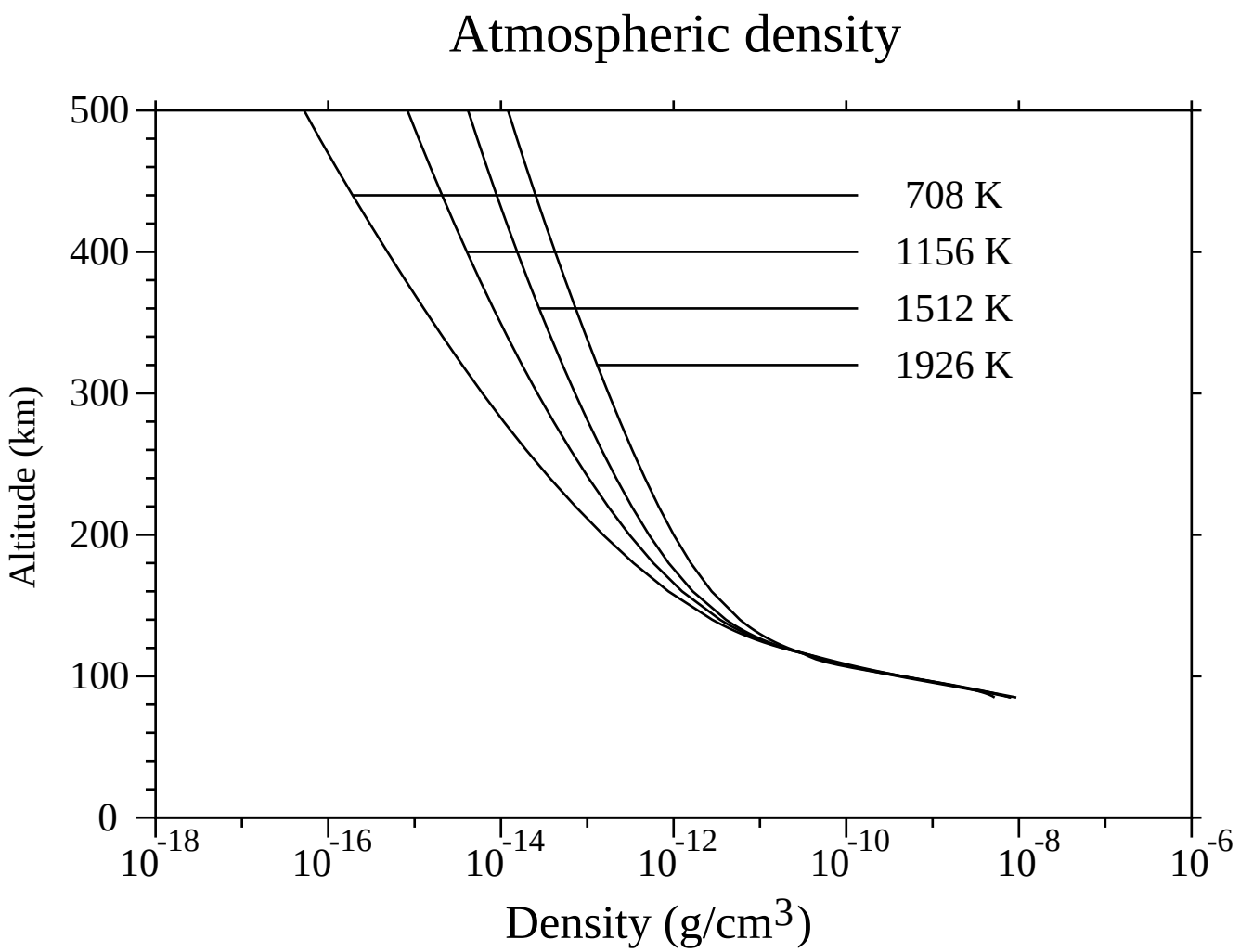

Kuva 3: The density of upper atmosphere at different exospheric temperatures.

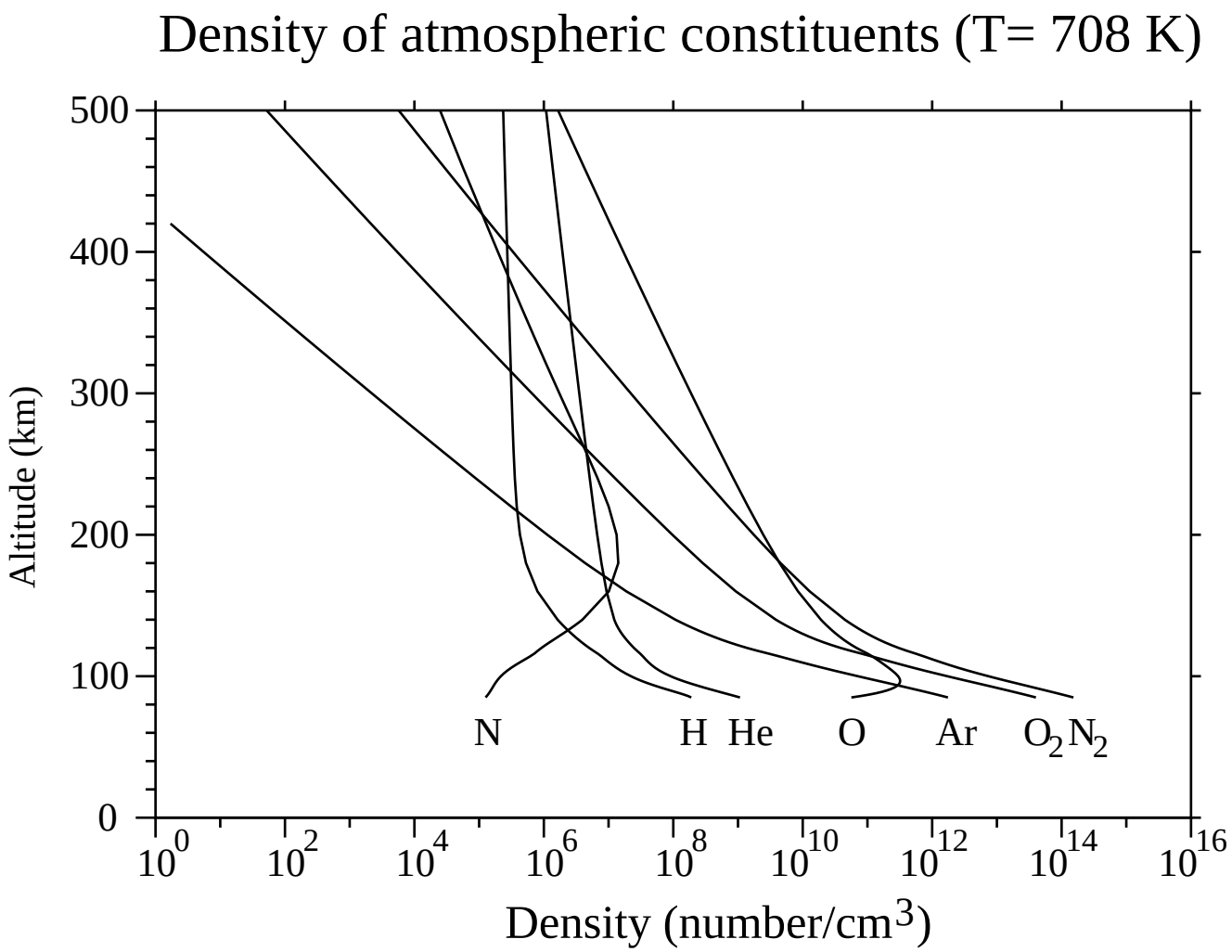

Kuva 4: The density profiles of different constituents at exospheric temperature 708 K.

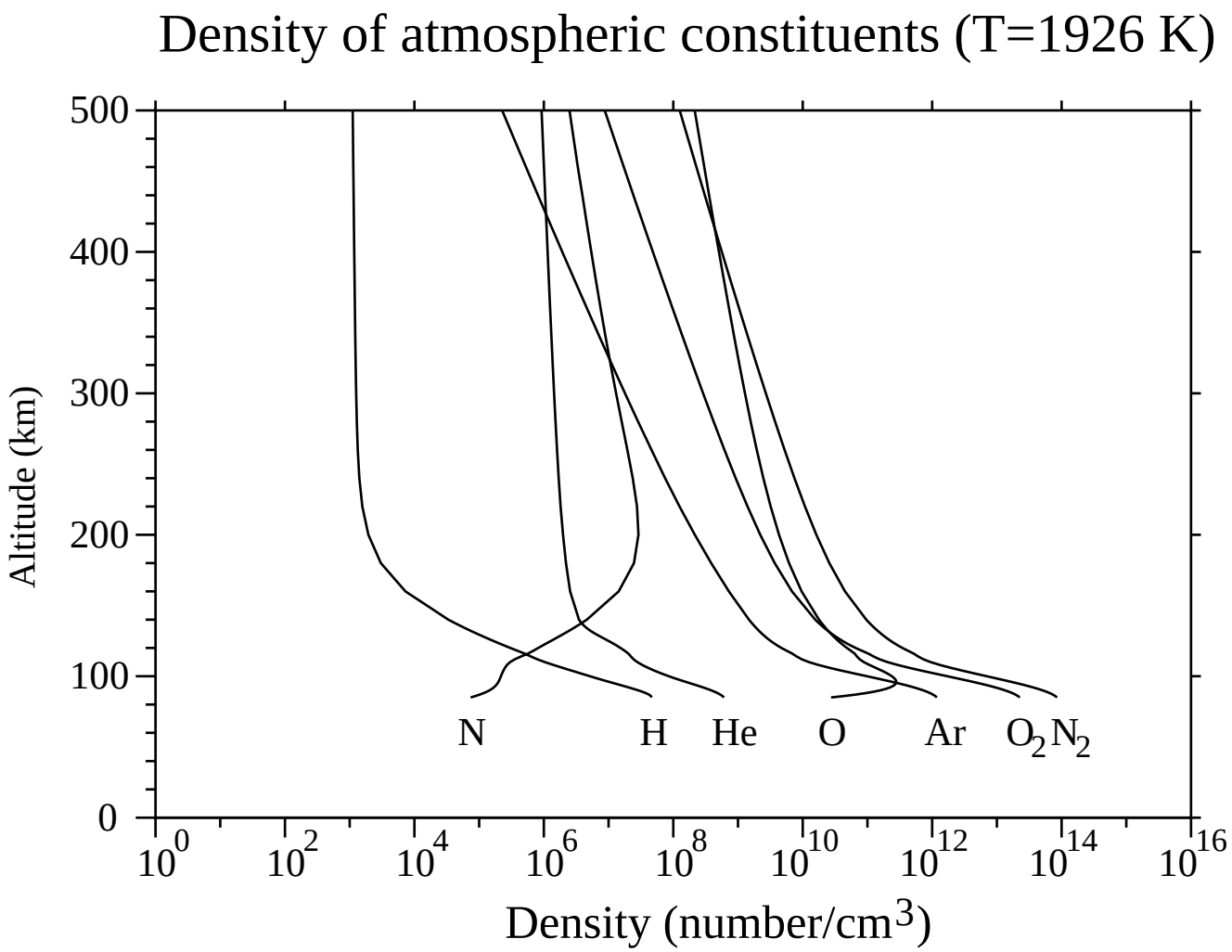

Kuva 5: The density profiles of different constituents at exospheric temperature 1926 K.

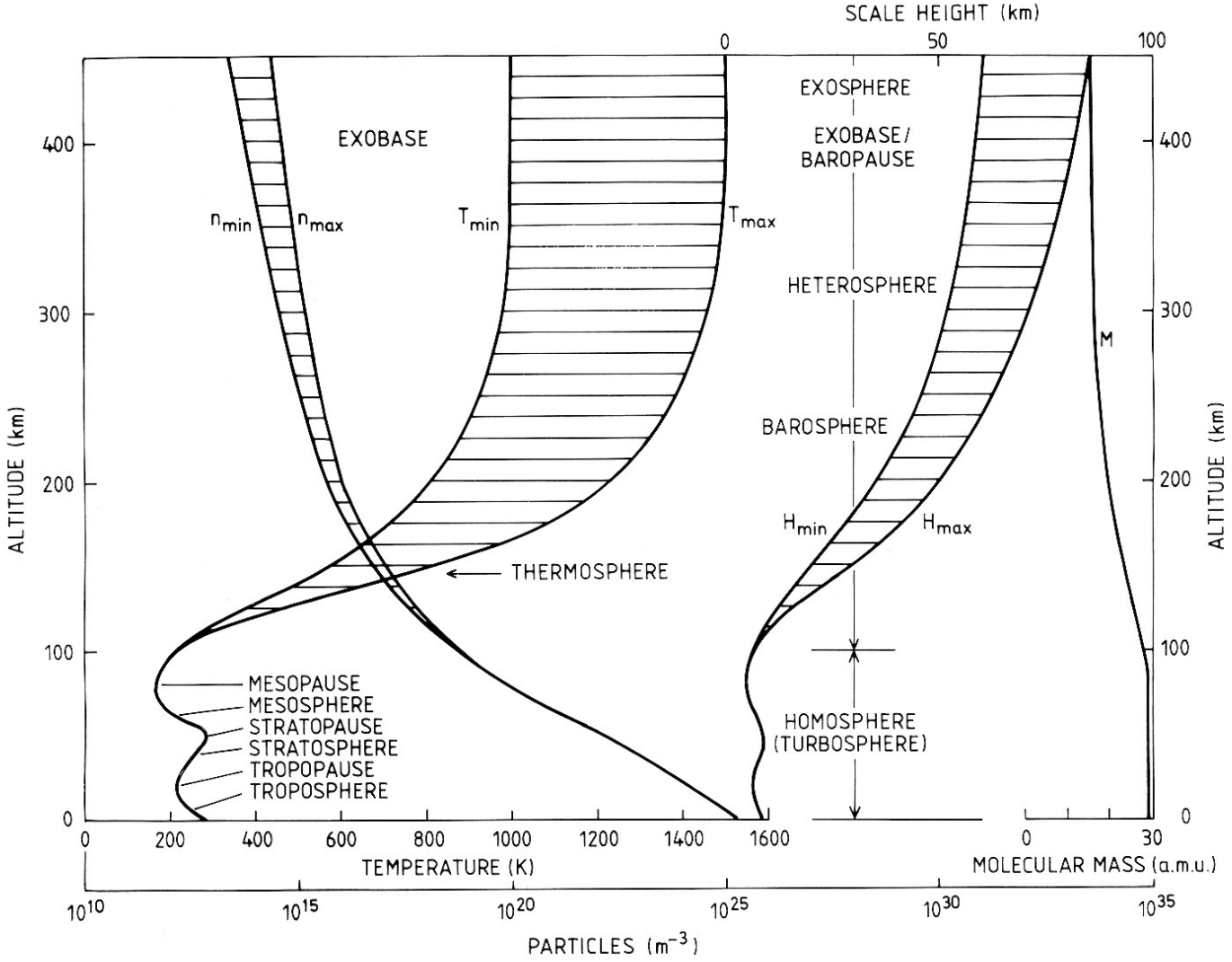

Fig. 3.1. Model height profiles of the temperature T, density n, molecular mass M, and scale height H, distributions in the Earth's atmosphere below 450 km. The different regions are also indicated by their characteristic names according to temperature or composition. The variability in the different parameters with respect to solar activity is indicated by the hatched areas.

AURORAL ELECTRONS

Solar UV radiation produce photoelectrons in the atmosphere. The population of these photoelectrons is an embedded source of ionization. The production rate of photoelectrons is not a measurable quantity.

An additional source of ionization is due to energetic charged particle precipitation of solar and magnetospheric origin. These are associated principally with the aurora. The intencity of primary auroral electrons is a measurable quantity.

Primary auroral electrons ionize the atmospheric gases producing secondary electrons that are equivalent of the photoelectrons produced by photoionization.

In this chapter we will survey the characteristics of energetic electron fluxes. Auroral electrons undergo numerous collisions in their passage through the atmosphere and we will focus to the processes they overcame.

1.1 UV irradiance and primary auroral electrons

The solar UV irradiance is highly variable. However it is responsible of several thermospheric and ionospheric parameters, e.g. density and composition at a given

pressure level, neutral and plasma temperature, ion density and composition as we have already seen.

That is associated with the diurnal, seasonal as well as geographic variations. Also the 11 years cycle is connected to the solar activity.

Charged particles associated with auroral phenomena are temporally and spatially much more variable in strength. They are much more unpredictable than solar UV radiation.

Since charged particle motion in the collisionless magnetosphere is controlled by the geomagnetic field, the precipitation pattern of auroral particles is aligned by the magnetic dipole field.

The auroral characteristics that are needed to study this phenomenon are the identity of the charged particles: electrons, protons and possibly the heavier ions, the energy spectrum and the angular distribution of the stream.

1.2 Electron transport in the atmosphere

Passage of solar irradiance $I(\lambda)$ through the atmosphere implies that the pho-

tons only suffer complete destruction. They are **not** multiple scattered and they do **not** reappear as photons at a different wavelength.

Electron transport behave different way. They are not destroyed in the course of passage throug the atmosphere. They are effectively stopped or more accurately, they become indistinguishable from the ambient thermal electron population.

The electrons are not absorbed. They are scattered elastically or inelastically. Both types have their own cross sections and probabilities.

1.2.1 Elastic scattering

The precipitating primary electrons do not gain energy in collisions with neutral atoms and molecules. *There is effectively no energy change in collision with the more massive atoms, molecules and ions! The main effect in elastic scattering is the angular deflection of the electron.* The elastic scattering cross section is of the form of

$$\sigma_e(E', E; \mu', \mu) = \delta(E - E')P_e(E; \mu', \mu)\sigma_e(E) \tag{1}$$

where $P_e(E; \mu', \mu)$ is the phase function for angular deflection at an energy E with μ' and μ the cosine of pitch angle before and after the collision. The E'

and E refer to the electron energy before and after the collision and $\sigma_e(E)$ is the magnitude of the cross section at energy E.

1.2.2 Inelastic scattering

The precipitating primary electrons will lose the energy in collisions with neutrals and ions. *They lose energy in every collision!*

Inelastic scattering involves a change in the internal energy of the atmospheric collision partner. This could be excitation of electronic, vibrational and rotational states accompanied by a discrete energy loss.

It could be also ionization and molecular dissociation accompanied by continuous energy loss above the threshold. Ionization is not only energy loss process. It is also a source of secondary electrons.

Individual electrons are not labelled. They can be degraded primaries or fresh secondaries. Measurements of electron intensities cannot distinguish between them.

The cross section for excitation of discrete states is

$$\sigma_{in}^{d}(E', E; \mu', \mu) = \Sigma_j P_j^d(E; \mu', \mu)\delta(E' - E - W_j)\sigma_j(E) \tag{2}$$

where W_j is the excitation threshold energy of state j. The other varibles are the same than in the equation 1.

Within the ionization a secondary electron is produced. **The cross sections for ionization and production for secondary electrons** are

$$\sigma_{in}^{I}(E'_p, E_p; \mu', \mu) = \Sigma_j P_j^I(E_p; \mu', \mu)\frac{d\sigma}{dW}(E'_p, W = E'_p - E_p) \tag{3}$$

$$\sigma_{in}^{s}(E'_p, E_s; \mu', \mu) = \Sigma_j P_j^s(E_s; \mu', \mu)\frac{d\sigma}{dW}(E'_p, W = E_s + I) \tag{4}$$

The energy loss W is the sum of the ionization potentials I and the energy of the secondary electron E_s. Energy conservation requires that $E_p + E_s + I = E'_p$. The differential cross section $d\sigma/dW$ is used for continuous energy loss processes.

The cross section for molecular dissociation is similar to equation 3

$$\sigma_{in}^{D}(E'_p, E_p; \mu', \mu) = \Sigma_j P_j^D(E_p; \mu', \mu)\frac{d\sigma}{dW}(E'_p, W = E'_p - E_p) \tag{5}$$

and **the cross section for dissociative ionization of molecules**

$$\sigma_{in}^{DI}(E'_p, E_p; \mu', \mu) = \Sigma_j P_j^{DI}(E_p; \mu', \mu) \frac{d\sigma}{dW}(E'_p, W = E_s + I) \tag{6}$$

but this is included to equation 4

The total scattering cross section is then

$$\sigma_{tot} = \sigma_e + \sigma_{in}^d + \sigma_{in}^I + \sigma_{in}^D + \sigma_{in}^{DI} \tag{7}$$

The scattering depth, analogous to the optical depth, can be defined by

$$\tau = \Sigma_j \sigma_{tot} \int_z^\infty n_j(z) dz \tag{8}$$

The total number flux for a given event may be larger within the atmosphere than above the atmosphere but the electron spectra would be very different. It means that primary electrons produce a number of secondary electrons.

1.2.3 Primary, secondary, suprathermal and photoelectrons

In the upper atmosphere the electron density is always considerably less than the neutral gas density. The precipitating primary electrons therefore collide primarily with the neutrals.

The primary and secondary electrons continue to lose energy until they have energy of just above the thermal electron population. Then they are called suprathermal electrons.

The number of inelastic collision processes in the suprathermal regime is limited to excitation of low vibrational levels or rotational levels in molecules. They are capable to excite also lower excitation levels or states of different atoms.

The energy of suprathermal electrons is shared with the less abundant ambient thermal electrons by elastic collisions, resulting an increase of electron temperature.

Photoelectrons are primarily an embedded source in the atmosphere. At times there is also a small photoelectron flux from the geomagnetically conjugate hemisphere which becomes an external intensity source. Auroral electron precipitation is primarily an external source with the secondary electrons becoming the embedded source.

Note that the dimension of the electron intensity I is $cm^{-2}s^{-1}sr^{-1}J^{-1}$ or $cm^{-2}s^{-1}sr^{-1}eV^{-1}$ whereas the dimension of distribution function f is $cm^{-6}s^{3}$.

These are related by

$$I(\mathbf{x}, E, \mathbf{\Omega}, t) = \frac{v^2}{m} f(\mathbf{x}, \mathbf{v}, t) \tag{9}$$

where $\mathbf{x}$ is the position vector, $\mathbf{\Omega}$ is a unit vector for the direction of the velocity $\mathbf{v}$, $\mathbf{E}$ is the energy and $\mathbf{m}$ is the mass of electron.

The intensity $I(\tau, E, \mu)$ is a basic quantity for testing our understanding of the physical processes that govern photoelectrons and auroral electron transport. Rockets and satellites can make in situ measurements of the intensity.

The intensity enables us to compute ionization rates, dissociation rates, excitation rates and electron heating rates. This kind of computation is often made by Monte Carlo calculations.

The angular distribution of photoelectrons produced by solar UV-photons is nearly isotropic. It means that photoelectrons are initially uniformly ejected to every directions. In the simplest approximation a two stream approximation has been applied, where upward and downward fluxes have taken into account.

1.3 Electron energy deposition in the atmosphere

In the course of their passage through the atmosphere photoelectrons and auroral electrons lose their energy by a variety of inelastic collisions as described earlier. These collision reactions will be discussed in more detail because they are responsible for the physical and chemical changes in the atmosphere.

The overall energy loss suffered by electrons is called as **rate of energy deposition** at various heights in the atmosphere and it is given by

$$\varepsilon(z) = \Sigma_j \Sigma_k n_j(z) \int_{w_{j,k}}^{\infty} W_{j,k} \sigma_j^k(E) I(E,z) dE \tag{10}$$

The summation extends over all inelastic processes k, of all species j, for which the cross sections are σ_j^k and the energy loss is $W_{j,k}$.

The electron intensity $I(E, z)$ will be integrated over all directions. The species concentrations are denoted by $n_j(z)$. The intensity is not easily computed and often approximation is made.

Integration over altitude gives the total energy deposited within the atmosphere by the incoming as well as outgoing electron or photon flux.

In the case of auroral electron intensities, which are characterized by a wide range of energy and angular distribution, there are serious computational difficulties.

A.E. Grün made laboratory experiment in 1957, where he fired a beam of monoenergetic electrons into a chamber filled with nitrogen gas and measured the luminosity it created.

The geometry of the experiment is shown in Fig. 1. An intensity of light was measured through a narrow slit with a width of dz. It was scanned through the entire luminous range.

What happened in the chamber? A small fraction of molecular ions were produced by electron impact on N_2 molecules and excited to the state $B^2\Sigma$. Following chemical reaction is produced by a primary electron denoted by e^*

$$e^* + N_2 \longrightarrow e^* + N_2^+(B^2\Sigma) + e \tag{11}$$

Decay to the ground station results emissions in the First Negative system (1 NG). The vibrational band $v' = 0$ to $v'' = 0$ emits at a wavelength of 391.4

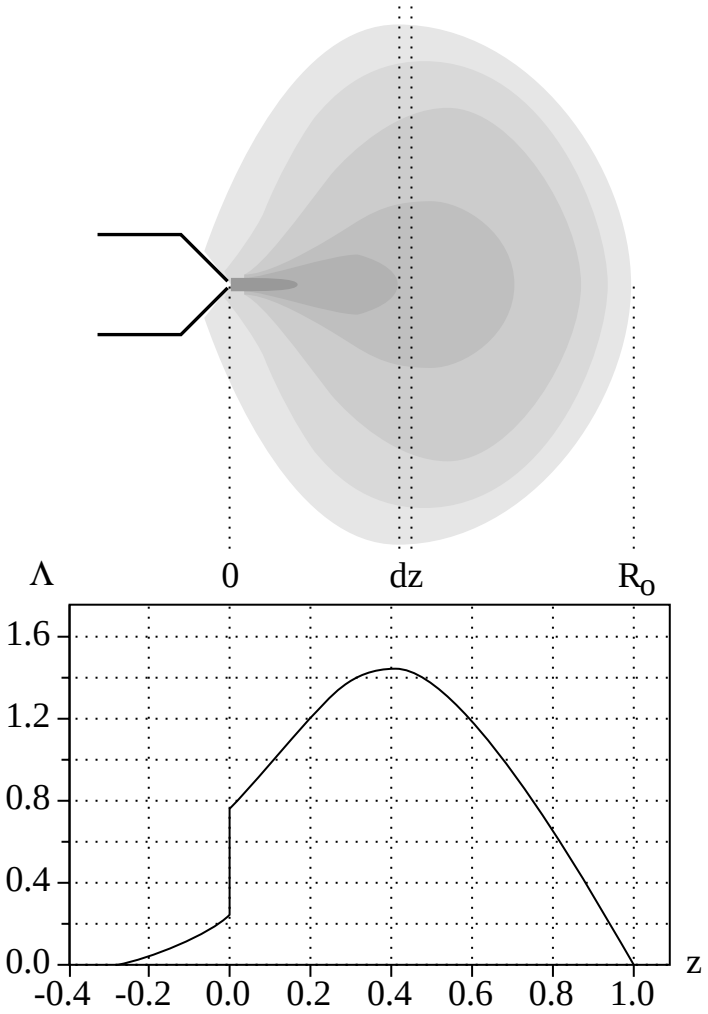

Kuva 1: The Grün's experiment.

nm

$$N_2^+(B^2\Sigma, v' = 0) \longrightarrow N_2^+(X^2\Sigma, v'' = 0) + h\nu \tag{12}$$

The emission cross section for the (0,0) transition, the rate of formation of ion pairs per 391.4 nm photon and the energy lost by the incident electron per ion pair formation are all well-established experimental parameters.

The variations of 391.4 m emission rate with distance from the source is a measure of the distribution of energy deposition along the path. It includes implicitly all the elastic and inelastic scattering processes that pertain to N_2 molecules.

1.3.1 Electron range and energy dissipation

An electron with initial energy E undergoes a number of collisions and it is finally stopped at a distance from the source identified as the effective range $R(E)$.

Its dimension is usually given as $g\ cm^{-2}$ or as $atm\ cm$, where atm refers to the mass density $g\ cm^{-3}$ of the atmosphere at standard pressure and temperature at sea level.

The **range** is an experimentally derived parameter and several investigators

have made measurements for different electron energy regime. In the energy interval of greatest importance for auroral primary electrons, $200\ eV < E < 50\ keV$, the result can be expressed approximately by

$$R(E) = 4.30 \times 10^{-7} + 5.36 \times 10^{-6} E^{1.67} \tag{13}$$

where E is in keV and $R(E)$ is in $g\ cm^{-2}$.

The energy is not dissipated uniformly along its range. Instead the distribution function reaches a maximum value at some distance from the source, which depends on the initial electron energy. The energy dissipation distribution $\Lambda(s/R)$ is a function of the fractional range s/R.

The atmosphere scattering depth s is given by

$$s = \int_z^\infty \rho(z) dz \tag{14}$$

where $\rho(z)$ is the mass density.

Normalization of the energy dissipation distribution function gives

$$\int_{-1}^{+1} \Lambda(s/R) d(s/R) = 1 \tag{15}$$

according to the energy conservation.

The curves in Fig. 2 apply to an electron beam directed perpendicular to the source plane. It corresponds to a unidirectional intensity normal to the atmosphere.

The energy deposition $eV\ cm^{-3}\ s^{-1}$ for monoenergetic electrons at energy E_p will be

$$\varepsilon(z, E_p) = q(z)\Delta\varepsilon_{ion} = FE_p\Lambda(s/R)\frac{\rho(z)}{R(E_p)} \tag{16}$$

where F is the electron flux $cm^{-2}s^{-1}$, E_p is the electron energy in eV, $\rho(z)$ is the mass density, $R(E_p)$ is the range and $\Lambda(s/R)$ is the energy dissipation function.

The energy deposition rate is the product of the ionization rate $q(z)$ and the energy loss per ion pair formation $\Delta\varepsilon_{ion}$.

In the upper atmosphere there are only three main species, N_2, O_2 and O. The energy loss per ion pair formation $\Delta\varepsilon_{ion}$ have been found experimentally.

The total ionization rate will be then

$$q(z, E_p) = \varepsilon(z, E_p)/\Delta\varepsilon_{ion} \tag{17}$$

In aurorae the electron spectrum is usually not monoenergetic. A typical spect-

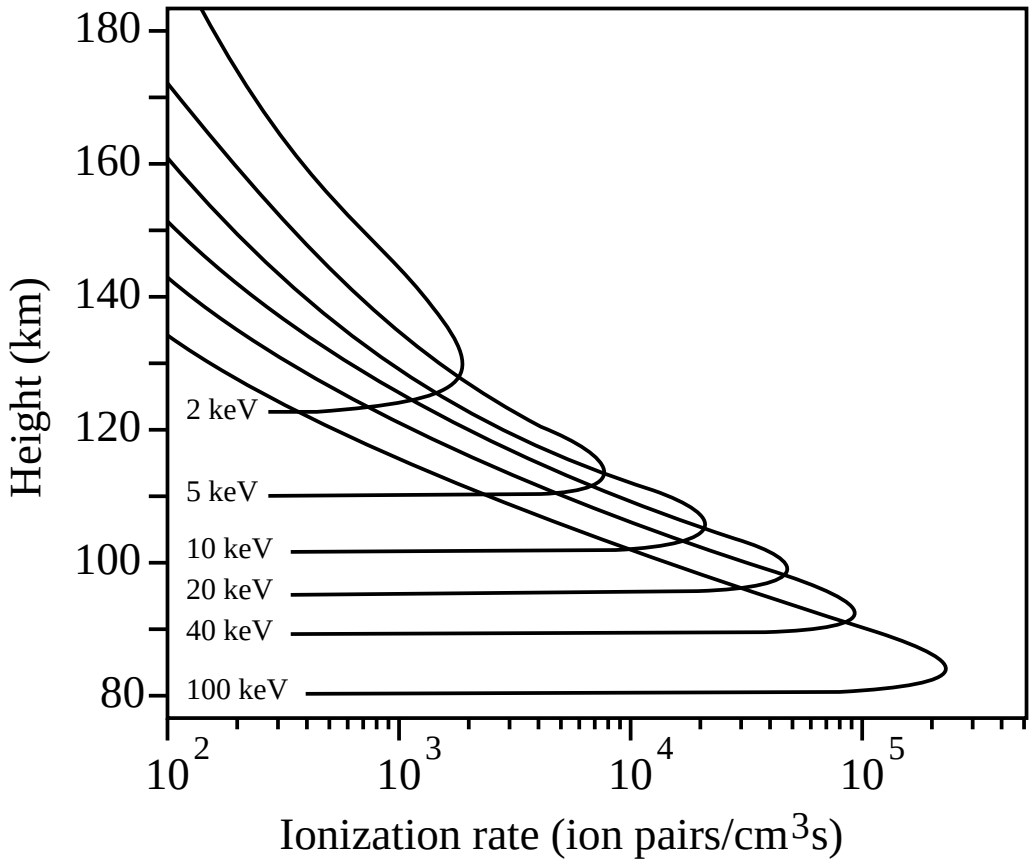

Kuva 2: Ionization rate curves at different primary electron energy.

rum has a distribution of the form

$$N(E)dE = E^{\gamma} \exp(-E/E_o)dE \tag{18}$$

where the parameters γ and E_o yield power law, exponential variations or Maxwellian distribution.

The ionization rate can be computed by using the spectrum with

$$q(z) = \int_0^{\infty} q(z, E)N(E)dE \tag{19}$$

Every ionization event produces a positive ion and a secondary electron. But what could be the energy of the newly produced secondary electron?

In the case of photoelectrons the incident photon destroys leaving the rest energy of the ionization process to kinetic energy of the particles.

In the case of ionization of primary auroral electrons they scatter forward direction. The much more numerous secondary electrons are emitted about isotropically at all angles. There will be a distribution of energy according to the ionization cross section.

The experimental results for the differential cross section for production of

electrons with energy E_s by incident beam of electrons with energy E'_p is

$$\frac{d\sigma}{dW}(E'_p, E_s) = \frac{\sigma'(E'_p)(1 - E_s/\overline{E})^{-2.1}}{\overline{E}\tanh[(E'_p - I)/2\overline{E}]} \tag{20}$$

where $\overline{E}$ is a spectral shape parameter, I is the ionization potential and $\sigma^I(E'_p)$ is the ionization cross section.

Differential cross sections are derived for ionization as well as for the production of secondary electrons for N_2, O_2 and O.

The total ionization rate for N_2 by taking into account different ionization cross sections will be

$$q^i_z(N_2) = q^i_z \frac{\sigma^i_{N_2}\, n_z(N_2)}{\sigma^i_{N_2}\, n_z(N_2) + \sigma^i_{O_2}\, n_z(O_2) + \sigma^i_O\, n_z(O)} \tag{21}$$

Corresponding formulas can be derived for $q_z(O_2)$ and $q_z(O)$. Thus the production rate of secondary electrons will be

$$P_z(E_s, E_p) = \Sigma_j \frac{d\sigma_j/dW}{\sigma^I_j} q_j(z, E_p) \tag{22}$$

In the sunlit atmosphere the photoelectrons and secondary electrons become indistinguishable.